METHYLPHENYLGERMYLENE AND ITS DIMER

GENERATION AND TIME RESOLVED

SPECTROSCOPIC STUDIES

OF METHYLPHENYLGERMYLENE AND ITS DIMER IN SOLUTION

By

ILEANA DANIELA DUMBRAVA, B.Sc.

A Thesis

Submitted to the school of Graduate Studies

in Partial Fulfillment of the Requirements

for the Degree

Master of Science

McMaster University

MASTER OF SCIENCE (2005)

(Chemistry)

McMaster University

Hamilton, Ontario

TITLE: Generation and time resolved spectroscopic studies of methylphenylgermylene and its dimer in solution

AUTHOR: Ileana D. Dumbrava, B. Sc.

SUPERVISOR: Professor William J. Leigh

NUMBER OF PAGES: xix, 175

ABSTRACT

Under 248 nm laser flash photolysis, the photodecomposition of 1,3,4-trimethyl-1-phenyl-1-germacyclopent-3-ene (**28**) in dry, deoxygenated hexane solution at 23 ^{0}C leads to the prompt formation of two transient species: phenylmethylgermylene (**29**) and its Ge=Ge doubly bonded dimer, 1,2-dimethyl-1,2-diphenyldigemene (**30**). The formation of **29** proceeds in high chemical yield as shown by the results of steady state trapping experiments with methanol and isoprene. The transient assigned to **29** exhibits λ_{max} = 490 nm and decays with second-order kinetics ($\tau \sim 2~\mu s$). The second transient, which is formed from the latter, is assigned to digermene **30** and exhibits λ_{max} = 420 nm and a lifetime, $\tau \sim 8~\mu s$. The assignments are based on comparisons to the spectra of other simple germylenes, such as dimethyl-, diphenyl and dimesitylgermylene as well as on the pattern of reactivity with trapping reagents in solution at room temperature.

Reactions studied include N-H, O-H and Sn-H insertion reactions, the [1+2] addition to isoprene and t-butylacetylene, and halogen atom abstraction from carbon tetrachloride.

Absolute rate constants for quenching of **29** with the above mentioned scavengers were obtained by direct measurement of the germylene decay kinetics, over the concentration range where the formation of the digermene was more than 70% quenched. This ensures that the decay of **29** was dominated by the reaction with the trapping reagent.

Absolute rate constants for reaction of the same reagents with **30** have also been determined for most of the scavengers studied. However, the digermene was found to be considerably less reactive than phenylmethylgermylene in all cases.

The trends in spectroscopic properties and reactivity of simple germylenes in solution are discussed.

ACKNOWLEDGEMENTS

TABLE OF CONTENTS

LIST OF SCHEMES

LIST OF FIGURES

LIST OF TABLES

CHAPTER 1

INTRODUCTION

1.1. Overview

The history of silicon and related elements dates back to the 19th century with the development of the Periodic Table. Mendeleev was the first who predicted the existence of germanium in 1871. Fifteen years later germanium was discovered in a mineral called argyrodite (Ag_6GeS_5) by *Clemens Alexander Winkler*.[1] The same scientist Winkler synthesized the first organogermanium compound in 1887, tetraethylgermane by reaction of tetrachlorogermane and diethylzinc[2] a quarter century later than the first organic compounds of silicon, tin and lead were obtained. The chemistry of organogermanium compounds started to develop in the second quarter of the twentieth century and flourished in the 60's when new sources of germanium were discovered.[3-5] Activity was stimulated by the advances made in the chemistry of organometallic compounds on the one hand and by the expanding range of applications of germanium and its organic derivatives on the other.

Germanium compounds have been extensively used in the fields of electronics,[6] as well as in medicine as anticancer, hypotensive and immunomodulating treatments.[7-10] Certain organogermanium compounds

possess low mammalian toxicity with a marked activity against certain bacteria, which makes them useful as chemotherapeutic agents.[10] In addition, the rapid expansion of organogermanium chemistry was due to a progressive decrease in the prices of elemental germanium and its derivatives.

The unique physico-chemical properties of divalent carbon species as reactive intermediates in organic chemistry have attracted considerable interest in recent years and initiated the search for other divalent species of Group 14. Silylenes, germylenes, stannylenes and plumbylenes are commonly referred to as "heavy carbene analogues" within the family of $[R_2M:]$ compounds, where M = C, Si, Ge, Sn, Pb. Simple germylenes [RR'Ge:] with R = R' = Me, Ph or R $\neq$ R' = Me, Ph are reactive species which are formed as intermediates in the course of thermal and/or photochemical reactions of a number of classes of organogermanium compounds.

Basically there are two methods for the direct study of these short-lived species: looking at them very quickly, immediately after their formation, which nowadays can be as short as a few nanoseconds or femtoseconds, or forming and trapping them under circumstances where they can be studied leisurely, using conventional spectroscopic tools.

Recent advances in spectroscopy, including matrix isolation and laser flash photolytic spectroscopies, allows researchers to study these very reactive and unstable species that otherwise cannot be isolated and characterized under

normal conditions. Generally the rate of conversion of these intermediates into reaction products is fast compared to their rate of formation, otherwise the intermediate would be an isolable compound or a species in rapid equilibrium with the reactants.

Through the application of fast laser techniques it has become possible to observe directly and obtain the lifetimes of short lived transient species. Furthermore, chemical methods have been developed for intercepting these species by means of chemical traps to form stable, isolable compounds with structures consistent with the reaction between the trap and the reaction intermediate. Clearly the added "trap" must intercept the reaction pathway only after the formation of the relevant intermediate, and the best evidence that this condition is met is provided by direct time-resolved monitoring of the reactive intermediate in the presence of the trap.

Species like carbenes $[R_2C:]$[11-17], free radicals $[R_3C\bullet]$[18-21], carbenium ions or carbocations $[R_3C^+]$[22, 23], carbanions $[R_3C^-]$[24, 25] and doubly-bonded systems $[R_2M=MR_2]$[26-29] or $[R_2M=CR]$[26, 30] where R = Me, Ph, Et, Mes; M = Si, Ge, Sn are classified as "reactive intermediates" simply because their reactions take place in the nano- to millisecond time scales.

When the "active" carbon in carbenes is substituted for Si and/or Ge in going from $[R_2C:]$ to $[R_2Si:]$[31-44] (silylenes) and $[R_2Ge:]$[27, 45-68] (germylenes) the

spectroscopic properties, reactivity and reaction mechanisms of such species change.

The focus of this study was to answer questions regarding these problems and find experimental evidence in support of proposed mechanisms.

The main objective of the present thesis was to synthesize a new photochemical precursor for phenylmethylgermylene (**29**) and to study its reactivity in solution by steady state and nanosecond laser flash photolysis methods.

1.2. Carbenes and Germylenes

1.2.1. Carbenes

1.2.1.1. Triplet versus singlet ground state

Starting with the pioneering work of Curtius[69] and Staudinger[70] the divalent carbon compounds referred to as carbenes have played an important role in understanding the chemistry of the divalent transient intermediates of Group 14.

The divalent carbon atom in carbenes contains six electrons in its valence shell: two in each covalent bond and two nonbonding electrons.[14, 15] Carbenes are often represented as [R_2C:], where R stands for a wide range of hydrocarbon substituents.[11] Most of these species are nonlinear with a trigonal (sp^2)

4

hybridization state and can exist either in a singlet or a triplet electronic state. The bent structure with both electrons paired and situated in the nonbonding (sp^2) orbital with σ character forms the lowest–energy singlet state $^1(\sigma^2)$. In the lowest–energy triplet state the electrons have parallel spins and occupy the nonbonding σ (sp^2) and π ($pxyz$) orbitals $^3(\sigma^1 p^1)$ (Figure 1).[71] In carbenes, these two electronic states are generally similar in energy. As a result, the identity of the ground state (singlet or triplet) varies depending on the substituents.

Singlet (100-110°)   Triplet (130-150°)

$E_{singlet} \sim E_{triplet}$

R = Me, Et, Bu, Ph.
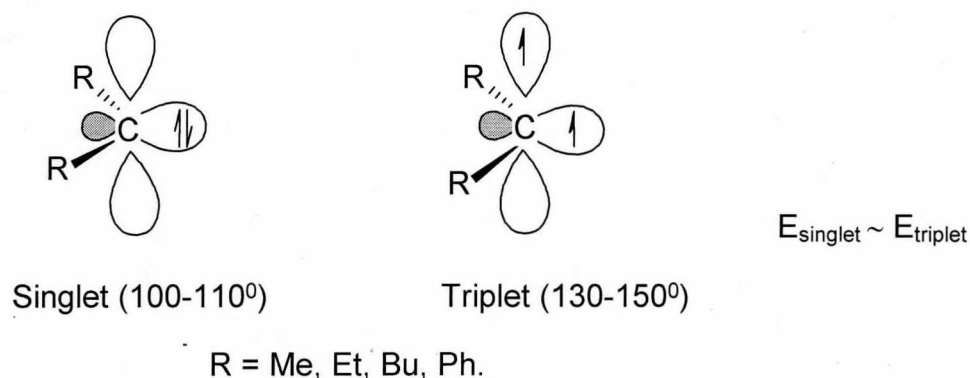
Figure 1. Electronic configuration of carbenes.

The ground-state spin multiplicity is a fundamental feature of carbenes and dictates their reactivity.[72] Singlet carbenes with a filled and a vacant orbital possess ambiphilic (electro- or nucleophilic) character whereas triplet carbenes with two singly occupied orbitals exhibit diradical behaviour.

The triplet is the ground state for most simple carbenes such as [CH_2:] and simple alkyl derivatives. The reason that most carbenes are more stable as triplets is that the energy to be gained by bringing the electron in the p orbital down into the sp^2 is insufficient to overcome the repulsion that exists between two electrons in a single orbital.[73] Recent high–level calculations, which are in perfect agreement with experimental determinations,[74-76] show that the singlet–triplet gap in [CH_2:] has a value of 9–9.1 kcal mol^{-1}, in other words, 9–9.1 kcal mol^{-1} is required to pair up the two electrons. Therefore, a singlet ground state is favored by a large σ-p energy difference; Gleiter and Hofmann[77] suggested that a value of at least 40-46 kcal/mol is necessary to impose a singlet ground state, whereas a value below 35 kcal/mol leads to a triplet ground state. Experimental observations[78] and theoretical calculations[79] showed that the typical valence angles of monosubstituted singlet carbenes fall in the range 100–110^0 (*e.g.* dimethylcarbene has a singlet ground state and bond angle of 111^0)[80] while the values of triplet carbenes are larger 133–150^0 (e.g. di(tert-butyl)carbene has a triplet ground state and bond angle of 143^0).[81] Based on these data the influence of substituents on the carbene ground state spin multiplicity can be analyzed in terms of steric and electronic effects.

The influence of substituent electronegativity on carbene multiplicity is well understood.[82] Inductive-electron–withdrawing substituents favor the singlet over the triplet state. In particular, Harrison *et al.*[83] showed that the ground state goes from triplet to singlet upon changing the substituents from electropositive lithium

via hydrogen to electronegative fluorine. Although inductive effects play an important role in determining the ground state multiplicity of a few carbenes (for example triplet Li-C-Li)[83], mesomeric (resonance) effects are more significant; π-electron-donating groups such as -F, -Cl, -Br, -I, -NR$_2$, -PR$_2$, -OR, -SR, -SR$_3$ (with R = alkyl, aryl) will interact with the p orbital, increasing the σ-p energy gap and favoring the singlet state over the triplet. The most familiar carbenes of this class are dihalocarbenes[84] and the stable diaminocarbenes[15] (Figure 2).
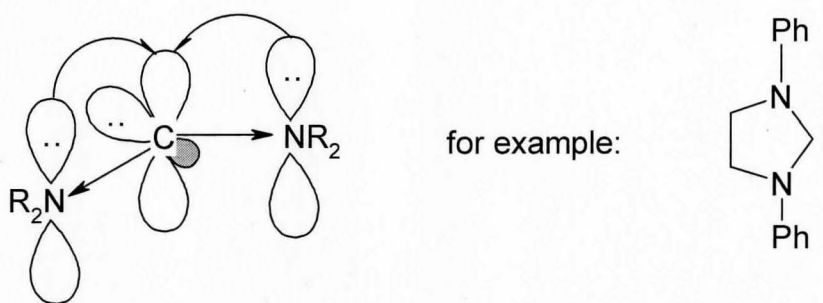
Figure 2. Electronic effects of substituents in diaminocarbenes.

On the contrary, π-electron–withdrawing groups such as W = -COR, -CN, -CF$_3$, -BR$_2$, -SiR$_3$, -PR$_3^+$, -SOR, -SO$_2$R and conjugating groups including alkenyl, alkynyl and aryl lower the σ-p gap energy and thus the ground state for these carbenes is expected to be a triplet. Representatives of this class of carbenes are diborylcarbenes[15] (Figure 3).
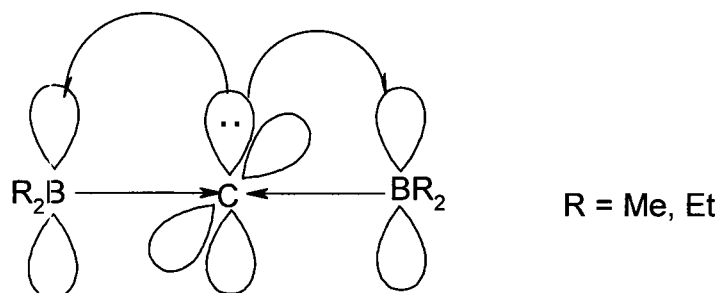
Figure 3. Electronic effects of substituents in diborylcarbenes.

It can be concluded from a valence bond point of view that electron-donating groups stabilize the singlet state more efficiently than the radical-like triplet state, whereas electron-withdrawing groups have the opposite effect.

The magnitude of ΔE_{ST} is also influenced by the carbon-carbon bond angle. A carbene with a linear geometry was found by calculations to provide the maximum value for ΔE_{ST} and consequently stabilizes the triplet state. Thus, increasing the bulkiness of the carbene substituents broadens the carbene bond angle and favors the triplet state.[85] Dimethylcarbene has a bent singlet ground state (111^0)[80, 86], while di(tert-butyl)[81] and diadamantylcarbene[86] are ground state triplets with bond angles of 143^0 and 152^0, respectively (Figure 4).
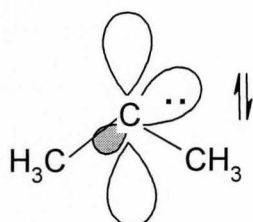
Ad = 1-Adamantyl

Dimethylcarbene (111°)   Diadamantylcarbenes (152°)

Figure 4. The influence of bond angles on the ground states of carbenes.

However, not all carbenes featuring a large bond angle have a triplet ground state. Steric effects dictate the ground-state spin multiplicities only when the electronic effect is small.[87, 88]

1.2.1.2. Characteristic reactions of singlet carbenes

The chemical behavior of carbenes is strongly dependent upon the spin multiplicity of the ground state. Triplet carbenes react by two-step radical pathways, whereas singlet carbenes undergo single-step reactions. Typical singlet carbene reactions are insertion reactions (insertion into O-H, Si-H, Ge-H, Sn-H bonds), stereospecific addition to olefins and dienes, reaction with Lewis Bases, and dimerization.[16] Singlet carbenes add to olefins in a concerted manner and during the addition the geometry of the alkene is preserved, so the reaction is stereospecific. Generally, carbenes undergo 1,2-addition with conjugated dienes, yielding vinylcyclopropanes[89] (Scheme1).
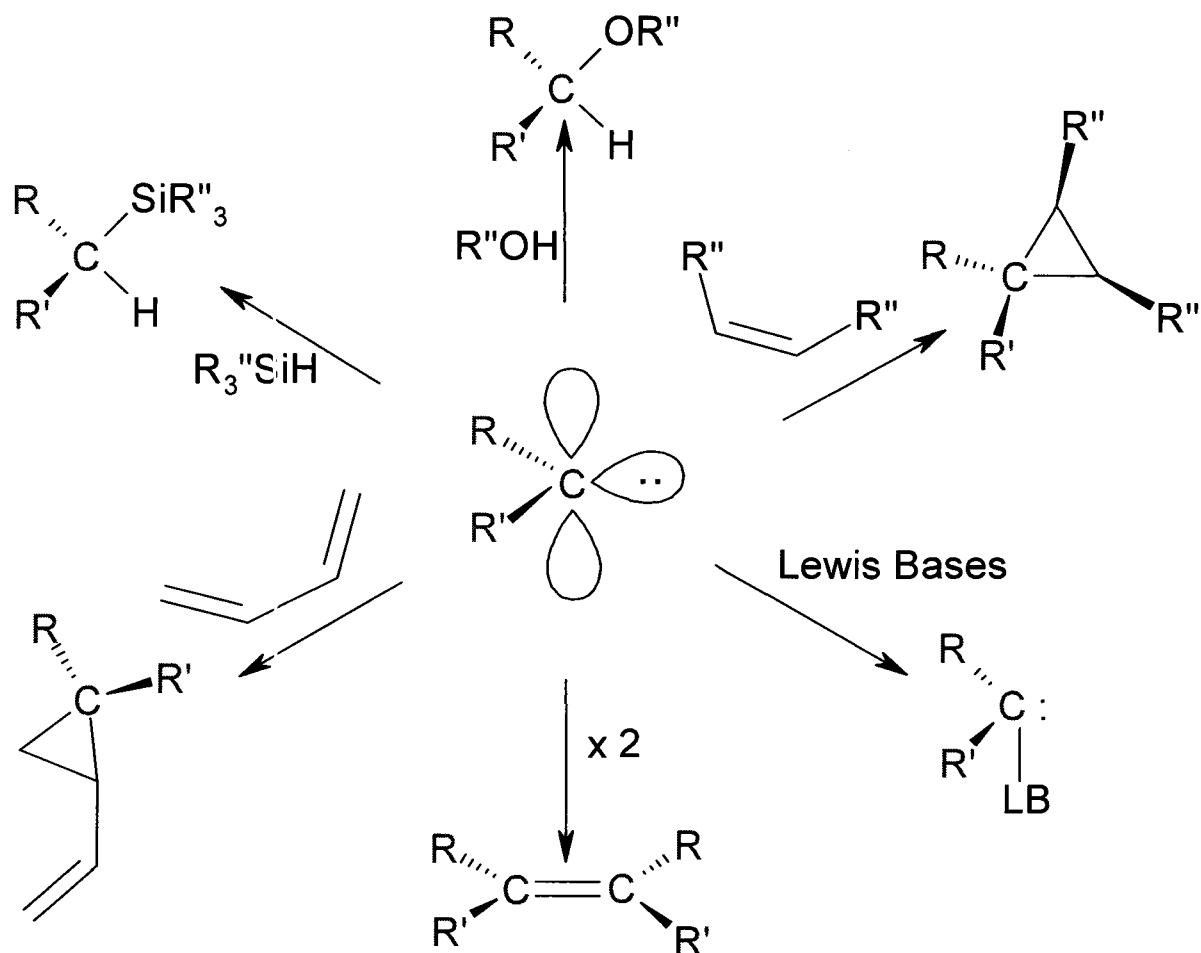
Scheme 1. Characteristic reactions of singlet carbenes.

R = R' = Me, Ph; R" = Me, Et.

1.2.2. Silylenes and Germylenes

1.2.2.1. Ground electronic state

One important difference between carbenes and heavier Group 14 metallylenes, silylenes and germylenes is the nature of the ground electronic state. While carbenes are found with singlet and triplet ground electronic states, each with a distinctive chemistry, only singlet germylenes have been found experimentally so far.[36] Almost all known silylenes possess singlet ground states as well. According to recent experiments and high-level calculations, the singlet ground state of the parent compound [H_2Si:] lies 21 kcal/mol lower than the first triplet state.[75, 90, 91] No experimental determinations of the singlet/triplet splitting in germylenes have been done so far. Therefore, the energy of the singlet/triplet splitting in [H_2Ge:] was estimated at *ca.* 23-24 kcal/mol by *ab initio* calculations, slightly greater than that reported for [SiH_2][92, 93] (Figure 5).

R = R' = CH$_3$, Ph; R = Me; R' = Ph; M = Si, Ge

Singlet (86^0-111^0)   Triplet (> 130^0)
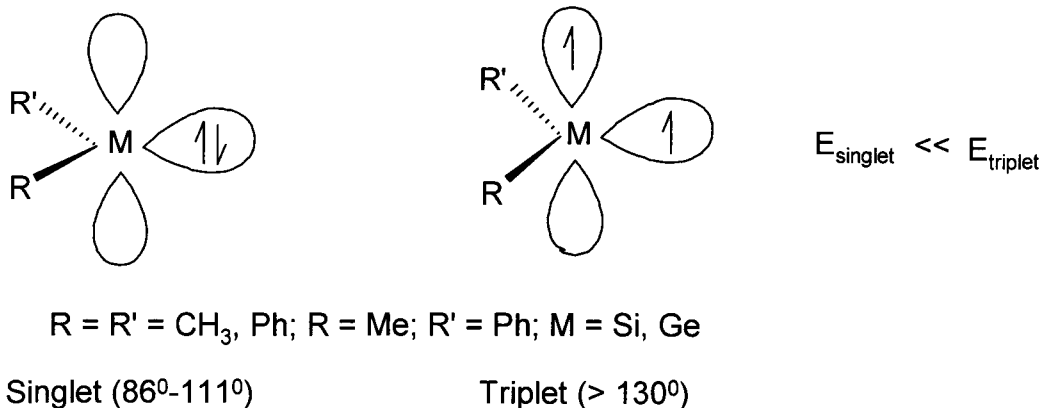
Figure 5. Ground electronic state for [RR'Si:] and [RR'Ge:].

This reversal in the multiplicity of the ground state has a great impact on the reactivity of the heavier carbene analogues. The difference in the ground state multiplicity on going from [CH$_2$:] to [SiH$_2$:] and [GeH$_2$:] has been rationalized based on the HOMO-LUMO gap. The calculated HOMO-LUMO gap for [SiH$_2$:] is 52 kcal/mol, significantly larger than that for [CH$_2$:] (27 kcal/mol).[94] The energy gained in forming a triplet configuration is not enough to compensate for the large HOMO-LUMO separation and thus [SiH$_2$:] assumes a singlet state. Thus, for simple silylenes and germylenes the ground state is the singlet, because the separation of the nonbonding electrons necessary to attain the triplet configuration requires an increase in energy larger than the accompanying decrease in electron-electron repulsion.

However, there are other factors that should be taken into account to explain the effects observed. In addition to the pairing energy and electrostatic effects, the small extent of s and p mixing in silicon and germanium seems to

play an important role. The higher p-character of the M-substituent bonds in silylenes and germylenes compared to that in carbenes accounts for the larger stabilization of the singlet state but also for the smaller bond angles in silylenes and germylenes. HMH valence angles in the singlet states of [H_2Si:] and [H_2Ge:] are 91.98^0 [95] and 91.28^0 [96], respectively, compared to that in [CH_2:] of 105^0.[97] These differences can be explained as the consequence of the relatively large difference in size of 3s, 4s, 3p, and 4p orbitals versus 2s and 2p ones. On the other hand the larger size of the lone pair orbital in silylenes and germylenes compared with carbenes results in lower electron-electron repulsion in silylenes and germylenes, thus favoring the singlet state for the heavier analogues. Moreover, as a result of the larger size of the lone pair orbitals, the larger bond lengths in silylenes and germylenes (*e.g.* for [CH_2:] was determined a bond length 1.08 Å compared with 1.52 Å for [SiH_2:] and 1.60 Å for [GeH_2:])[14] also contribute to the decrease in the electron-electron repulsion, favoring the singlet state for these species.

Another factor influencing the energy of the ground state is the degree of mixing between the HOMO and the empty orbital. Stronger mixing between these orbitals leads to a lowering in the energy of the HOMO and a higher HOMO-LUMO energy difference[98] (Figure 5).

Steric effects can also influence the singlet-triplet gap. For [SiH_2:] singlet-triplet crossing occurs at a valence bond angle of ~ 125^0-130^0.[99-101] This result indicates that silylenes with a triplet ground state can be formed when the angle

around the central metal is higher than 130^0. This is in accord with the finding that the ground-state multiplicity of the carbon analogues [R_2C:] can easily be switched from triplet to singlet by modification of the substituents at R. Thus, if sufficiently bulky groups are attached to silicon a ground state triplet can be expected by means of opening up the angle at silicon. The enlargement of the bond angles caused by insertion of isopropyl and t-butyl groups was encouraged. Computational studies predicted that [(t-$Bu_3Si)_2Si$:] and [:Si((Si(i-propyl)(t-butyl)$_2$)], [:Si(Si(i-propyl)$_3)_2$] should have triplet ground states,[100-102] and in 2003 Sekiguchi *et al.*[100] reported the first observation of a triplet ground state silylene, bis(tri-tert-butylsilyl)silylene, and its chemical behaviour.

1.2.2.2. Direct detection of silylenes and germylenes

Germylenes and silylenes are reactive species, which are formed as intermediates in the course of thermal and/or photochemical reactions of a number of organogermanium or organosilicon compounds. Three main approaches have been applied for the study of these species: (i) time–resolved techniques (ii) stabilization of the intermediates in low temperature matrices and characterization by different spectroscopic methods such as UV, IR or ESR spectroscopy (iii) stabilization of the intermediates through electronic and steric effects of the substituents.

The lowest energy electronic absorption of germylenes can be represented as a transition between the singlet S_0 and the excited singlet S_1 states, by promotion of an electron into the p orbital perpendicular to the molecular plane (Figure 6).
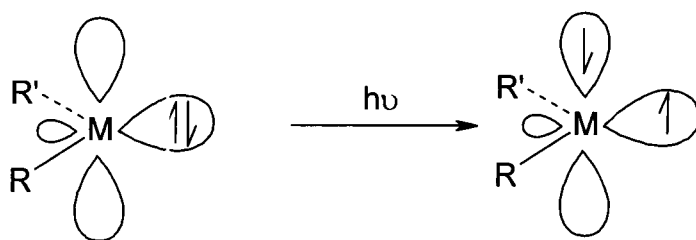
R = R' = Me or Ph; R = Me, R' = Ph; M = Si, Ge

Singlet S_0　　　　　　　　　　　　　Singlet S_1

Figure 6. Electronic excitation of germylenes and silylenes.

Thus, the lowest energy electronic transition is of the n, p type, and should occur upon absorption of energy in the visible or UV region of the electromagnetic spectrum. Therefore, UV–VIS absorption spectroscopy is a convenient method for the direct detection of these species, especially in low–temperature matrices or in solution using flash photolysis techniques.

Matrix isolation techniques are widely used for the observation of reactive intermediates. In a general sense the term matrix isolation encompasses a range

of techniques in which guest molecules are trapped in rigid host materials and are thereby prevented from undergoing diffusion. There are different types of matrices, among which inert gas matrices and organic glasses are the most frequently employed.

Dissolving the germylene precursors in a suitable solvent and rapidly cooling it below its freezing point produces the organic glasses. The resulting matrix is then irradiated and analyzed. In the case of silylenes and germylenes, matrix isolation in hydrocarbons, for example 3-methylpentane (3-MP) or sometimes mixtures of 3-MP and other hydrocarbons, are usually used.[78, 103] A common feature of the spectra obtained is the presence of one or more broad absorption bands. The assignment of the observed bands to specific species is based on the stoichiometry of the precursor decomposition, the exclusion of alternative possible products with known spectral characteristics, or the use of different precursors for generation of the same transient.[104]

One important aspect of UV–VIS spectroscopy is that it provides a link between the matrix isolation techniques and the time–resolved spectroscopy in solution. Actually, these two methods are complementary in that the matrix isolation technique can yield insight into the electronic and molecular structure of reactive intermediates, while time-resolved techniques provide information on reactivity.

With the advent of nanosecond flash photolysis (nLFP) techniques, it became possible to study short–lived species (10 ns to ~ 50 μs) in solution at

room temperature. The technique allows measurement of their UV–VIS absorption spectra and lifetimes, and measurement of rate constants for their reaction with trapping agents.

In the nLFP technique (see Figure 7), a solution of a stable precursor is photolyzed with a pulse from a UV laser to produce the transient of interest. The formation and decay of the transient is monitored by an optical detection system consisting of a xenon lamp, monochromator, and photomultiplier tube. The output of the photomultiplier tube is fed to a transient digitizer and the signal is finally fed to a computer for storage and kinetic analysis. Reaction kinetics are investigated at a fixed wavelength by monitoring changes in the absorption or optical density (Δ OD) of the solution with time. The spectrum of the transient is constructed from measurements of these time profiles at a series of wavelengths.[11, 20, 67, 105-108]
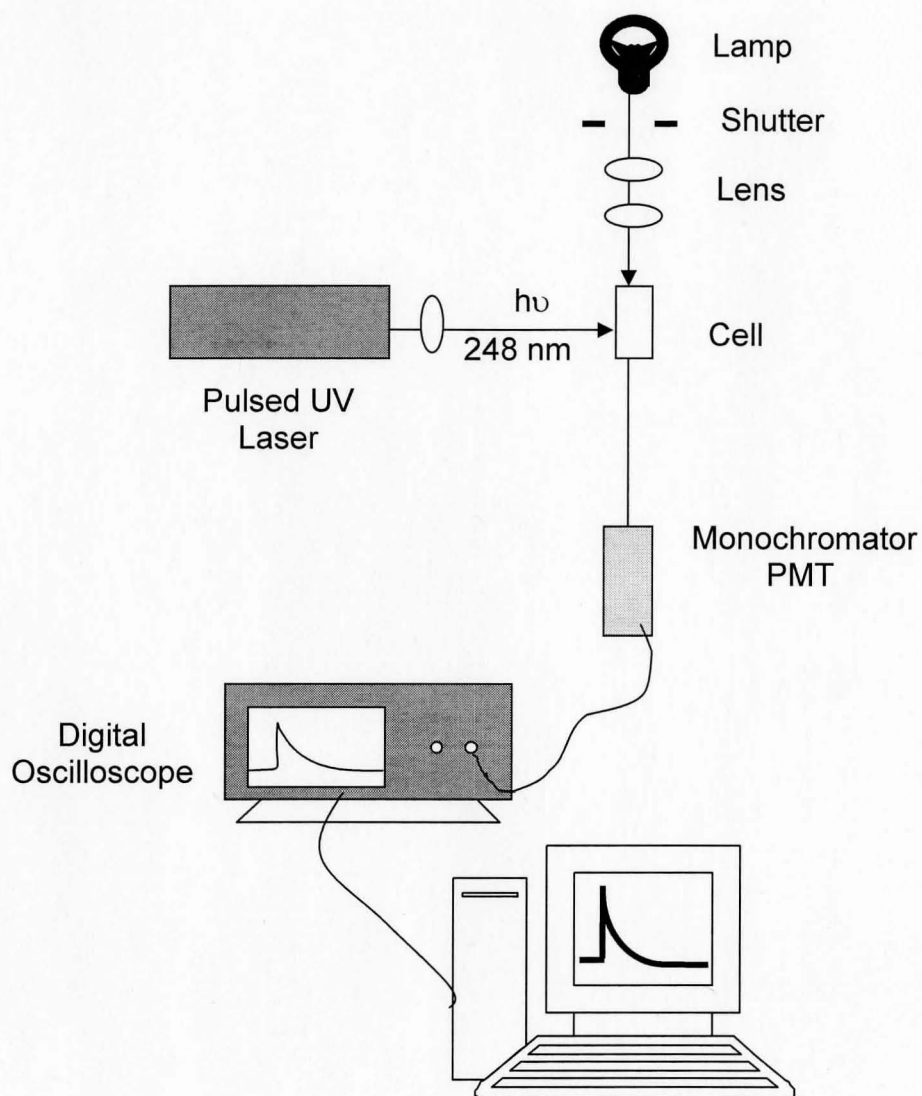
Figure 7. Schematic representation of the laser flash
photolysis system.

UV–VIS spectra of the same species recorded by both methods (matrix
isolation and nLFP techniques) ensure that the same chemistry is observed in
rigid media and in solution.

1.2.3. Precursors and Electronic Spectra of Germylenes

The electronic transition of germylenes due to promotion of one electron from HOMO to LUMO (n-p transition-Figure 6) is spin-allowed but is space-forbidden (both orbital overlap and orbital symmetry forbidden).[109, 110]

Carbonyl compounds exhibit weak bands in their UV-VIS spectra due to n-π^* transitions, which are analogous to the n-p transition in germylenes. One of the oxygen nonbonded electrons is promoted into a π^* orbital upon absorption of light of the proper energy. A very dilute solution shows a strong absorption band for the π-π^* transition but often no indication of n-π^* absorption. This weaker band can be detected only with more concentrated solution. The molar absorptivities ε ($M^{-1}cm^{-1}$), for the π-π^* transition in unsaturated carbonyl compounds are on the order 10^4 but are 10^2 or less for the n-π^* transition.[111] The lowest energy transition in germylenes, as in carbonyl compounds, is characterized by a low value of the extinction coefficient (ε). For example, in the case of [Ph$_2$Ge:] the value for the extinction coefficient at λ_{max} = 500 nm is ε_{max} = 1650 $M^{-1}s^{-1}$).[67] The value of the extinction coefficient ε reported by our group is in good agreement with the value reported for the stable germylene [TbtMesGe:], Tbt = 2,4,6-tris[bis(trimethylsilyl)methyl]phenyl, Mes = 2,4,6-Me$_3$C$_6$H$_2$ at 295 K, λ_{max} = 575 nm , ε_{max} = 1600 $M^{-1}s^{-1}$.[112] Due to its low intensity, this transition can be easily hidden by absorptions due to other species present in the system and in any event will be difficult to detect in dilute solution by UV-VIS spectroscopy. Medium

effects and inadequate precursors, which after thermal and/or photochemical reactions generate not only the transient of interest but also other labile by-products, absorbing strongly in the same region as the species of interest, are other interfering factors that make the direct detection and identification of germylene by UV-VIS spectroscopy difficult.

Despite the great deal of experimental data accumulated in recent years, the search for efficient photochemical precursors and reliable values for rate constants continues to be an important aspect of the chemistry of germylenes.[113] From this point of view a brief review of the most studied sources of germylenes will be presented. These include:

- 1-germacyclopent-3-ene derivatives (**1**)[57, 59, 60, 62, 67, 68]

- cyclopolygermanes (**2**)[52, 53]

- 7-germanorbornadiene derivatives (**3**)[50, 114]

- polygermanes or disilagermanes (**4**)[46-48], and

- germetanes (**5**).[115-117]
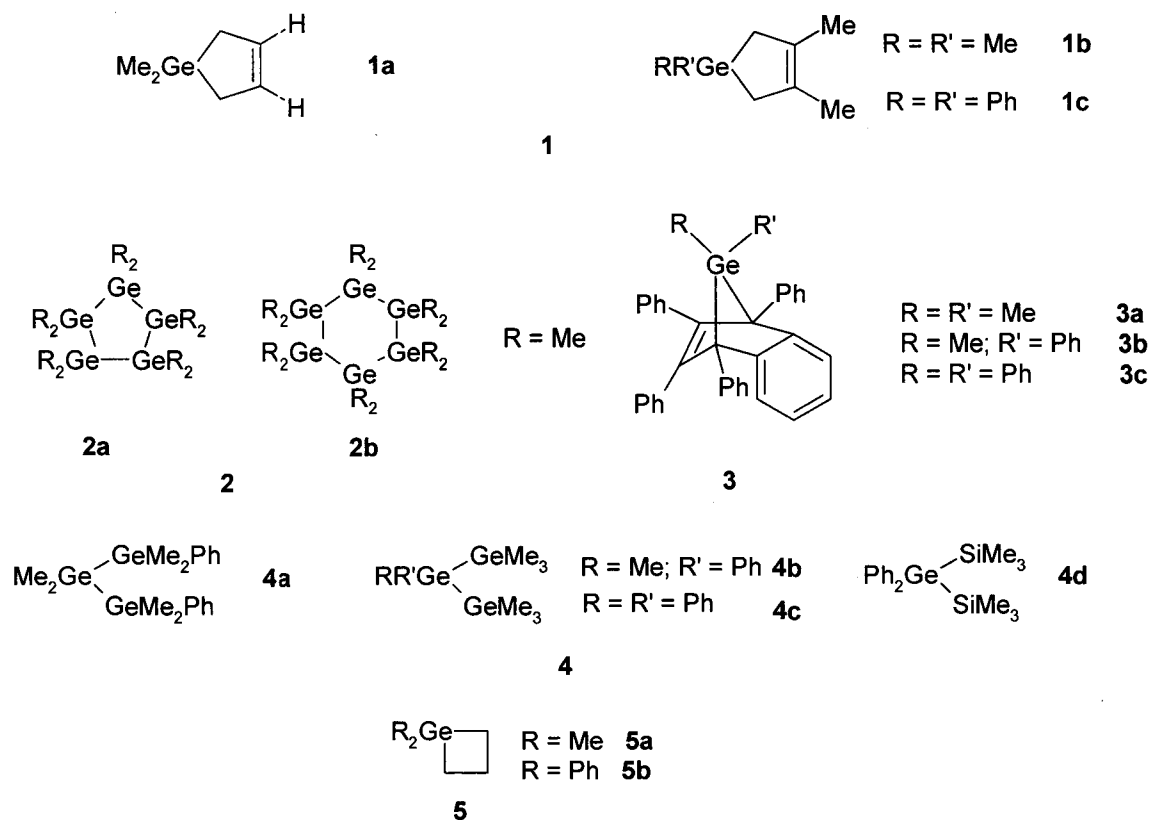
Table 1 presents some representative spectroscopic data that illustrates that the absorption maxima reported for the same germylene [R_2Ge:] and digermene [$R_2Ge=GeR_2$] formed from different precursors differ remarkably from each other, where R = Me, Ph. The largest span in the reported absorption maxima (values ranging from 370 to 506 nm) exist for [Me_2Ge:], whose UV spectrum has been studied the most.

| Transient | Precursor | Medium | Transient/λ_{max}(nm) | | Reference |
			[R_2Ge:]	[(R_2Ge)$_2$]	
[Me$_2$Ge:]	1a	Gas phase	480	-	59, 60
	1b	C$_6$H$_{14}$	480	370	67
	2a	C$_6$H$_{12}$	490	370	53
	2b	C$_6$H$_{12}$	450	370	52
	4a	C$_6$H$_{12}$	422	320	46
	2a	3-MP matrix, 77K	506	-	53
	3a	3-MP matrix, 77K	420	-	50, 114
[PhMeGe:]	4b	C$_6$H$_{12}$	430	320	48
	4b	3-MP matrix, 77K	456	-	48, 51
	3b	3-MP matrix, 77K	440	-	114
[Ph$_2$Ge:]	4c	3-MP matrix, 77K	460	-	48
	1c	C$_6$H$_{14}$	500	440	67
	4c	C$_6$H$_{12}$	450	330	48
	4d	C$_6$H$_{12}$	445	320	47
	3c, 4d	3-MP matrix, 77K	466	-	50, 114

Table 1. Comparison of reported absorption maxima of simple germylenes [R_2Ge:] and digermenes [(R_2Ge)$_2$], illustrating the discrepancies that exist in the literature.

The limited number of studies on phenylmethylgermylene, [PhMeGe:] (29) also reveal inconsistency in the values of the absorption maxima, which span from 430 nm to 456 nm.

It should be noted (see Table 1) that variation in the position of the absorption peaks is often observed in case of the corresponding digermenes as well.

Such poor consistency from one study to another can partly be explained by the factors mentioned above. In addition, many of the precursors used are laborious to synthesize (for example 7-norbornadiene derivatives (**3a-c**), cyclopolygermanes (**2a-b**), oligogermane (**4a**)).[45]

However, it has been suggested that the presence of by-products in the medium under investigation is the most important interfering factor in the detection and identification of germylenes by UV absorption spectroscopy.[113]

Following this idea the question that arises is why most of the photochemical sources used until now are not clean and eficient photochemical precursors for the germylene of interest. A clean photochemical precursor should be:

- synthesized in high yield following a simple procedure,

- stable and easy to handle,

- yields the germylene of interest upon photolysis, in high chemical and quantum yield.

The arylated oligogermanes (**4a-c**) and disilylgermanes (**4d**) used as simple germylene precursors by other workers often undergo competing Ge-M bond

homolysis and [1,3]-sigmatropic rearrangements, which form germanium centered radicals and conjugated germene derivatives in significant yields.[45, 67, 68, 117-119] Although the germylene is the major photoproduct in all cases, as verified by steady state photolysis experiments, its extinction coefficient (ε) is too small compared to those associated with these other relatively minor products to permit reliable detection and study (Scheme 2).

$$[Ph_2Ge:] \xrightarrow{\text{x 2}} Ph_2Ge=GePh_2$$
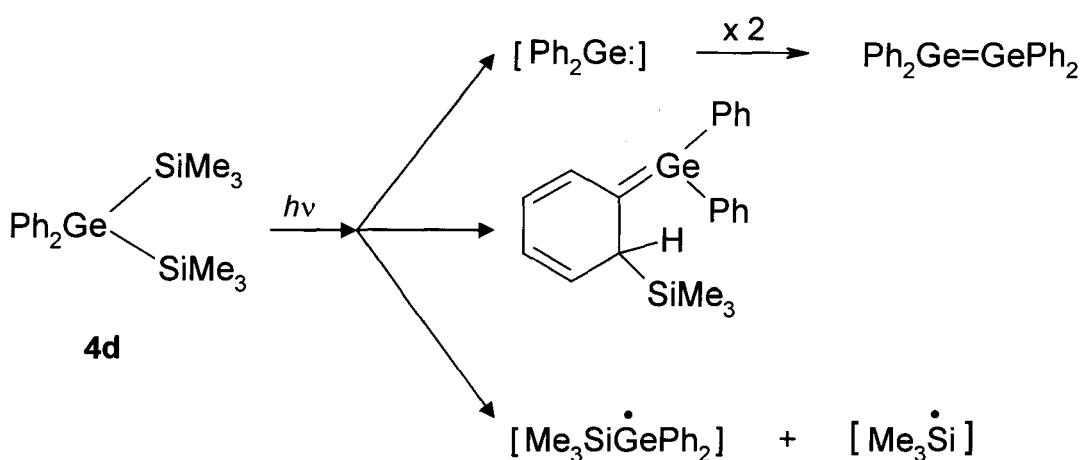
Scheme 2. Formation of germanium centered radicals and conjugated germene derivative upon irradiation of a disilylgermane (4d) precursor to [Ph$_2$Ge:].

7-Norbornadiene derivatives are the most-used sources of free germylenes[27] and evidently do not undergo competing reactions like 4a-d, but these compounds are difficult to prepare and handle.

From our experience[67], these molecules tend to undergo rapid thermal decomposition. Furthermore, this class of photochemical precursors has been studied until now only in matrixes, although laser flash photolysis experiments with **3a** were mentioned in Neumann's review.[27] The results have evidently been published only in a Ph. D. thesis.

Photolysis of cyclopolygermanes c-$(GeMe_2)_5$ (**2a**) and c-$(GeMe_2)_6$ (**2b**) leads to the formation of [Me_2Ge:], the lower cyclopolygermane analogues c-$(GeMe_2)_{n-1}$ (where n = 6,5), unidentified high-boiling products containing germanium, and compounds attributed to the accidental oxidation of the starting material **2a** or **2b** by oxygen.[52, 53] It is unclear, however, why the absorption assigned to [Me_2Ge:] generated from cyclo-$(GeMe_2)_5$ is red-shifted relative to that obtained upon its generation from cyclo-$(GeMe_2)_6$ under the same conditions[52, 53] (Scheme 3).

$$\text{c-}(GeR_2)_n \xrightarrow{\quad h\nu \quad} [:GeR_2] + \text{c-}(GeR_2)_{n-1} + \text{ side products}$$

R = Me, Ph; n = 3-6
2
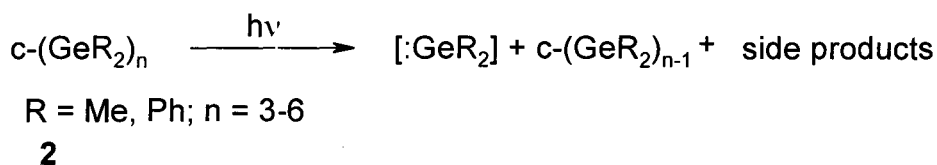
Scheme 3. Photolysis of cyclopolygermanes.

The photolysis of diarylgermetanes (**5**) yields ethylene and reactive 1,1-diarylgermenes as the major products, in addition to minor amounts of cyclopropane and the corresponding diarylgermylene (Scheme 4). [115-117]

$$R_2Ge\boxed{} \xrightarrow{\Delta \text{ or } h\upsilon} [R_2Ge{:}] \ + \ R_2Ge{=}CH_2 \ + \ C_2H_4 \ + \ \triangle$$

5
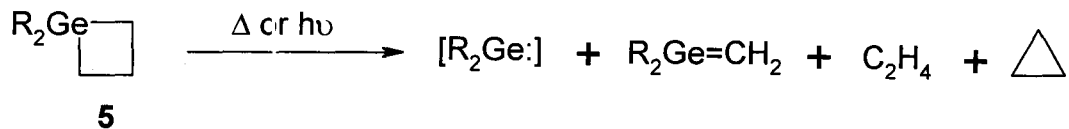
R = Aryl

Scheme 4. Thermal and/or photochemical decomposition of

diarylgermetanes (**5**).

The corresponding germenes are the only transients that can be detected in laser flash photolysis experiments with these compounds. In conclusion, the formation of co-products in the system under investigation can interfere with the signal due to the major (germylene) product, complicating the identification and study of the germylene of interest by UV-VIS spectroscopic methods.

In view of the fact that most of the precursors present in the literature are not clean sources of germylenes, the development of more reliable precursor(s) to simple germylenes is necessary if they are to be studied in a meaningful way by time-resolved spectroscopic methods. One possibility that might be used for the generation of dialkylgermylenes is the photolysis of bis(mesitylsilyl)germanes, in which the mesityl groups (Mes = 2,4,6-trimethylphenyl) serve as a chromophore, and the ortho-methyl groups block photorearrangement processes. For example, in the silylene literature it is known that photolysis 2,2-dimesityl-1,1,1,3,3,3-hexamethyltrisilane (**6**) affords dimesitylsilylene (**7**) and

hexamethyldisilane (**8**); the silylene can be readily detected and characterized by laser flash photolysis.[33] The mesityl substituent with its methyl groups in the ortho positions of the phenyl ring block the [1, 3]-silyl migration, which normally leads to the hexatriene intermediate (**9**)[33] (Scheme 5).

9   **6**   **7**   **8**
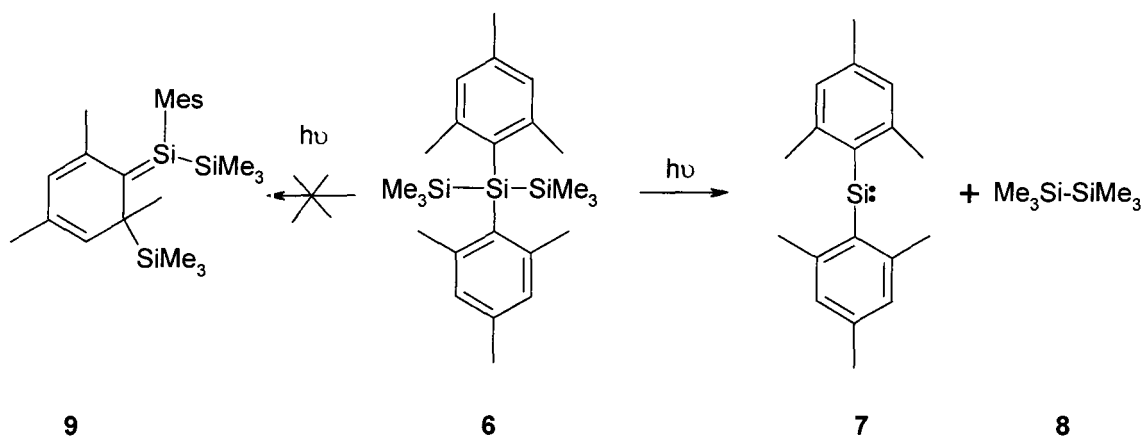
Scheme 5. Laser flash photolysis (266 nm) of 2,2-dimesitylhexamethyltrisilane (**6**) in dry, deoxygenated cyclohexane solution at room temperature.

Similarly, the analogous disilylgermane derivative (**10**) is a clean source of dimesitylgermylene.[54, 120] Laser flash photolysis (nLFP) of a solution of *bis*(trimethylsilyl)dimesitylgermane (**10**) allowed the detection of both dimesitylgermylene (**11**, λ_{max} ~ 580 nm) and its digermene dimer, tetramesityldigermene (**12**, λ_{max} ~ 420 nm) (Scheme 6).[54, 67, 114, 120]

$(Me_3Si)_2Ge(Mes)_2$ Mes = 2,4,6-trimethylphenyl

10
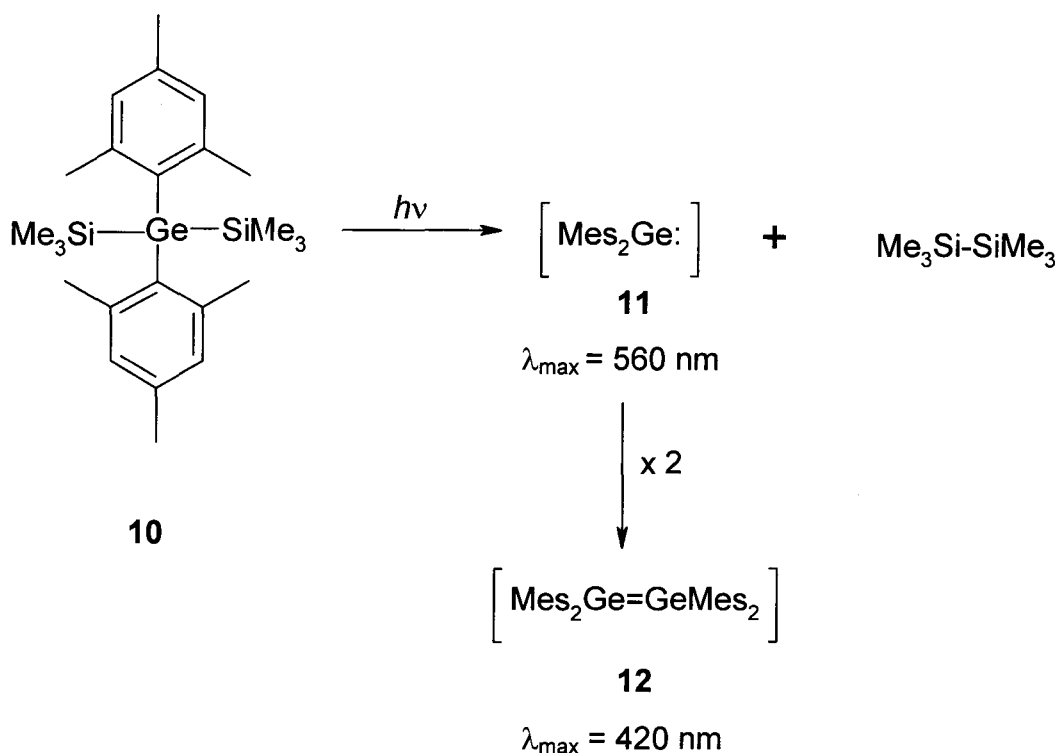
Scheme 6. Laser flash photolysis of $(Me_3Si)_2Ge(Mes)_2$ (**10**) in dry, deoxygenated cyclohexane solution at 298 K with 248 nm pulses.

Following this idea, one of our initial goals was to synthesize a potential precursor to $[Me_2Ge:]$ in the form of $Me_2Ge(SiMe_2Mes)_2$. Unfortunately, we could not overcome a number of problems that occurred in our attempts to synthesize

the target molecule. We therefore decided to shift our attention to developing an efficient photochemical precursor to phenylmethylgermylene (**29**), since the necessary synthetic chemistry is more straightforward.

Following earlier studies of [SiH$_2$:] and [SiMe$_2$:],[121] Becerra *et al.* decided to explore the UV photodecomposition of germacyclopent-3-ene (**13**)[57] and 3,4-dimethyl-1-germacyclopent-3-ene (**14**)[57, 59] as potential sources of [GeH$_2$:], and 1,1-dimethyl-1-germacyclopent-3-ene (**1a**) and pentamethyldigermane[59, 60] as sources of [Me$_2$Ge:].

R$_2$Ge⟨⟩   R = H   **13**
            R = Me **1a**

R$_2$Ge⟨⟩   R = H   **14**

3,4-Dimethyl-1-germacyclopent-3-ene (**14**) exhibits a strong UV absorption at

λ = 198 nm, ε = 3.2 x 10^3 dm^3 mol^{-1} cm^{-1},[57] and the 1,1-dimethyl-1-germacyclopent-3-ene (**1a**) at λ = 190 nm, ε = 2.1 x 10^3 dm^3 mol^{-1} cm^{-1}.[60]

End-product analysis after gas phase photolysis of the compounds at 193 nm showed that the major (hydrocarbon) photoproducts are 2,3-dimethyl-1,3-butadiene[57] from **1a** and 1,3-butadiene[60] from **13**, which accounted for ~ 70% of

the total products formed. This strongly suggests that the major

photodecomposition pathway is as follows:

R = H; R' = Me   **14**
R = Me; R' = H   **1a**
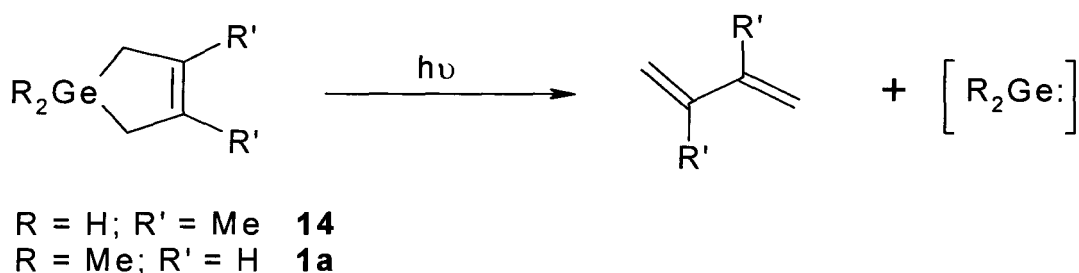
Scheme 7. Major photodecomposition pathway of **14** and **1a**.

Moreover, the transient absorption spectrum formed from **1a** and

pentamethyldigermane[59, 60] shows identical spectral features (λ = 480 nm),

indicating that a common species has been detected. This species was assigned

to dimethylgermylene.

In conclusion, these photochemical precursors extrude the corresponding

germylenes cleanly and efficiently upon photolysis in the gas phase with 193 nm

light, in amounts sufficient for their detection by time-resolved UV-VIS

spectroscopy.

Recently, our group has reported the photochemistry of the 1,1-diphenyl

analogue of **14** (**1c**).[67] The compound can be synthesized in high yield in just

three steps, and yields the expected germylene [Ph_2Ge:] in high chemical and

quantum yield. Moreover, it was shown that this molecule can easily be modified

so that other simple germylene derivatives like [Me$_2$Ge:] and [Mes$_2$Ge:] might be obtained. Flash photolysis of **1c** in dry deoxygenated hexane generated a transient assigned to [Ph$_2$Ge:] (λ_{max} = 500 nm; $\varepsilon \sim$ 1650 M^{-1}cm^{-1}) which decays with second-order kinetics. Moreover, its dimer, tetraphenyldigermene, [(Ph$_2$Ge)$_2$] is formed *via* a second order kinetic process that occurs in concert with decay of the germylene. The digermene exhibits an absorption maximum at 440 nm and lifetime $\tau \sim$ 50 μs in hexane at 23 °C.[67]

Far-UV (193 nm) laser flash photolysis of 1,1,3,4-tetramethylgermacyclopent-3-ene (**1b**)[67] yields transients assigned to dimethylgermylene (λ_{max} = 480 nm) and tetramethyldigermene (λ_{max} = 370 nm). The absorption spectrum of the initially-formed transient is in good agreement with the gas phase spectrum reported by Becerra *et al.*[59, 60]

Results consistent with literature data[54, 114, 120, 122] were also obtained upon laser flash photolysis of 3,4-dimethyl-1,1-dimesitylgermacyclopent-3-ene (**15**), which yields dimesitylgermylene (**11**, λ_{max} = 560 nm) and tetramesityldigermene (**12**, λ_{max} = 410 nm).[67]

R$_2$Ge
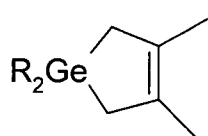
R = Ph	**1c**
R = Mes (2,4,6-Me$_3$C$_6$H$_2$)	**15**
R = Me	**1b**

As a following step the synthesis and study of a potential photochemical precursor to **29** was undertaken. The principal question we wanted to answer is: how does the reactivity of simple germylenes change upon substitution of the Ph group for Me in going from [Ph$_2$Ge:] to [PhMeGe:] and [Me$_2$Ge:]?

The major goal of this thesis was thus to contribute to the development of a consistent image of the generation, detection, reactivity and kinetic properties of simple germylenes in solution. Issues connected with the identification of the anticipated [PhMeGe:] (**29**) and its dimers, E- and Z-1,2-dimethyl-1,2-diphenyldigermene (**30**) and a study of their reactivities in solution have been addressed and will be discussed in detail.

1.2.4. Characteristic Reactions of Singlet Germylenes

Our laser flash photolysis system employs UV-VIS spectrometry as the method of transient detection, and thus gives only limited structural information on the transient species being examined. Therefore, these studies are generally accompanied by chemical trapping experiments in order to gain conclusive information on the nature of the intermediate produced. Chemical trapping experiments are carried out by photolysing the precursor in solution in the presence of a suitable scavenger, to establish that the expected trapping

products of the intermediate of interest are formed under similar conditions to those used to detect them directly. Additional confirmation of a transient assignment is obtained by the determination of absolute rate constants for reaction that the transient is known to undergo. It is also important to demonstrate a lack of reactivity toward reagents that a given transient should *not* react with.

A modified version of the scheme originally proposed by Gaspar[31] and Atwell and Weyenberg[34] can be used to describe the general chemistry of germylenes, and is shown in Scheme 8.

The germylene [RR'Ge:] after generation from its precursor, may undergo three different types of reaction with species present in the system:

(1) It may dimerize or polymerize if such reactions are kinetically favored. The dimer generally behaves as a reactive intermediate too, and it may also undergo reaction with other molecules present in the system.

(2) It may interact with the precursors if these contain reactive bonds.

(3) It may experience either insertion or addition reactions with added co-reactants. The formed adducts further undergo rearrangements to give the final product (Scheme 8).

Adducts

$[R_2Ge:]$

+precursor   insertion

Precursor $\xrightarrow{h\nu}$ $[R_2Ge:]$ $\xrightarrow{\text{+ reactants}}$ Adducts

insertion or addition

dimerize

$(R_2Ge)_n$ $\xleftarrow{\text{polymerize}}$ $[(R_2Ge)_2]$ $\xrightarrow{\text{+ reactants}}$ Adducts
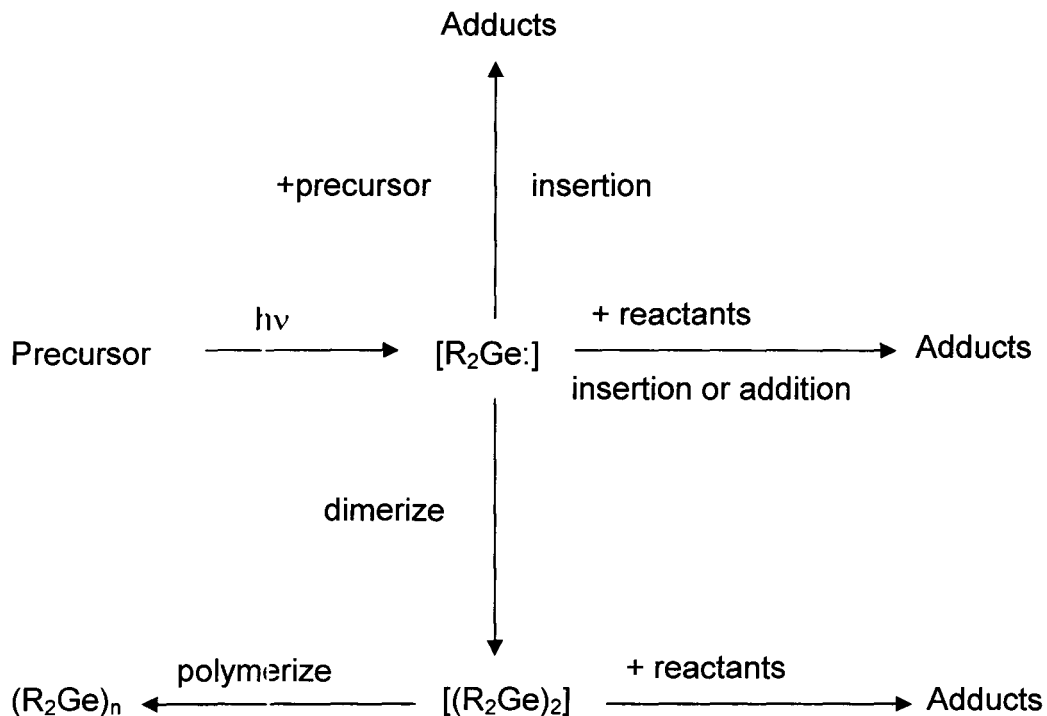
Scheme 8. The overall chemical fate of a germylene in a reacting system.

In the following subsections the chemical properties of singlet germylenes will be described in terms of four principal modes of reaction: dimerization, insertion into Si-H, O-H, C-Cl bonds, interaction with Lewis Bases and addition to alkenes and dienes (Scheme 9).

R = Me, Ph; R' = Me, Et.
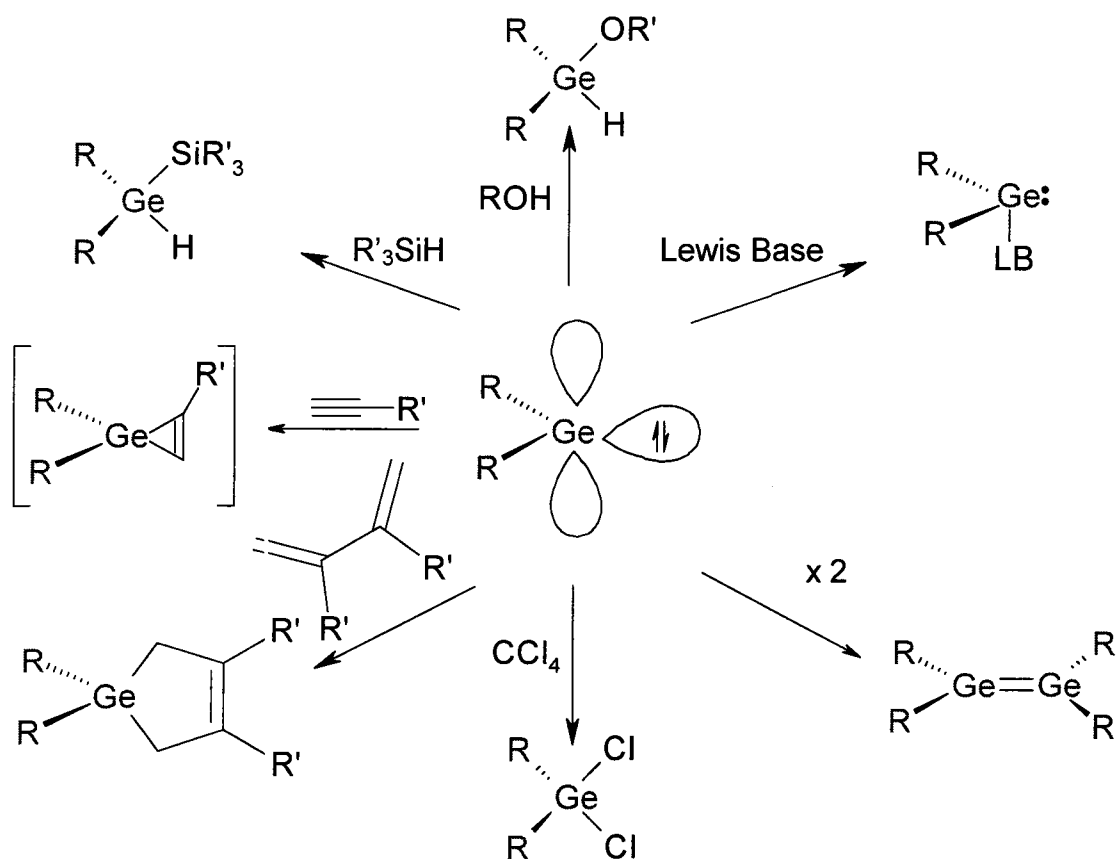
Scheme 9. Characteristic reactions of singlet germylenes.

1.2.4.1. Dimerization

Monomeric germylenes [R_2Ge:] (where R = Me, Ph, Mes) dimerize or polymerize in the absence of a trapping agent to give intermediates capable of undergoing further insertion, abstraction, and addition processes (Scheme 10).[54, 67, 123]

$$
\begin{array}{c}
\text{RR'Ge} - \text{GeRR'} \\
\text{RR'Ge} - \text{GeRR'}
\end{array}
$$

$\uparrow$ dimerization

Precursor $\xrightarrow{h\upsilon}$ $\big[\, \text{RR'Ge:} \,\big]$ $\xrightarrow{\text{dimerization}}$ $\big[\, \text{RR'Ge=GeRR'} \,\big]$

$\big[\, \text{RR'Ge} \,\big]_{2n}$ $\xleftarrow{\text{oligomerization}}$ $\big[\, \text{RR'Ge:} \,\big]$

$\big[\, \text{RR'Ge:} \,\big]$ $\downarrow$

$\big[\, \text{RR'Ge} \,\big]_{2n+1}$ $\xleftarrow{n\,\text{RR'Ge=GeRR'}}$ $\begin{array}{c}\text{RR'Ge}\\ \text{RR'Ge} - \text{GeRR'}\end{array}$

R = R' = Me; R = R' = Ph; R = Me; R' = Ph
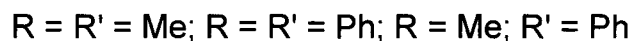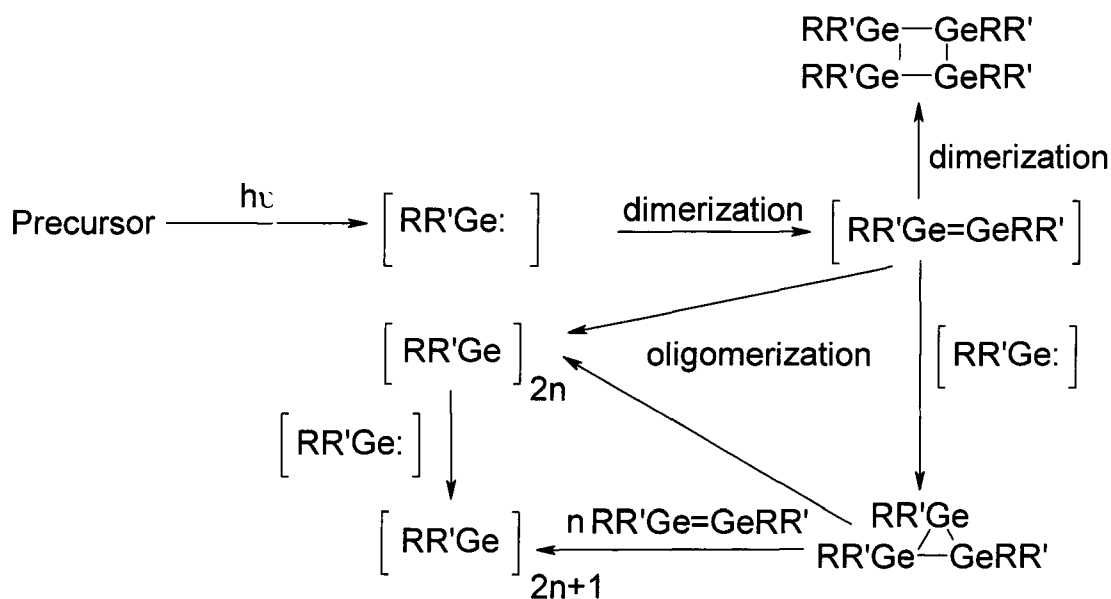
Scheme 10. Oligo- and polymerization of germylenes in the absence of trapping agents.

The results indicate that simple germylenes dimerize very rapidly with absolute rate constants comparable to the diffusion rate $k \sim 2 \times 10^{10}$ $M^{-1}s^{-1}$ in hexane solution.[27, 31, 67] The digermene can further participate in insertion, addition of another [R_2Ge:] (Scheme 4) or dimerization reactions (Scheme 4, 5). Finally, polygermanes ($R_2Ge)_n$ of undetermined structure are formed (Scheme 11).

$$[R_2Ge:] \xrightarrow{\text{x 2}} [R_2Ge=GeR_2] \xrightarrow{\text{polymerize}} (R_2Ge)_n$$
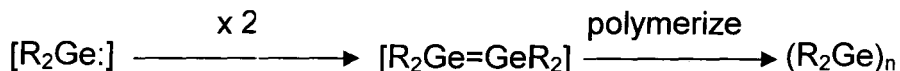
R = Me or Ph; R = Me, Ph, n = 4, 5, 6...

Scheme 11. Dimerization (polymerization) of simple germylenes.

It has been known for some time that if the substituents are large enough (e.g. 2,6-Et$_2$Ph), the only product formed is the dimer, further polymerization is suppressed, and the resulting digermene is stable.[124] Tetramesityldigermene is also stable toward oligomerization.[54] Even larger ortho-substituents stop the dimerization of the monomeric diarylgermylene; for example, bis(2,4,6-tri-t-butylphenyl)germylene has been isolated in the solid state at -10 ^{0}C.[125]

1.2.4.2. Insertion into σ bonds

The insertion of germylenes into single bonds is the best-studied type of reaction of these divalent species, and leads to the formation of stable products. As pointed out by Atwell and Weyenberg[34], in the case of silylenes the chemical bonds undergoing insertion are usually between a hydrogen atom and a more electronegative element such as oxygen or nitrogen; similar considerations apply to germylenes as well. As evidenced by experimental and theoretical studies[126] these processes often proceed by initial formation of a donor-acceptor complex, which results further to lead to the formation of the insertion product. Density

functional theoretical studies of germylene insertion into C-H, Si-H, N-H, O-H

bonds[126] show that optimal overlap between the lone-pair orbital of the

heteroatom X and the empty p orbital on germanium is achieved by an

orthogonal plane approach of the two molecules (Scheme 12).

Precursor

$\downarrow$ $h\upsilon$

[RR'Ge:]   +   X—H $\xrightarrow{\text{insertion}}$ H—RR'Ge—X

RR'Ge—X —H

R = R' = Me
R = Me; R' = Ph   X = Si, O, N
R = R' = Ph
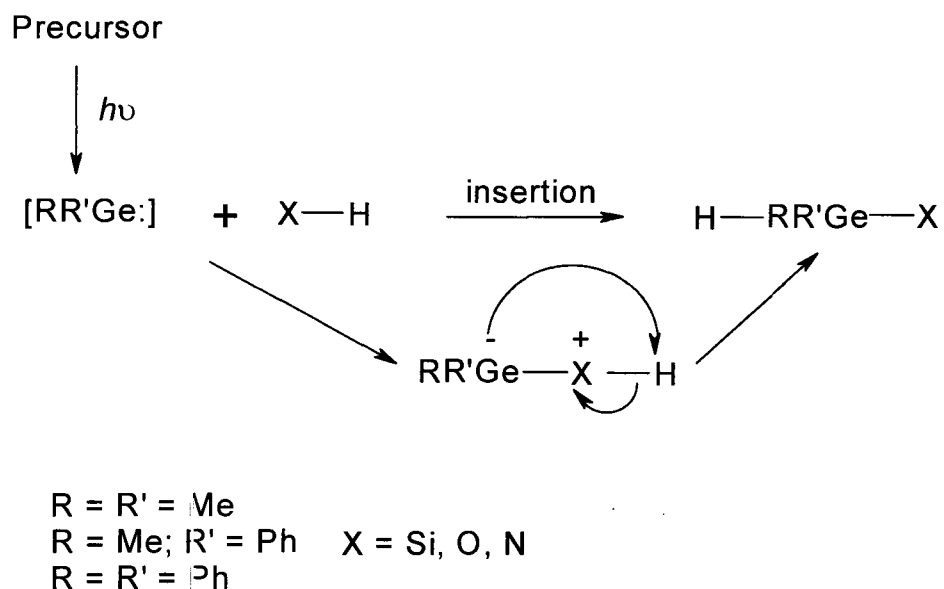
Scheme 12. Germylene insertion into X-H bonds.

Theoretical results also predict[126] that the insertion products adopt a

pentacoordinate conformation on the germanium centre. Furthermore the

calculations[126] have established that the chemical behavior of germylenes is

quite similar to that of silylenes, but unlike the behavior of singlet carbenes for

which X-H bond insertion is often concerted, this difference in the behavior of

carbenes and higher Group 14 analogues is linked to the singlet-triplet splitting,

which plays an important role in determining the activation energy of the insertion reaction.

1.2.4.2.1. Insertion into Si-H bonds

Si-H bond insertions have been employed to trap various kinds of germylenes (Scheme 13).

Precursor

$$[RR'Ge:] \quad + \quad Et_3Si-H \quad \longrightarrow \quad Et_3Si-Ge-H$$

R = R' = Me
R = R' = Ph
R = Me; R' = Ph.
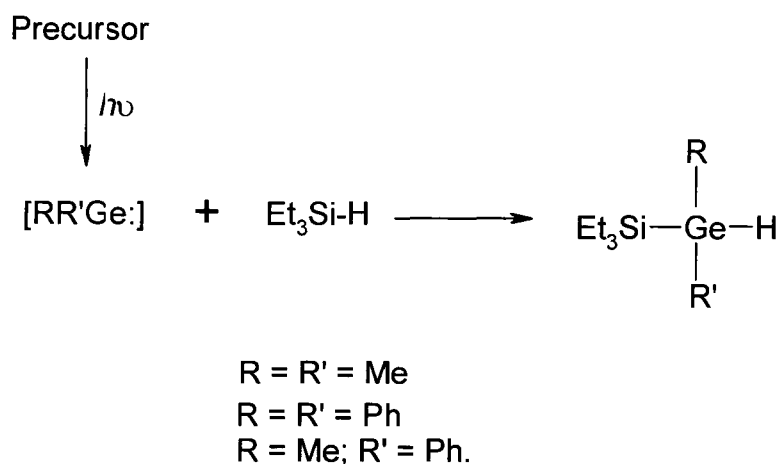
Scheme 13. Insertion of simple germylenes into the Si-H bond.

In spite of the fact that silanes (e.g. methylsilane, ethylsilane, trimethylsilane) are common scavengers, reported liquid-phase rate constants show a large degree of scatter (~ 10^4-10^6 $M^{-1}s^{-1}$) for the same germylene generated from different precursors, and demonstrate the uncertainties in the

identification of germylenes and determination of their reaction kinetics in solution.[46, 48, 60]

1.2.4.2.2. Insertion into O-H bonds of alcohols and carboxylic acids

It is known that silylenes insert into O-H bonds *via* zwitterionic donor-acceptor intermediates[31, 41, 42] which in the cases of primary and secondary alcohols undergo rearrangement to yield the formal O-H insertion products (Scheme 14).[32] Tertiary alcohols form adducts which can revert to silylenes upon warming.

Complexes of alcohols with sterically hindered silylenes were observed spectroscopically[42, 127] in annealed 95:5 3-MP/ROH matrices. The observed changes in the UV spectrum upon annealing of the matrix were dependent upon the steric bulk of the alcohol used. For ROH = EtOH or i-PrOH the intensity of the silylene band decreased as the matrix was warmed and a new band was observed to grow in. Upon further warming the new band decayed and no new bands were observed. Analysis of the resulting solution showed a quantitative conversion to the expected insertion product RR'SiH(OR). In the case of t-BuOH, upon annealing of the matrix the silylene dimerized to disilene and no trapped product was observed (Scheme 14).[42, 128]

Precursor
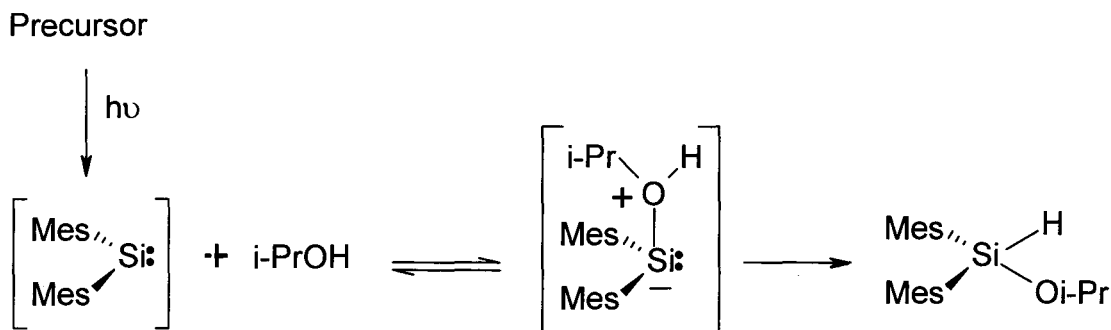
Scheme 14. Reaction of dimesitylsilylene with i-PrOH.

Although theoretical calculations have predicted a significant lifetime for the zwitterionic complex[129], the direct observation of silylene-alcohol complexes in fluid solution at room temperature has not been reported.

Few experimental and theoretical data are available which characterize the oxidation chemistry of germylenes. Mochida *et. al.*[46, 52, 53] and Konieczny *et al.*[47] studied the reaction of alcohols with germylenes. They concluded that simple germylenes [R_2Ge:] where R = Me, Ph either do not react with alcohols or they react so slowly that a rate constant cannot be established. However, the formation of alkoxygermanes from germylenes has been reported by several groups.[130-136] The UV spectra of germylene-alcohol complexes, from the reaction of several diarylgermylenes with alcohols in a 3-MP matrix at 77K were reported by Ando *et al.*[114] On the basis of their earlier results for germylene-ether complexes[114] and those obtained by Gillette *et al.*[42] for silylene-ether complexes they assigned the species with absorption maxima at 320-367 nm to germylene-alcohol complexes (Table 2).[114]

Germylenes	λ_{max} (nm)				
	EtOH	i-PrOH	n-BuOH	t-BuOH	Ref.
[Ph_2Ge:]	320	324	325	332	114
[Mes_2Ge:]	333	339	359	362	114
[Ar_2Ge:]	332	341	343	367	114

Table 2. UV Absorption maxima (nm) of germylene-alcohol complexes
in 3-MP/IP (3/7) Matrices; Ar = 2,6-diethylphenyl.

Again, evidence for the formation of germylene-alcohol complexes in fluid
solution at room temperature has never been reported.

Substituted organogermanium hydrides of the type $ROMe_2GeH$ have been
reported previously (Scheme 15).[130, 132]

$$[Me_2Ge\text{:}] + ROH \xrightarrow[70\ ^{o}C]{SiO_2} ROMe_2GeH$$
$$\textbf{16}$$
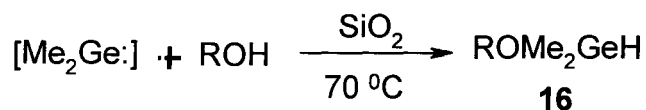
R = Me (a), $CHMe_2$ (b), CH_2Ph (c), Ph (d)

Scheme 15. Reaction of dimethylgermylene with different alcohols.

Compounds **16a-c** and organomethoxygermanes of the type $R'_2(MeO)GeH$ (**17**) are stable in solution only in the absence of base. Even gentle evaporation of the solvent generally results in rapid decomposition with release of methanol and the formation of germylenes, which condense to form polymers at room temperature (Scheme 16).[130-132]

$$\underset{\mathbf{17}}{\overset{\displaystyle R\diagdown\diagup H}{\underset{\displaystyle R'\diagup Ge \diagdown OMe}{}}} \xrightarrow[\displaystyle -MeOH]{} [RR'Ge:] \xrightarrow{\text{polymerize}} 1/n(RR'Ge)_n$$
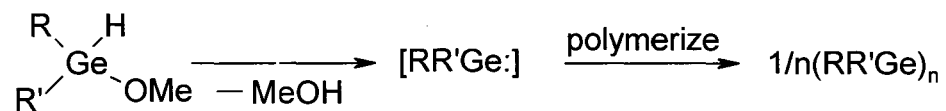
R = Me, Et, Ph; R' = X, OMe.

Scheme 16. Decomposition of organomethoxygermanes.

This decomposition is strongly catalysed by bases[130, 131], in particular methoxide ions, and can be explained by an α-elimination process (Scheme 17).
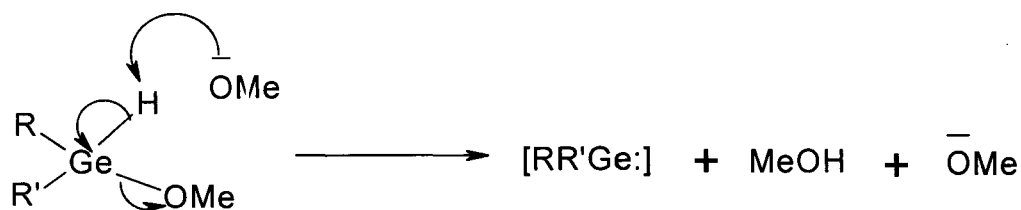
$$R = Me, Et, Ph$$
$$R' = X, OMe$$

Scheme 17. Base catalysed decomposition of organomethoxygermanes.

Stable products of insertion of [Me_2Ge:] into the more acidic O-H bonds of carboxylic acids (Scheme 18) have also been reported.[132]

Precursor

$$\downarrow h\upsilon$$

$$[Me_2Ge:] + RCOOH \longrightarrow RCOOMe_2GeH$$
17a, b
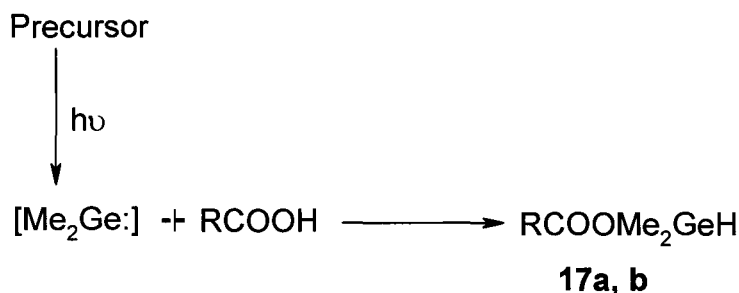
$$R = cyclohexyl (\mathbf{a}), Ph (\mathbf{b})$$

Scheme 18 Insertion into the O-H bond of carboxylic acids.

When R = cyclohexyl, **17a** can be isolated, but undergoes α-elimination (Scheme 16,17) at ~ 100 °C.[132] With R = Ph, product **17b** could be distilled at 95°C without decomposition.[132] Another example of a stable insertion product into more acidic O-H bonds is the reaction of dimethylgermylene with salicylic

acid. One equivalent of [Me$_2$Ge:] inserts first into the carboxylic acid OH bond to

give **18a**, which reacts further by insertion into the phenolic O-H bond to yield

18b (Scheme 19).[132]
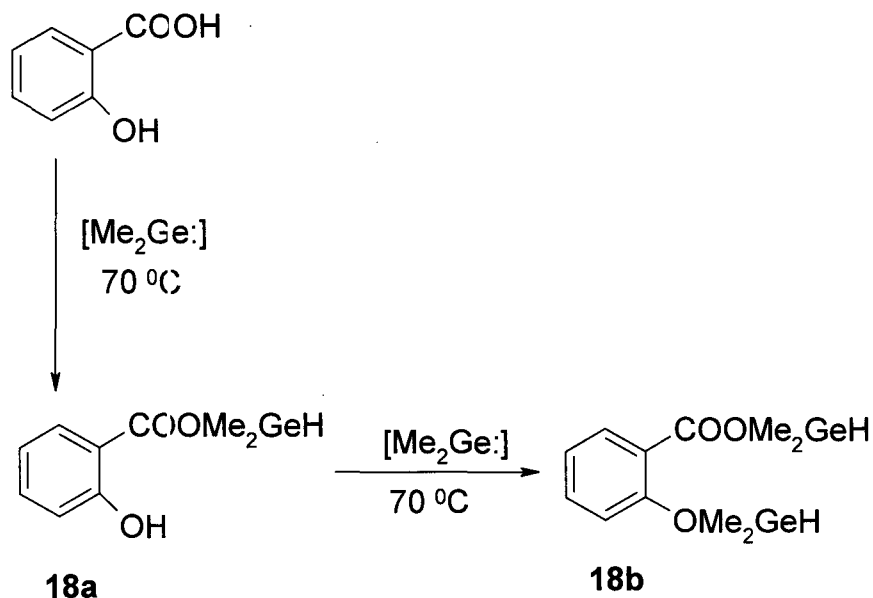
Scheme 19. Insertion of dimethylgermylene into
the O-H bonds of salicylic acid.

The reaction of ketodicarboxylic acid (**19**) with dimethylgermylene gives a

bis-acyloxygermaniumhydride, (**20**) which has been used as an intermediate in

the synthesis of vitamin D$_3$ (Scheme 20).[132]
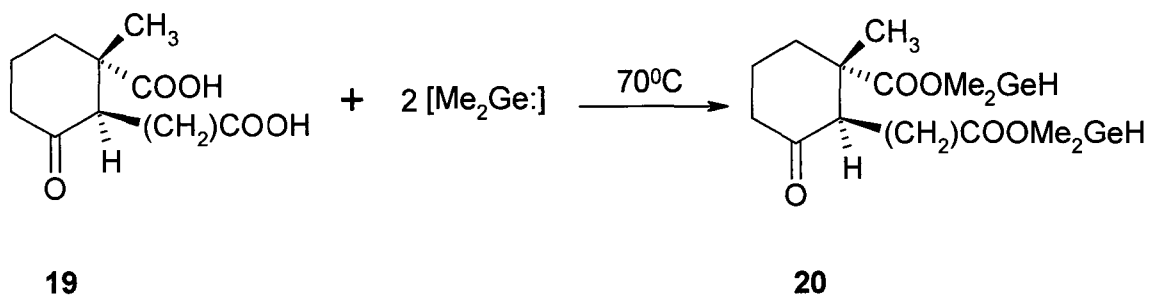
Scheme 20. Insertion of $[Me_2Ge:]$ into the O-H bond of **19**.

The measurement of absolute rate constants for the reaction of simple germylenes with AcOH has not been reported so far. Recent work from our laboratory offers for the first time information on the reactivity of simple germylenes towards AcOH, and absolute rate constants have been reported.

1.2.4.2.3. Insertion into C-Cl bonds

Insertion into C-X bonds, (X = Cl, Br, I) has been employed to trap germylenes and digermenes formed by various methods.

Dimethylgermylene inserts into the carbon-halogen bond of alkyl halides such as CCl_3X (X = Cl, Br), $PhCH_2X$ (X = Br, I), and Ph_2CHCl.[137] It was suggested that a two step radical reaction takes place, involving halogen atom abstraction followed by radical recombination.[137, 138] Absolute rate constants for the reactions of $[Me_2Ge:]$, $[PhMeGe:]$ and $[Ph_2Ge:]$ with CCl_4 were reported by Mochida *et al.*[49, 52, 53], Wakasa *et al.*[48] and Bobbit *et al.*[45], respectively.

Again, there are rather large variations in the rate constants for these reactions.[45] The results are also different from the rate constant measured in our group for [Ph$_2$Ge:], which is one order of magnitude lower than the previously reported value.[67]

The large number of products formed upon irradiation of the photochemical precursor used by Mochida's group (PhGeMe$_2$GeMe$_3$) suggests that Ge-Ge bond homolysis with the formation of germanium centered radicals is the dominant primary photoprocess, and the photoextrusion of dimethylgermylene is relatively inefficient. In the case of the photochemical precursor used by Gaspar and his group (PhGeMe$_2$SiMe$_3$), competition from [1,3]-sigmatropic rearrangement to yield a conjugated germene derivative is evident.[54] It is clear that the precursors employed for the photochemical generation of transient germylenes in solution need to be considerably better behaved than the compounds employed in earlier studies. Our recent work demonstrates that the germacyclopent-3-ene system is an ideal template from which other transient germylenes might be generated and studied in solution. The 1,1-dimesityl compound (**22**) yields [Mes$_2$Ge:] in significantly higher photochemical yields than hexamesitylcyclotrigermane (**21**), which our group has studied previously [67] Measurements of the absolute rate constants for reaction of CCl$_4$ with [Mes$_2$Ge:], generated from the two precursors are in progress in our laboratory.[67, 68] These values will represent a useful guide against which to verify

our results due to the fact that between different studies previously reported for

dimesitylgermylene, [Mes$_2$Ge:][50, 54, 114, 120] exist a good agreement.

$$\begin{array}{c} \text{Mes}_2 \\ \text{Ge} \\ \diagup \diagdown \\ \text{Mes}_2\text{Ge}-\text{GeMes}_2 \end{array}$$

21

Mes$_2$Ge
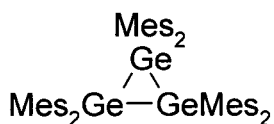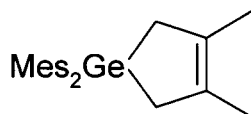
22

1.2.4.2.4. Intermolecular complexes of germylenes with Lewis bases
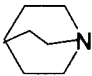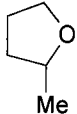
As might be expected from the earlier discussion of the reaction of

silylenes and germylenes with alcohols, these species also form Lewis acid-base

complexes with ethers, trialkylamines, trialkylphosphines, and dialkylsulphides

("LB:" Scheme 21).

R = R' = Me
R = R' = Ph   M = Si, Ge.   LB: = :OR"$_2$, :SR"$_2$, :NR"$_3$, :PR"..
R = Me; R' = Ph.
                                       LB:= Lewis Base.
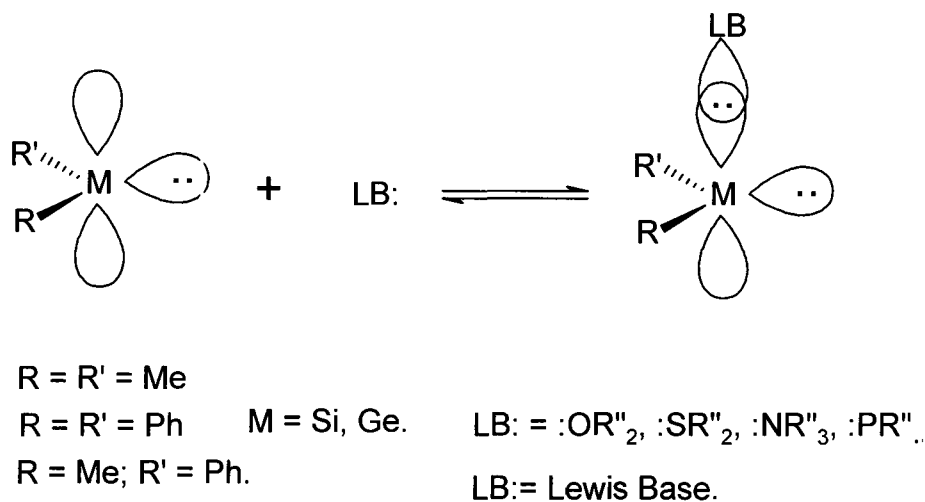
Scheme 21. Lewis acid-base complexes with diorganogermylenes and -silylenes.

Spectroscopic characterization of complexes of diorganogermylenes with heteroatom-containing substrates has been carried out in hard and soft matrices.[114, 120] These Lewis acid-base complexes are analogous to those observed in the case of silylenes,[41, 42, 128, 139] for which there is significant variation in the position of the UV absorption maximum with substitution at the metallylene centre and with the n-donor atom. Absorption bands due to the complexes of germylenes with compounds containing P, N, O and S atoms were observed from 306 to 376 nm,[114, 120] similar to those obtained for silylenes of similar structure (Table 3).[42]

Reagent	Medium	$\lambda_{max}[RR'Ge]$ (nm)				
		Ph_2Ge	Mes_2Ge	Ar_2Ge	Ar'_2Ge	Ref.
Bu_3P		-	306	314	334	114, 120
[structure] N		334	349	356	363	114, 120
Me_2S	3-MP/IP (3/7) 77K	326	348	357	357	114, 120
[structure] O Me		325	360	369	376	114, 120

Ar = 2,6-diethylphenyl   Ar' = 2,4,6-triisopropylphenyl.

Table 3. Absorption maxima (nm) of diorganogermylene complexes with Lewis bases.

The absorption bands due to the germylene complexes are shifted to shorter wavelengths compared to those of the corresponding free germylenes.[114, 120] The positions of the absorption maxima of these complexes have been suggested to provide an indication of the strength of the acid-base interaction between the germylene and the donor.[114] The stronger the interaction of the lone pair electrons of the Lewis base with the empty p-MO of the germylene the more stable is the complex, the higher is the energy of the LUMO in the complex, and the larger is the hypsochromic shift of the complex relative to that of the free germylene. In the case of silylenes it was suggested that the strength of these

complexes decreases in the following series of n-donors: amines > phosphines > ethers > sulfides.[140] The experimentally observed shifts in the absorption maxima of such complexes of germylenes with heteroatom-containing substrates (Table 3 and Figure 8) do not follow uniformly the mentioned trend.[114, 120]

23   **24**   **25**   **26**
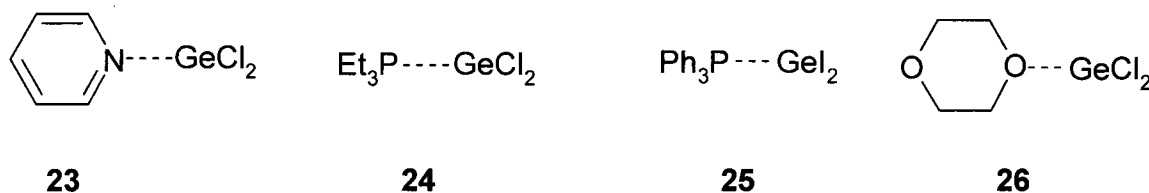
Figure 8. Examples of dihalogermylene complexes with Lewis bases.

1.2.4.2.5. Addition to olefins and dienes

Insertion and addition are two of the most important reactions of carbenes and their higher Group 14 analogues. While the most convenient method for trapping carbenes involves their addition to the double bonds of olefins to yield cyclopropane derivatives, the corresponding reaction of silylenes and germylenes is complicated by the fact that most sila- and germacyclopropanes are relatively unstable species that undergo secondary reactions. With the exception of conjugated dienes, addition reactions to C-C unsaturated bonds are rarely clean and straightforward.

The results reported in the literature demonstrate that singlet silylenes and germylenes resemble closely the carbenes in their addition to olefins and conjugated dienes. Silylenes, like singlet carbenes, have been shown to undergo stereospecific addition reactions with olefins, leading to the formation of three membered rings.[141-145]

Furthermore, they add to terminal and internal alkynes, forming a multitude of four-, five-, and six membered germanocycles.[27, 146-150] Depending on substituents and reaction conditions, germanium heterocycles containing one, two or even three germylene units, or acyclic germanium compounds were obtained, or nothing at all. It was assumed that the formation of a germirene[27, 146-148] represents the first step, but this has not been clearly demonstated so far. Dimerization or polymerization of the germylene is in most cases competitive with the formation of addition products.

Another major difference between silylenes, germylenes and carbenes is the addition to dienes. Carbenes usually undergo [1+2]-addition to yield vinylcyclopropanes,[89] while the major products from silylenes or germylenes are usually five-membered rings.[36, 40, 45, 151-159] Concerted [1+2]-*cis*-addition seems to be the rule,[45, 154, 159, 160] but the resulting vinylmetalliranes are much less stable, and rearrange fairly rapidly to the corresponding 1-metallacyclopent-3-ene isomer (Scheme 22).[36, 154]

Precursor
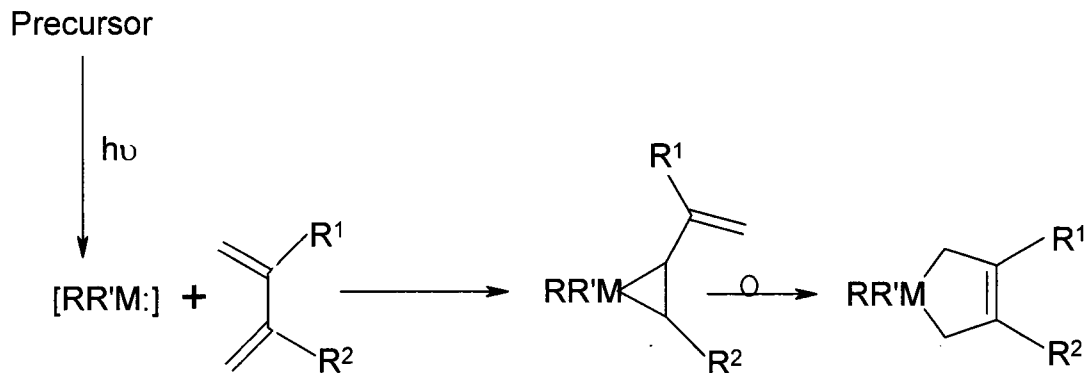
Where M = Si,Ge;

R = R' = Me, Ph; R = Me; R' = Ph; R^1 = R^2 = H, Me.

Scheme 22. Addition of silylenes and germylenes to butadiene (s).

The reported liquid-phase rate constants for reaction of germylenes with dienes also show a large scatter (from 10^4-10^9 $M^{-1}s^{-1}$).[45-49, 52, 53]

1.3 Objectives of this Work

The majority of the studies cited in the literature have produced convincing arguments for the formation of transient germylenes in solution. However, the spectroscopic data and reaction rate constants reported for these species from different precursors shows little consitency from one study to another. It has been suggested that this problem is due to the fact that the arylated oligogermane or disilylgermane precursors that have usually been used for their generation do not represent clean and highly efficient sources of simple germylenes. Upon irradiation they generate not only the germylene of interest but transient germanium centered radicals and conjugated germene intermediates, which absorb strongly in the same spectral region (400-500 nm) where the germylenes of interest are expected to absorb. Obviously, interference from these products may well influence the measurement of the absolute rate constants as well.

A major focus of our group in recent years has been to resolve those discrepancies by the development and study of a class of clean and efficient photochemical precursors to simple germylenes, to allow the study of these species in solution by laser flash photolysis techniques. The first such molecules (**1b, 1c**) proved to be outstanding, and have allowed unequivocal spectra of [Ph_2Ge:] and [Me_2Ge:] and the digermene dimers to be measured in solution for the first time.

The goal of my work was to extend this previous work to **28**, a proposed photochemical precursor for [PhMeGe:] and its corresponding digermene dimers. This work has involved the synthesis and characterization of **28**, steady state trapping studies of its photochemistry in solution, and a study of the UV-VIS spectra and reactivity of [PhMeGe:] and **30** toward selected germylene/digermene scavengers.

CHAPTER 2

RESULTS AND DISCUSSION

2.1. Photochemical Precursors of Phenylmethylgermylene and 1,2-Dimethyl-1,2-diphenyldigermene

At present in the literature, there are reported three photochemical sources for the generation of phenylmethylgermylene (**29**) and its dimer, 1,2-dimethyl-1,2-diphenyldigermene (**30**): the 7-germanorbornadiene derivative **3b**[114], the substituted trigermane **4b**[46, 48] and a polygermane (PhMeGe)$_n$ with (M_w = 5.0 x 10^3, M_n = 3.6 x 10^3)[49]. Unfortunately, this work is characterized by little consistency in the spectroscopic properties and reactivity of **29** towards different trapping agents. Consequently, we have focused our efforts on the synthesis of a versatile class of compounds for the photochemical generation of simple germylenes, in particular **29**.

Recent research in our group has led to the synthesis of **1c** along with the first measurements of the spectroscopic properties and absolute reactivities of diphenylgermylene and its dimer, tetraphenyldigermene in solution. Building on these results, we developed the goals of the work described in this chapter:

- to prepare a clean and highly efficient photochemical precursor to **29**;

- to measure UV-VIS absorption spectra of **29** and its corresponding digermene **30**,

- to measure absolute rate constants for reaction of **29** and **30** with different scavengers.

Another goal was to compare the spectroscopic properties and absolute reactivities of **29** with those of other germylenes, to see whether a consistent trend exists in going from [Ph_2Ge:] to [Me_2Ge:] *via* [PhMeGe:]. Moreover, the results should allow us to make comparisons between the spectroscopic properties and reactivities of simple germylenes and the homologous silylenes.

2.2. Synthesis of 1,3,4-Trimethyl-1-phenyl-1-germacyclopent-3-ene (28)

1,3,4-Trimethyl-1-phenylgermacyclopent-3-ene (**28**) was synthesized in 70% overall yield by the route shown in Scheme 23.

The first steps involve synthesis of $GeCl_2$-dioxane from germanium tetrachloride and 1,1,3,3-tetramethyldisiloxane in the presence of 1,4-dioxane (82%), followed by reaction of that product with 2,3-dimethyl-1,3-butadiene to obtain 1,1-dichloro-3,4-dimethyl-1-germacyclopent-3-ene (**27**) in 93% yield. The next two steps involved the sequential addition of PhMgBr and MeMgBr to **27** in diethyl ether. The final product (**28**) was purified to >99% (GC) purity by vacuum distillation and column chromatography, and identified by analytical and spectroscopic methods (^{1}H NMR, ^{13}CNMR, GC, GC/MS, FTIR). Our results are in

excellent agreement with analytical and spectroscopic data previously reported by Bobbitt et al.[45]
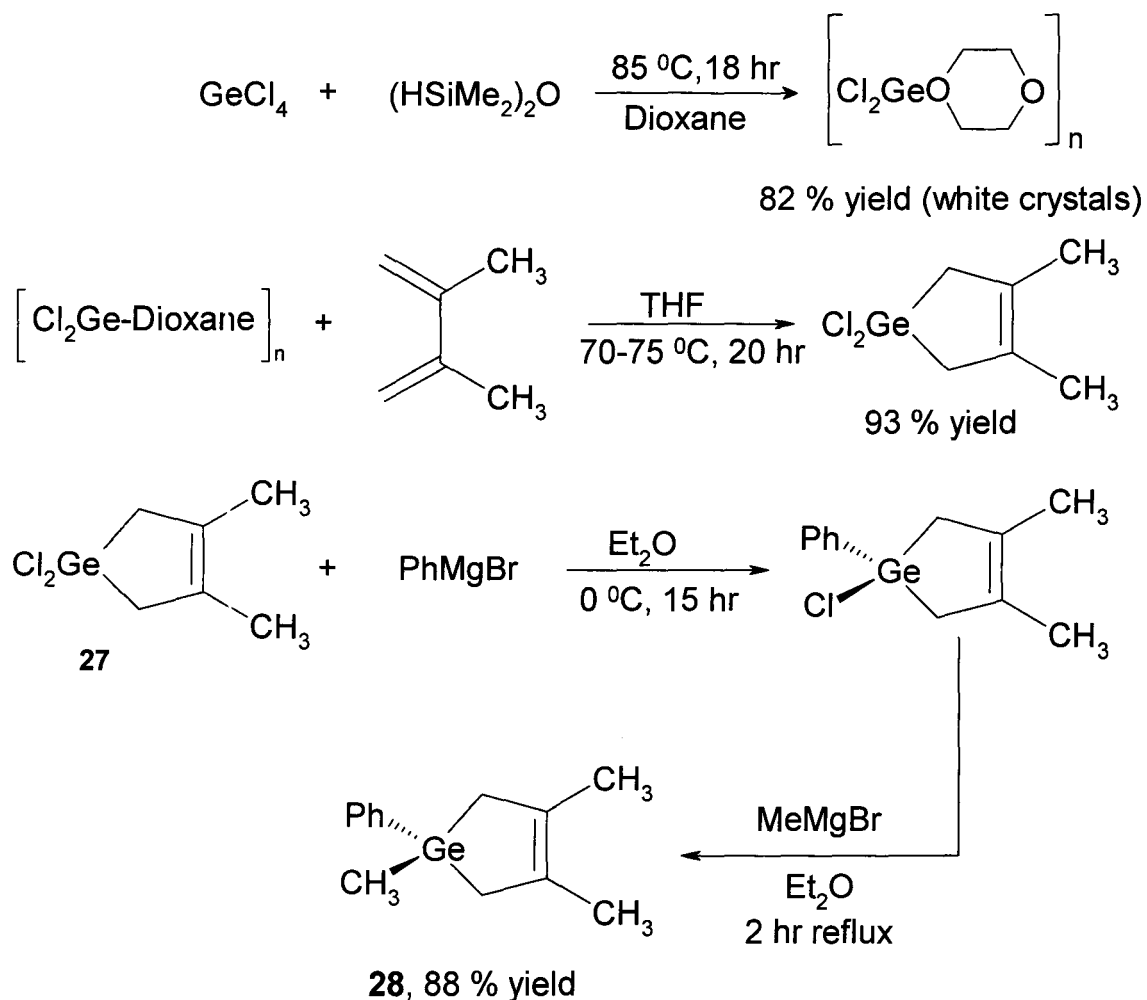
Scheme 23. Synthesis of 1,3,4-trimethyl-1-phenyl-1-germacyclopent-3-ene (**28**).

2.3. Steady State Photolysis of 1,3,4-Trimethyl-1-phenyl-1-germacyclopent-3-ene (28) in the presence of Isoprene

Steady-state photolysis of an argon saturated hexane solution of **28** (0.025 M) containing an internal standard (*n*-dodecane) and 0.1 M isoprene, with low pressure mercury lamps (254 nm) in a merry-go-round apparatus, led to the formation of 2,3-dimethyl-1,3-butadiene (**DMB**) and the expected germylene-trapping product, 1,3-dimethyl-1-phenyl-1-germacyclopent-3-ene (**31**; see Scheme 24).
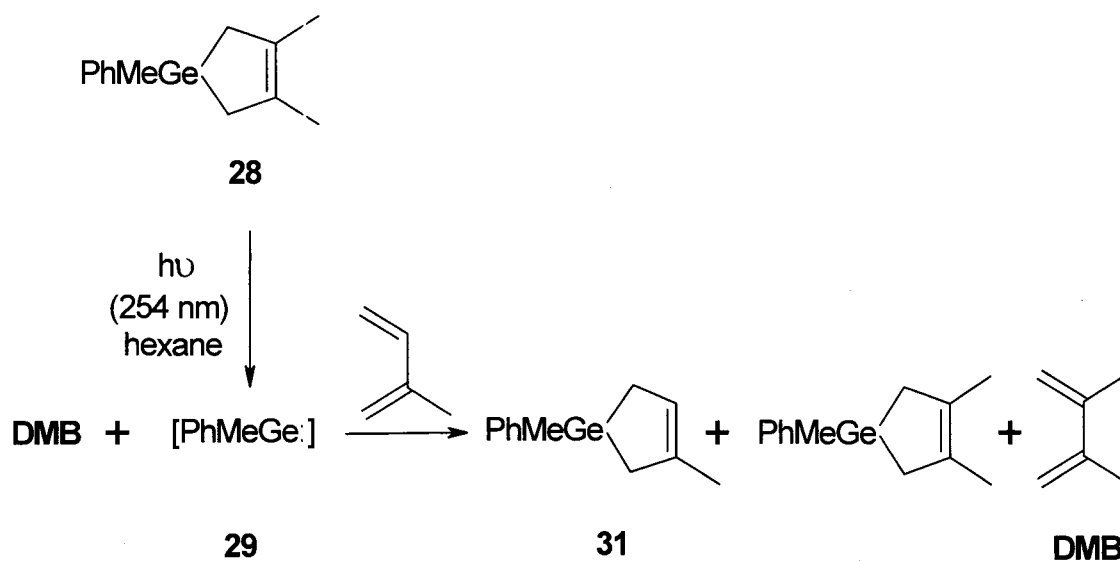
Scheme 24. Steady-state lamp (254 nm) photolysis of **28** in dry, deoxygenated hexane solution in the presence of (0.1 M) Isoprene.

GC analysis of the crude photolysate indicated that the trapping product, **31**, was exclusively formed in a chemical yield exceeding 96% at conversions below *ca.* 20%. The product was identified by comparisons with an authentic sample, prepared in an analogous fashion as **28**. The identity of **31** as the photoproduct from **28** was verified by co-injection of the crude photolysed product with the authentic sample on two different GC columns (see Figure 9).
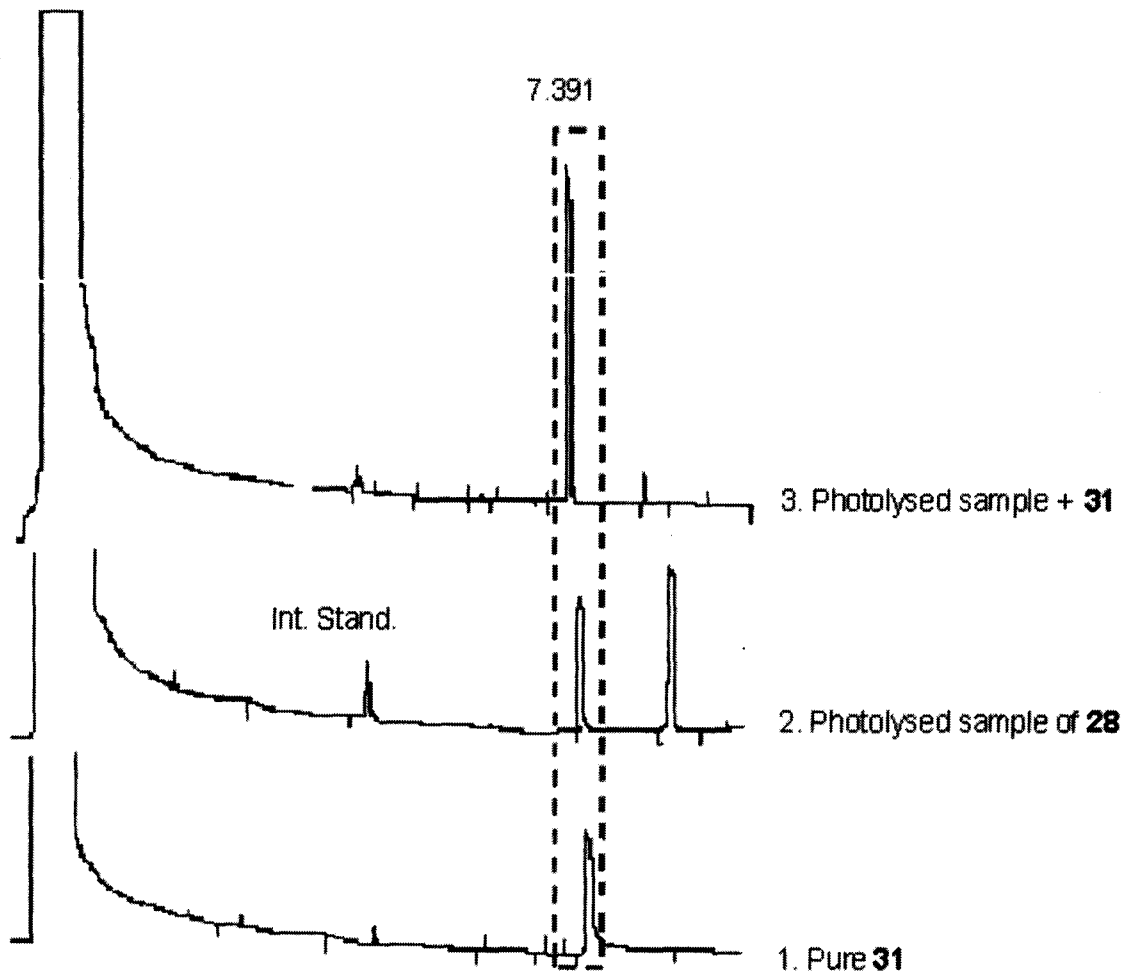
Figure 9. GC analysis of the pure, crude photolysed and co-injected (crude photolysed and authentic) sample in hexane solution in the presence of an internal standard (n-dodecane).

Plots of [31] / [Int.Std.] and [28] / [Int.Std.] / versus time from the lamp photolysis (254 nm) experiment are shown in Figure 10. The conversion of 28 to 31 was monitored by GC.
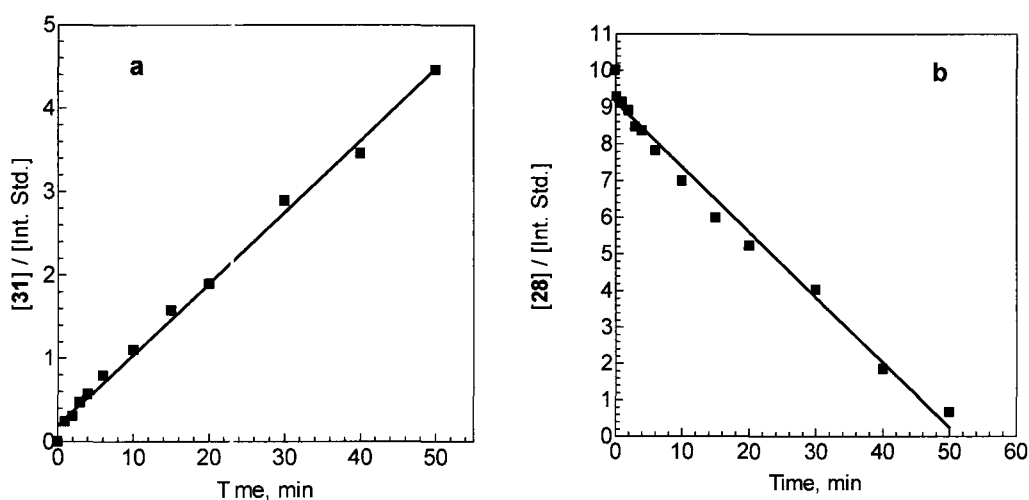
Figure 10. Photolysis of 28 (0.025 M) with 0.1 M Isoprene in dry, deoxygenated hexane solution at room temperature. (a) [31] / [Int. Std.] vs. time; (b) [28] / [Int. Std.] vs. time.

The mechanism for the reaction of germylenes with dienes has been the subject of considerable debate.[45, 153, 159, 160] Atwell and Weyenberg[158, 161, 162] in 1968-73 proposed the formation of a vinylsilirane intermediate (32) in the reaction of silylenes with 1,3-dienes. This intermediate undergoes a rearrangement to the final product, the corresponding 1-silacyclopent-3-ene derivative (Scheme 25).[36, 151, 152, 163, 164]

Precursor
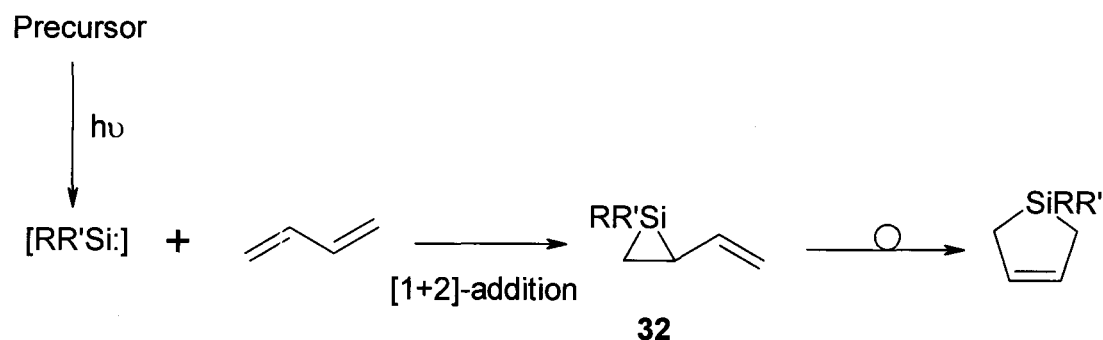
R = R' = Me, Et, Ph or combination of these substituents.

Scheme 25. Addition of silylenes to 1,3-butadiene.

Considerable experimental evidence, based on trapping experiments[152] and the formation of other kinds of end-products *via* competing reactions of the initial 1,2-adduct[36, 151, 152, 163, 164] were accumulated before the isolation of a vinylsilirane intermediate by Zhang and Conlin.[155]

By analogy with the behavior of silylenes, Bobbitt *et al.*[45, 157], Lei *et al.*[165], Becerra *et al.*[60] and Neumann *et al.*[27, 153], concluded that in the case of singlet germylenes the [1+2]–addition occurs first and the unstable intermediate rearranges to the final [1+4]–adduct. The isomerization is likely to be fast and therefore unaffected by the presence of a scavenger at low concentrations.

Ab initio calculations[166] suggest that germiranes are less stable than siliranes, which has been confirmed by the results of Becerra *et al.*[60]

We suggest a similar pathway for the reaction of **31** with isoprene:

[1+2]-addition with the formation of a three-membered ring followed by rearrangement to the final [1+4]-adduct (see Scheme 26).
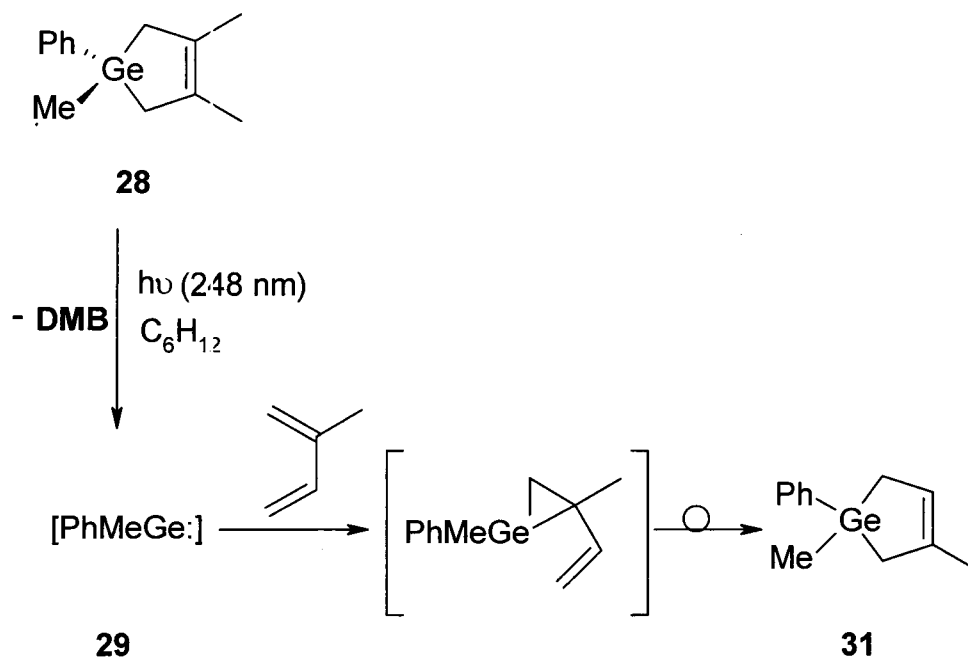
Scheme 26. Proposed stepwise addition of **29** to isoprene with the formation of **31**.

It is noteworthy that the results for **28** are analogous to those found previously for the photolysis of **1c** in the presence of isoprene.[67, 68]

2.4. Steady State Photolysis of 1,3,4-Trimethyl-1-phenyl-1-germacyclopent-3-ene (28) in the presence of Methanol

Photolysis of argon-saturated cyclohexane-d_{12} solutions of **28** (0.05 M) in the presence of MeOH (0.5 M) with low-pressure mercury lamps (254 nm) led to the formation of 2,3-dimethyl-1,3-butadiene (**DMB**) and the germylene trapping product, methoxymethylphenylgermane (**33**) (Scheme 27).
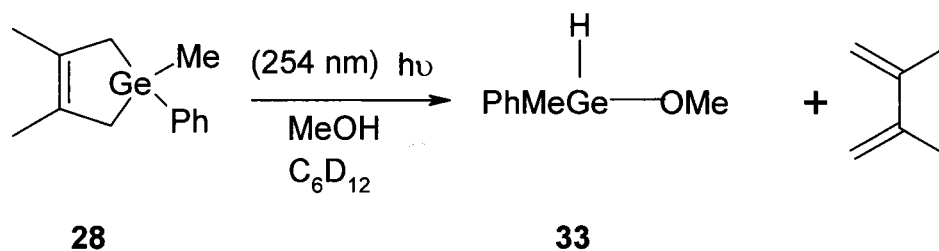
Scheme 27. Lamp (254 nm) photolysis of **28** in the presence of 0.5 M MeOH in C_6D_{12} solution at room temperature.

The identity of **33** was established by (600 MHz) ^{1}H NMR spectroscopy (Fig. 11 and the experimental section) and GC\MS analysis of the crude reaction mixtures.
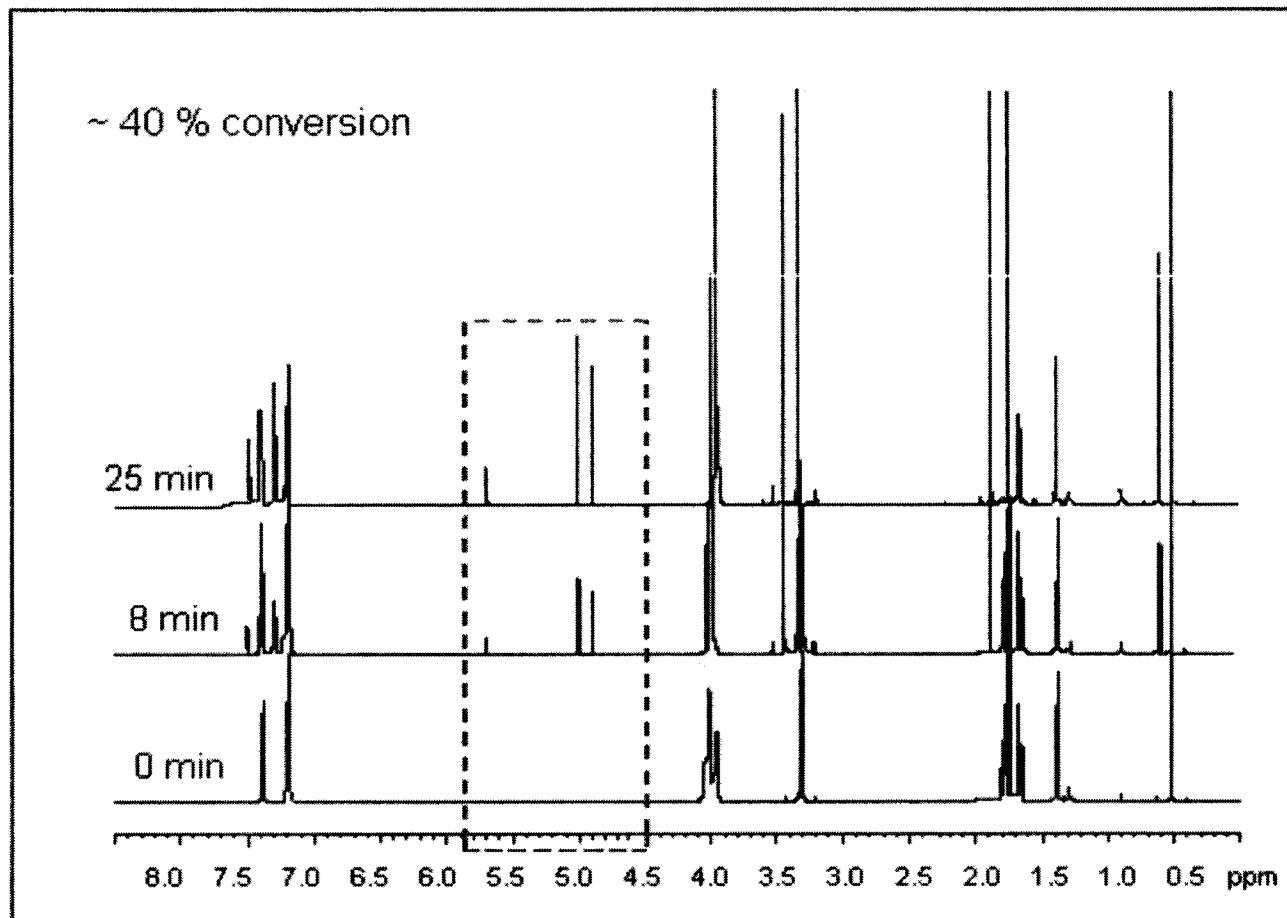
Figure 11. Lamp photolysis (254 nm) of a solution of 28 in deuterated benzene containing 0.5 M MeOH. The expected trapping product, 33 was identified by 1H (600 MHz) NMR spectroscopy.

The spectroscopic data for **33** can be compared to those reported previously for the analogous product of photolysis of **1c** in the presence of MeOH,[68] and other reported data.[130-133, 136] Figure 11 shows that the signal assigned to the Ge-H in **33** occurs at δ = 5.7 ppm, which is similar to the corresponding Ge-H formed in the spectra of Me$_2$GeHOMe, **34a** (δ = 5.20 ppm, in C$_6$D$_6$)[132] Ph$_2$GeHOMe, **34b** (δ = 6.22 ppm, in C$_6$D$_6$)[67], Mes$_2$GeHOMe, **34c** (δ = 6.67 ppm, in C$_6$D$_6$).[29] Figure 11 shows also that in the absence of MeOH at 0 min no signal due to the Ge-H or diene was observed, but after 8 min and 25 min at ~ 40 % conversion, the signals due to the Ge-H and diene grow in and are clearly evident. Furthermore, the spectra show peaks at δ = 0.6 ppm and δ = 3.45 ppm, which compare favorably to the GeMe and GeOMe resonances, respectively, in methoxydimethylgermane, **34a** (δ = 0.24 ppm and δ = 3.30 ppm in C$_6$D$_6$). [132, 130]

$$\overset{\displaystyle H}{\underset{\displaystyle R_2Ge}{|}}\!\!-\!\!-\text{OMe}$$
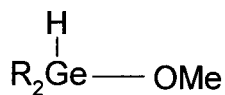
34

a. R = Me; **b.** R = Ph; **c.** R = Mes.

As can be seen from Figure 11, the photolysis is quite clean, with no evidence for the formation of other products in yields greater than *ca.* 5 % after ~ 40 % conversion of **28**.

2.5. Direct Detection and Identification of Phenylmethylgermylene and 1,2-Dimethyl-1,2-diphenyldigermene by Laser Flash Photolysis

Laser flash photolysis of continuously flowing, deoxygenated solutions of **28** (*ca.* 9 mM) in dried hexane (Na/K amalgam) with the pulses from a KrF excimer laser (248 nm, *ca.* 25 ns, 100 ± 5 mJ) leads to the formation of two transient species. The behavior observed is illustrated in Figure **12a**, in the form of transient absorption spectra recorded for the solution in point-by-point fashion throughout selectable time windows after the laser pulse, in this case 96-218 ns and 3.4-3.6 μs, respectively. The first transient is formed with the pulse and exhibits an absorption maximum at λ_{max} = 490 nm; its lifetime is ~ 2 μs. The other is much longer-lived and exhibits λ_{max} = 420 nm; it grows in over the first *ca.* 1μs and then decays with mixed first- and second-order kinetics and a lifetime of ~ 8 μs. The absorption due to this second intermediate overlaps partially with that of the initially formed transient. Typical transient decay/growth profiles recorded at 420 nm and 490 nm are presented in Figure **12b**.
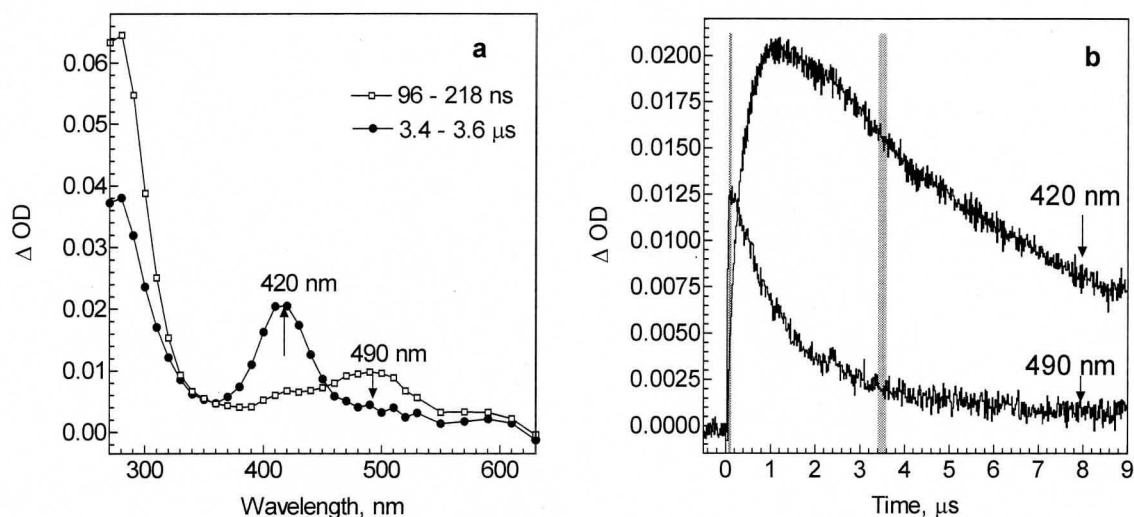
Figure 12. **a**) Transient absorption spectra generated by laser flash photolysis of **28** in dried, deoxygenated hexane solution at 23 ^{0}C. **b**) Typical transient decay/growth profiles recorded at 420 nm and 490 nm, respectively.

Traces recorded at 510 nm and 410 nm were *ca.* 20% and 30% weaker respectively, than those recorded at 490 nm and 420 nm, but the degree of overlap is lower. A representative decay trace recorded at 510 nm is shown in Figure 13.It fits well to the expression of Equation 1 for second-order decay, leading to a value of k_{decay} = (1.37 ± 0.01) x 10^5 s^{-1} for the second-order rate coefficient.

$$\Delta (OD)_t = \Delta (OD)_\infty + \Delta (OD)_0 / (1 + 2k[PhMeGe:]_0\, t) \qquad (1)$$
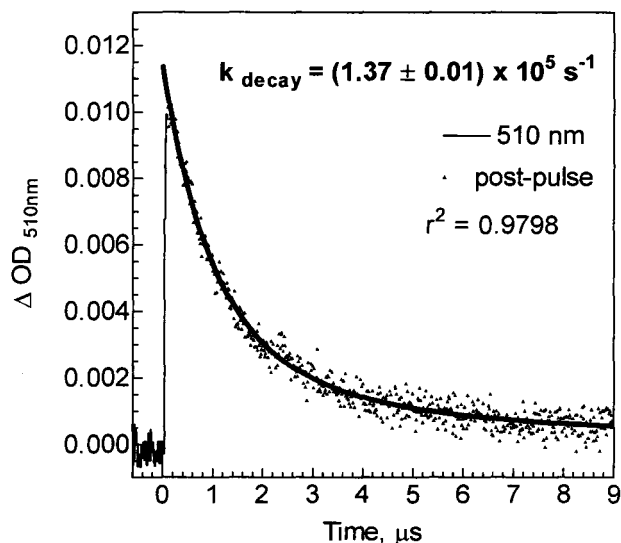
Figure 13. Decay trace profile of **29**, generated by laser flash photolysis of a *ca.* 9 mM solution of **28** in dried, deoxygenated hexane solution at 23 ^{0}C recorded at 510 nm; it fits well to the Equation (1) for a second-order decay kinetics; solid line represent the best fit of the data to a second order exponential decay.

In view of the fact that the 420 nm transient grows in on a similar time scale as the decay of the 490 nm species, we suggest that the latter is formed from the former *via* a second order kinetic process. Thus, we assign the first transient, formed right after the laser pulse with λ_{max} = 490 nm to **29**, and the subsequently formed species with λ_{max} = 420 nm to the corresponding 1,2-dimethyl-1,2-diphenyldigermene (**30**).

These assignments are not consistent with those reported by other workers for the same species,[46, 48, 49, 51, 114] but our confidence that the observed transients are **29** and **30** is based on the reasonable agreement between their

absorption maxima and those obtained in our laboratory for other simple germylene and digermene derivatives (Table 4).[67, 68]

R	R'	λ_{max}RR'Ge (nm)	λ_{max}RR'Ge=GeRR' (nm)	Ref.
Me	Me	480	370	67
Ph	Me	490	420	this work
Ph	Ph	500	440	67, 68
Mes	Mes	560	410	67

Table 4. UV-VIS absorption maxima of simple germylenes and digermenes in dry, deoxygenated hexane solutions at 23 ^{0}C.

Table 4 shows also the effect of substituent on the n-p transition. The introduction of aryl groups on germanium results in small red shifts compared to [Me$_2$Ge:]. The following series demonstrate this point: [Me$_2$Ge:] (480 nm) < [PhMeGe:] (490 nm) < [Ph$_2$Ge:] (500 nm) < [Mes$_2$Ge:] (560 nm). Much larger red shifts are observed in the spectra of the corresponding digermenes (Table 4).

Comparison of the values of the absorption maxima for simple germylenes[54, 67, 68] and silylenes[33, 41, 167-169] of identical substitution provides good additional support for these assignments (Table 5).

R	R'	$\lambda_{max}RR'Si$ (nm)	Ref.	$\lambda_{max}RR'Ge$ (nm)	Ref.
Me	Me	460	41, 167-169	480	67
Ph	Me	480	37	490	this work
Ph	Ph	495	167	500	67, 68
Mes	Mes	580	33	560	54, 67, 68

Table 5. Comparison of UV-VIS absorption maxima of simple silylenes and germylenes of identical substitution in hydrocarbon solvents at room temperature.

On the basis of all these results, it is reasonable to assume that the intermediate with λ_{max} = 490 nm is **29** and the transient with λ_{max} = 420 nm is **30** (Scheme 28).
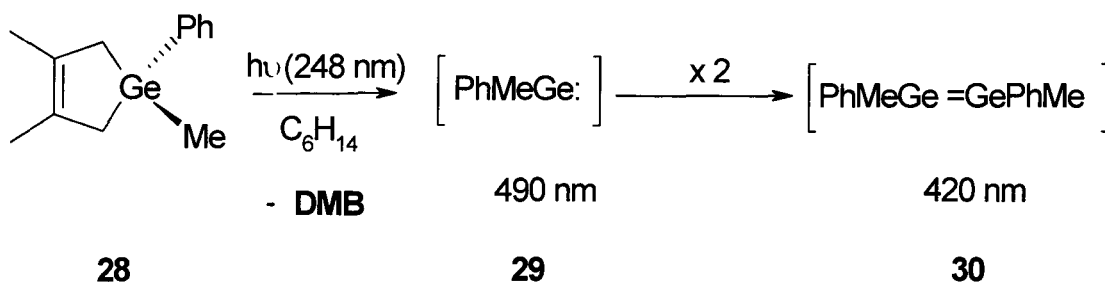
Scheme 28. Laser flash photolysis (248 nm) of **28** in dried, deoxygenated hexane solution at 23 °C.

Figure 12**b** shows that the dimer, **30** is not stable over the timescale during which is formed and consequently a quantitative agreement between the germylene decay and its dimer growth kinetics cannot be expected.

The UV-VIS spectra of both transients observed from photolysis of **28** shows a distinct, significantly more intense band centered at *ca.* 280 nm. Similar features are observed in the transient absorption spectra of diphenylgermylene and tetraphenyldigermene.[67] These are most reasonably assigned to the $S_0 \rightarrow S_2$ transitions in **29** and **30**; however, we are less confident of the latter assignment because absorptions in this region have not been studied over an extended time scale.

As was previously observed,[67] accurate and reliable data can be obtained only when the experiments employed scrupulously dry solvents and glassware and deoxygenated conditions. With **28**, the strongest signals are obtained using hexane that had been dried by distillation from sodium/potassium amalgam.[67] It was demonstrated that the use of untreated HPLC-grade hexane ([H_2O] ~ 1.5 mM) as a solvent afforded signals due to [Ph_2Ge:] and its dimer which are ~ 45% and ~ 65 % weaker respectively, compared to those recorded in the dried solvent.[67] In our case, an experiment performed using glassware which was not dried enough showed roughly 20% and 40% weaker signals due to **29** and **30**, respectively, compared to experiments carried out with oven-baked glassware and sample cells. These results indicate that the initially formed intermediate in

the photolysis reacts with water or other hydroxylic impurities, resulting in a reduction in the intensities of the recorded signals observed for both species. Indeed, such behavior was suggested by Klein *et al.* in 1993[132], for [Me_2Ge:], generated photochemically from a 7-gemanorbornadiene precursor in wet benzene. Moreover, Ando *et al.*[114] have reported UV spectroscopic evidence for diarylgermylene-aliphatic alcohol complexes in low temperature matrices, where they absorb in the 320-367 nm regions.

2.6. Irreversible Scavengers

Following the main objectives of this thesis we have to investigate the reactivity of **29** and **30** in hydrocarbon solution with different scavengers. Based on the behavior observed the various reactions that were studied can be classified as either irreversible or reversible.

2.6.1. Acetic acid as a quencher

We presented above laser flash photolysis evidence for the occurrence of dimerization when **29** is generated in solution in the absence of an added trapping agent. Convincing evidence for the formation of the species of interest

(the germylene) upon photodecomposition of the chosen precursor and its participation as an intermediate in reactions is its conversion into expected end-products in the presence of suitable scavengers. However, there are limitations on using these trapping experiments in that the added species must not affect the course of the reaction being studied other than by reacting with the intermediate. Clearly the added "trap" must therefore intercept the reaction pathway only after the suspected intermediate has been formed.

Since the bulk of the data to be discussed below is derived from kinetic studies of the reactivity of **29** and **30** in solution, it is appropriate to present a brief description of the way in which absolute rate constants are extracted from the data obtained using the laser flash photolysis technique. To extract the kinetic parameters that govern the transient's decay under particular experimental conditions, it is necessary to analyze the absorption–time profile obtained after the laser pulse. The analysis is simplest and most precise when the transient decays with first- or pseudo-first-order kinetics. Equation (2) characterizes the variation of the transient absorbance with time; in this situation $\Delta(OD)_t$ is the transient absorbance at time t after the laser pulse, $\Delta(OD)_0$ is the absorbance at the peak of the laser pulse and k_{obs} is the pseudo-first-order rate constant for decay.

$$\Delta(OD)_t = \Delta(OD)_0 \exp(-k_{obs}t) \qquad (2)$$

The rate constant k_{obs} in equation 2 is the sum of the rate constants for all first- and pseudo-first-order reactions that the transient undergoes under the particular conditions employed in the experiment–unimolecular reaction (k_{uni}) and reaction of the transient with other species, such as impurities (I) of unknown concentration or an intentionally added quencher (Q) of known concentration. The most likely impurities present in the system are oxygen, water and other hydroxylic impurities, as previously discussed. When the experiments employed scrupulously dry solvents and glassware and deoxygenated conditions and in the absence of intentionally added scavenger the decay of the transient should follow second order kinetics (Equation 3).

$$\left[\; R_2Ge{:} \; \right] \quad + \quad \left[\; R_2Ge{:} \; \right] \quad \xrightarrow{\; k_{dim} \;} \quad \text{Dimer} \qquad \text{second-order decay}$$
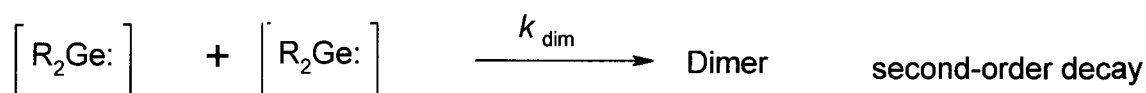
R = H, Me, Ph, Mes.

$$-d[R_2Ge{:}]/dt = 2k_{dim}[R_2Ge{:}]^2 \tag{3}$$

In the presence of an intentionally added reagent (Q) at low concentrations, the decay of the transient should follow mixed first- and second-order kinetics (Equation 4).

$$\left[R_2Ge: \right] + \left[R_2Ge: \right] \xrightarrow{k_{dim}} \left[R_2Ge=GeR_2 \right]$$

mixed first and second
order kinetics

$$\left[R_2Ge: \right] + Q \xrightarrow{k_Q} Products$$
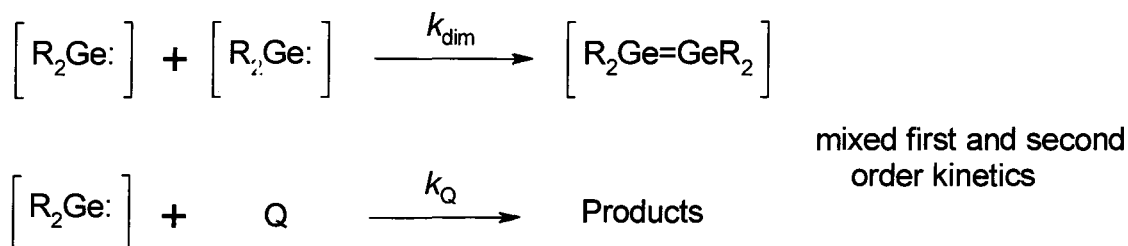
$$-d[R_2Ge:]/dt = \{2k_{dim}[R_2Ge:] + k_Q[Q]\}[R_2Ge:] \tag{4}$$

In order to determine simply and precisely the bimolecular rate constant k_Q for the reaction with the added scavenger, the decay of the transient should follow first-order kinetics (Equation 5).

$$-d[R_2Ge:]/dt \approx k_Q[Q][R_2Ge:] \tag{5}$$

Equation 5 will be true when $k_Q[Q] \gg k_{dim}[R_2Ge:]$ respectively, over the "high" concentration range where the decay of the germylene is dominated by the reaction with the added reagent and the dimerization is almost suppressed. In our case, we can tell when sufficient scavenger (Q) is added to accomplish this requirement by monitoring the digermene growth/decays. Thus, Equation 5 illustrates that the observable rate constant, k_{obs} is related to the scavenging rate constant, k_Q.

$$k_{obs} \approx k_Q[Q] \tag{5a}$$

A second method that can be used to obtain information on the efficiency of the germylene scavenging reaction involves monitoring the apparent yield of

the digermene in the presence of various concentrations of the scavenger, according to the Stern-Volmer equation (Equation 6).

In our situation, we define the digermene "yield" as the maximum transient absorbance measured at 420 nm (ΔOD_{max}) the absorption maximum of **30**. Equation 6 predicts that a plot of ratio of ΔOD_{max} in the absence and presence of the scavenger ($\Delta OD_{max,0}$ and $\Delta OD_{max,Q}$ respectively) versus scavenger concentration ([Q]) should be linear, with a slope equal to K_{SV}, the Stern-Volmer constant. The Stern-Volmer constant is related to the scavenging rate constant (k_Q) by equation 7, where τ is the lifetime of the precursor to the digermene in the absence of Q. This precursor is the germylene, and the lifetime is a second order lifetime due to the fact that it decays by second order kinetics in the absence of scavenger.

$$\phi^0/\phi \text{ or } \Delta OD_{max,\,0}/\Delta OD_{max,\,Q} = 1 + K_{SV}[Q] \qquad (6)$$

$$K_{SV} = k_Q\tau \qquad (7)$$

Equation (6) applies when:

(i) the quencher interacts only with the reactive intermediate involved in the product-forming process;

(ii) the product is formed from only one chemical species which is the one quenched by the scavenger, Q.[170]

The determination of K_{SV} provides an indirect method for determining absolute rate constants, for scavenging reactions for which k_Q cannot be measured directly.

Carboxylic acids have been used much less extensively than alcohols for trapping reactive germylenes and digermenes, although the corresponding O-H insertion products are evidently more stable than those derived from alcohols.[132] Quenching of transient germylenes and digermenes by acetic acid has proven to be a valuable tool in previous kinetic studies of simple germylenes in our laboratory.[67, 68]

Addition of increasing amounts of acetic acid (AcOH) to the deoxygenated hexane solution of **28** results in an enhancement in the decay rate of the signal attributed to **29** and a shortening of its lifetime (Figure **14a**). On the other hand, the intensity of the signal due to **30** is reduced, and it apparent growth rate is accelerated (Figure **14b**).
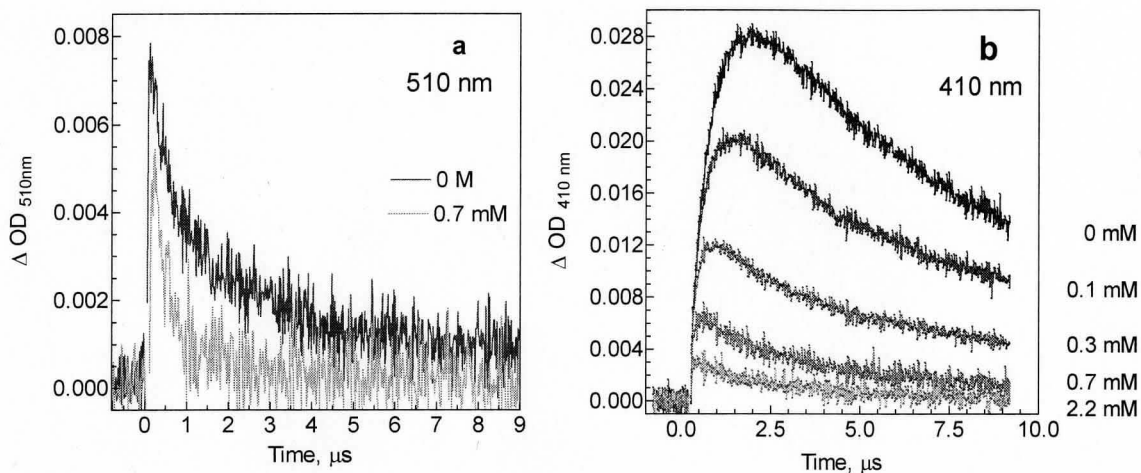
Figure 14. **a**. Decay profiles of **29** recorded at 510 nm in dried, deoxygenated hexane solution at 23 ^{0}C in the absence and in the presence of AcOH; **b**. Growth profiles of **30** recorded at 410 nm in the absence and in the presence of AcOH in dried deoxygenated hexane solution at 23 ^{0}C.

This is consistent with trapping of the germylene by AcOH, which competes with dimerization to digermene, **30**. The slightly accelerated decay of the latter, which can be clearly discerned in the trace recorded in the presence of 2.2 mM of the substrate (Figure 14**b**), indicates that **30** also reacts with AcOH, but much more slowly than **29** does (Scheme 29).
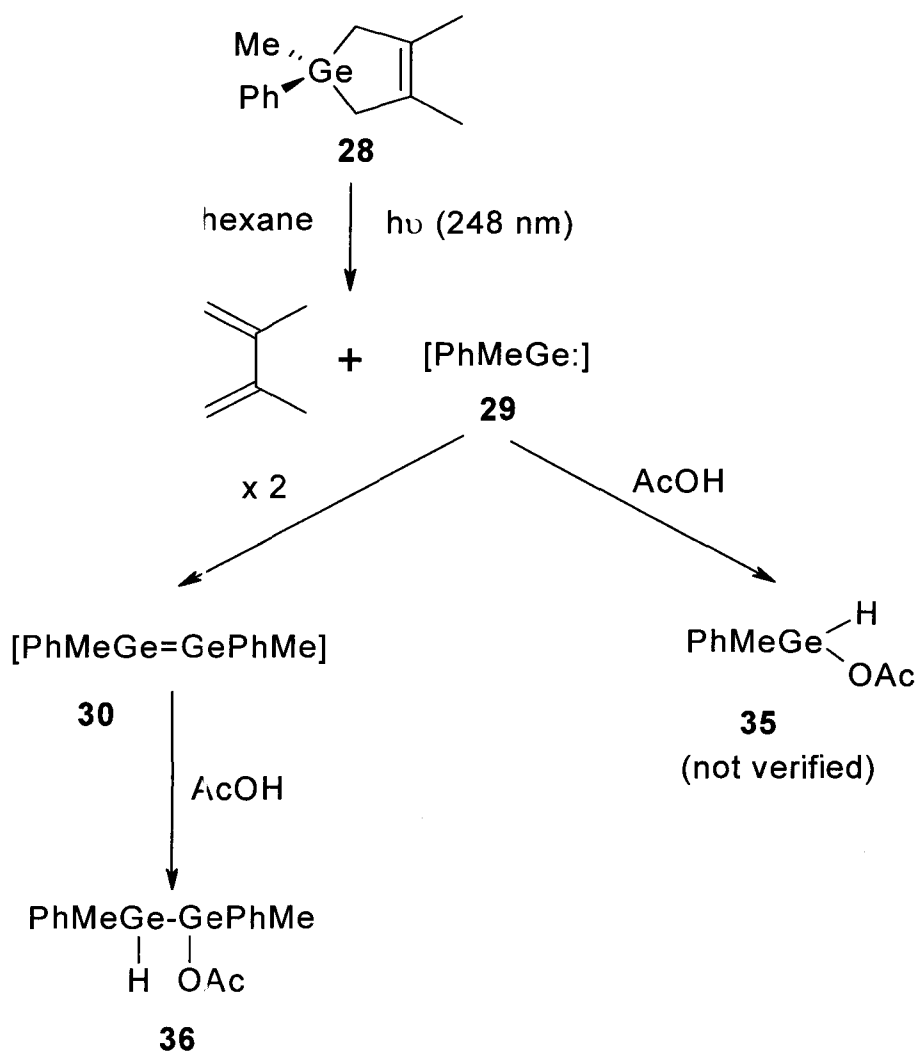
Scheme 29. Suggested course of trapping of **29** and **30** with AcOH.

It should be noted that the reaction with AcOH is quite clean, with exclusive formation of the O-H insertion product **35**. Similar behavior was observed in case of [Ph$_2$Ge:] and its dimer that support our assignments.[67]

Fig. 14 shows not only a reduction in the maximum intensities of the signal due to **30** after each addition, but a shift of the concentration maximum to shorter times, which occurs because dimerization dominates the early part of the

germylene decay where the concentration of the transient is highest. A lengthening of the decay of the digermene is also expected provided that it react more than one order of magnitude more slowly with AcOH than the germylene does; this is because in the absence of reaction with a scavenger the digermene decays with second-order kinetics (due probably to dimerization) and is thus concentration dependent. While the predicted lengthening of the decay of **30** is not observed, the other two effects are, which allows us to identify the reaction of [PhMeGe:] with AcOH as irreversible.

$$[PhMeGe:] \ + \ [PhMeGe:] \ \xrightarrow{\ k_{dim}\ } \ [PhMeGe=GePhMe]$$

$$[PhMeGe:] \ + \ AcOH \ (Q) \ \xrightarrow{\ k_Q\ } \ Products$$
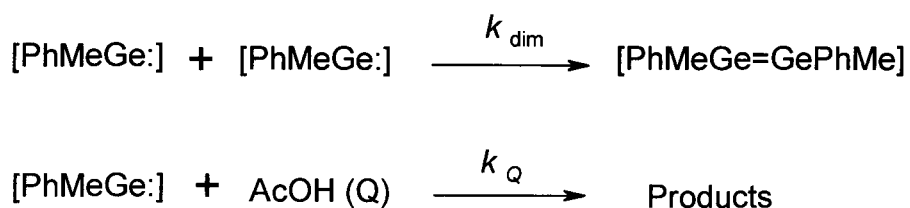
Scheme 30. Behaviour of phenylmethylgermylene in the presence of AcOH.

At concentrations above those required to reduce the digermene signal intensities to less than *ca.* 20 % of their values in the absence of added reagent (*ca.* 1.15 mM) the decay profile of **29** follows clean first-order kinetics and the germylene decays cleanly to the pre-pulse level.

Plots of the pseudo-first-order decay rate constant (k_{decay}) *vs.* trapping reagent concentration (AcOH) for both **29** and **30** were linear. Typical plots in hexane solution at 23 ^{0}C are shown in Figure 15.
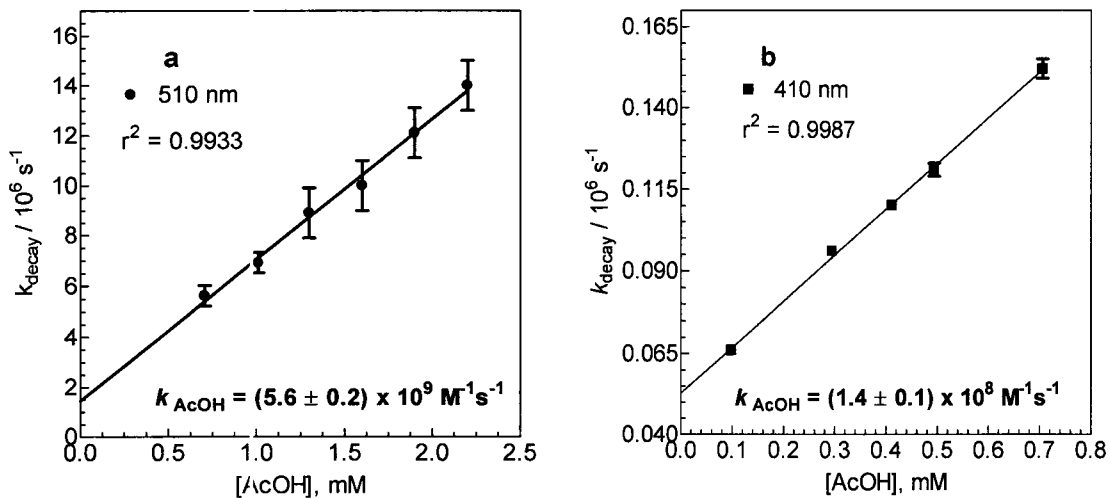
Figure 15. Plots of k_{decay} vs. [AcOH] for reaction of **29** (**a**) and **30** (**b**) with AcOH in dried, deoxygenated hexane solution at 23 ^{0}C recorded at 510 nm and 410 nm, respectively; the pseudo-first order rate constant for decay of **29** is obtained at concentrations at which the formation of **30** is more than 80 % quenched. The solid line represents the best fit (linear least squares analysis) of the data to equation 5, 5a.

The slope and intercept of such a plot affords the second order rate constant for quenching of the transient by Q (k_Q) and the (hypothetical) pseudo-first order rate constant for decay of the transient in the absence of trapping agent (k_0), respectively. The solid lines in figure 15 represent the best linear least squares fit of the data to equation 5, 5a. The values obtained are $(5.6 \pm 0.2) \times 10^9$ $M^{-1}s^{-1}$ for **29** and $(1.4 \pm 0.1) \times 10^8$ $M^{-1}s^{-1}$ for **30**.

In dilute solution of nonpolar organic solvents as hexane, AcOH exists as an equilibrium mixture of monomer and the cyclic hydrogen-bonded dimer even at submillimolar bulk concentration.[171] Fujii *et al.*[171] obtained the monomer-dimer equilibrium constant, $K = 3200 \ M^{-1}$ for acetic acid in hexane at 25 ^{0}C. Using this value of the monomer-dimer equilibrium constant K, we can calculate the values for the monomeric [AcOH]. Plots of the decay rate constants of Figure 15**a** for **29** against these new calculated values of monomeric [AcOH] led to a value of the rate constant of $(2.1 \pm 0.3) \times 10^{10} \ M^{-1}s^{-1}$.

Plots of the relative maximum intensities of the digermene signals at 410 nm in the absence and the presence of AcOH, $[(\Delta \ OD_{410})_{max,0}/(\Delta \ OD_{410})_{max,Q}]$ were linear suggesting adherence to the normal Stern-Volmer relationship of equation 6; K_{SV} was determined to be $5,300 \pm 100 \ M^{-1}$ (Figure 16).
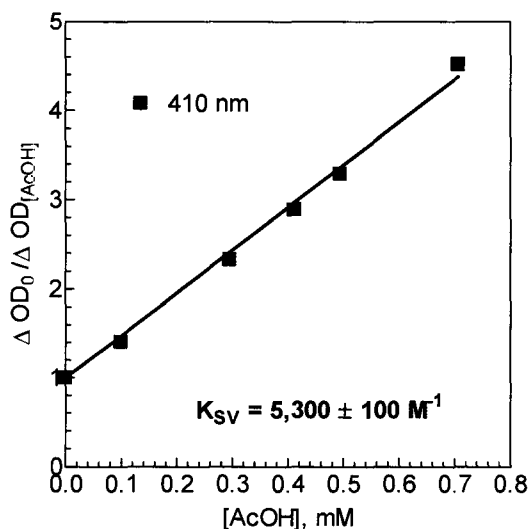
Figure 16. Stern-Volmer quenching of **30** by acetic acid
in dried, deoxygenated hexane solution at 23 ^{0}C, recorded at 410 nm.

The rate constants for reaction of **29** with AcOH are compared to the

corresponding values for [Ph$_2$Ge:] and [Mes$_2$Ge:][67, 68] in Table 6.

Species	k_{AcOH} 10^9/M^{-1}s^{-1}	Reference
Mes$_2$Ge	1.6 ± 0.3	67, 68
Ph$_2$Ge	3.9 ± 0.7	67, 68
MePhGe	5.6 ± 0.2	this work

Table 6. Values of the rate constants, k_{AcOH} for decay of simple germylenes in the
presence of AcOH in dried, deoxygenated hexane solution at 23 ^{0}C, at
concentrations at which the formation of the corresponding digermene
species is ~ 80% quenched. Errors are listed as ± 2σ.

2.6.2. n-Butylamine (n-BuNH$_2$) as a quencher

Addition of n-BuNH$_2$ to deoxygenated hexane solutions of **28**, caused, as in the case of AcOH addition, a shortening of the lifetime of **29** in proportion to the concentration of added reagent. A reduction in the maximum intensities of the signals due to **30** and a shift of the maximum to shorter times after the laser pulse is also observed on gradual addition of the n-BuNH$_2$. Representative data are shown in Figure 17.
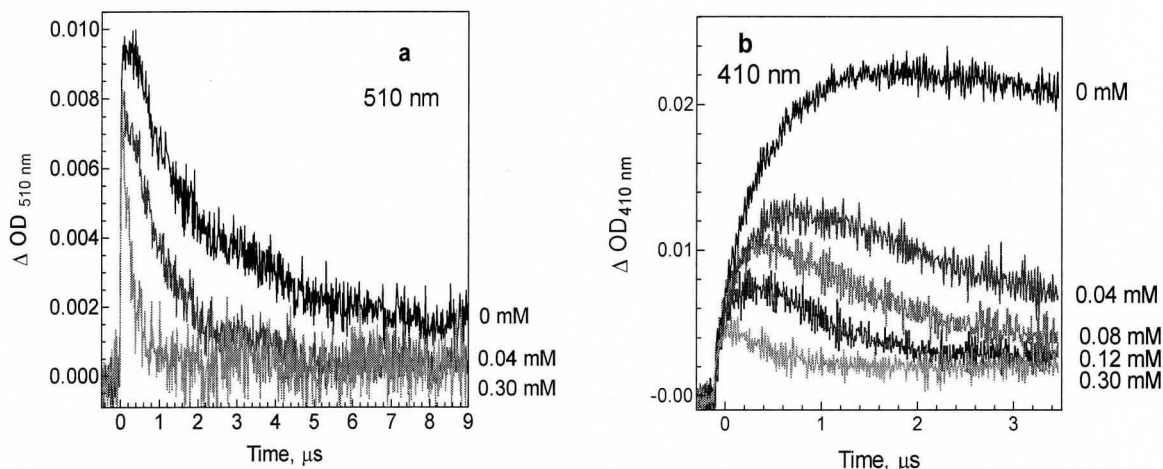
Figure 17. The effect of addition of n-BuNH$_2$ on decay/growth signal profiles of **29** and **30** recorded by laser flash photolysis at 510 nm and 410 nm, respectively in dried, deoxygenated hexane solutions at 23 ^{0}C.

This behavior is consistent with trapping of **29** by n-BuNH$_2$ in competition with dimerization to the digermene, as shown in Scheme 31.
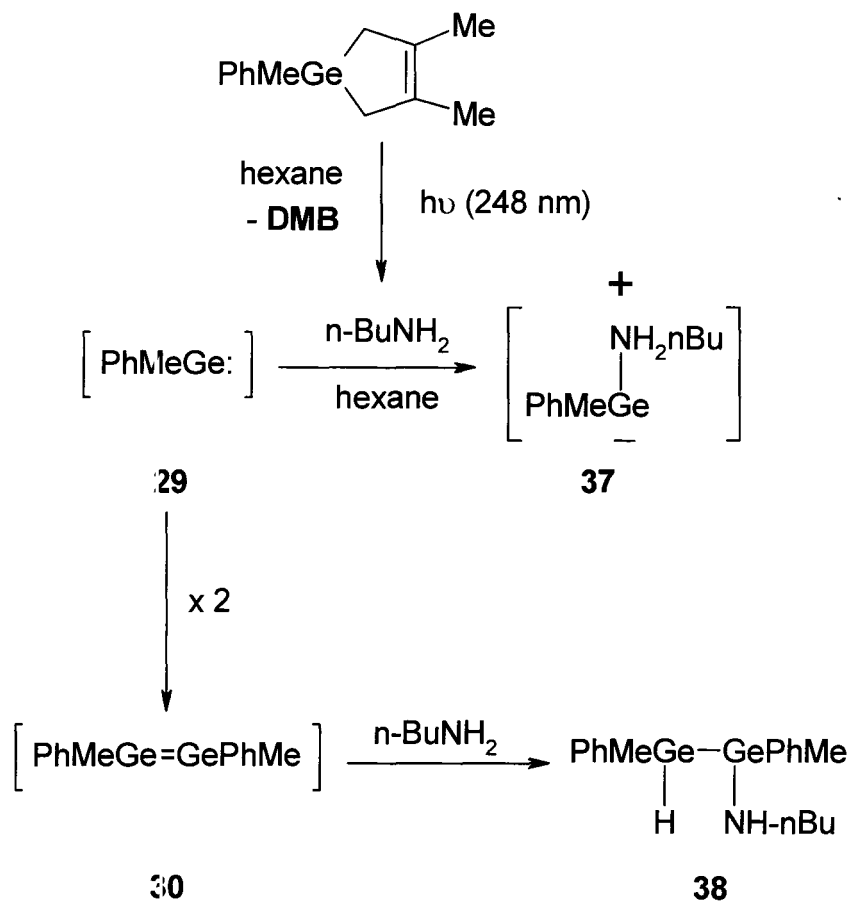
Scheme 31. Reaction of **29** and **30** generated by laser flash photolysis of **28** in presence of n-BuNH$_2$ in dry, deoxygenated hexane solution at room temperature.

Figure 17 snows that the progressive addition of the scavenger also results in a shorting of the lifetime of **30**.

As the concentration of the quencher is increased to the point where dimerization is more or less completely suppressed, (*e.g.* at 0.22 mM n-BuNH$_2$ 83% of **30** was quenched) the decay of the germylene evolves into pseudo-first

order kinetics. A plot of the pseudo-first-order decay rate constants (k_{decay}) *vs.* concentration of added *n*-BuNH$_2$ was linear and was analyzed according to equation 5. Representative plots are shown in Figure 18 for the quenching of **29** and **30** by *n*- BuNH$_2$. Linear least-squares analysis of the data to equation 5 gave acceptable fits. In the case of **29** a quenching rate constant k_Q = (1.2 ± 0.1) x 10^{10} $M^{-1}s^{-1}$ was obtained. A linear dependence of k_{decay} *vs.* *n*-BuNH$_2$ concentration was observed for **30** as well, and analysis of the data afforded a rate constant of (5.4 ± 0.3) x 10^9 $M^{-1}s^{-1}$ (see Figure 18). The solid lines in Figure 18 represent the best linear least squares fit of the data to equation 5, 5a.
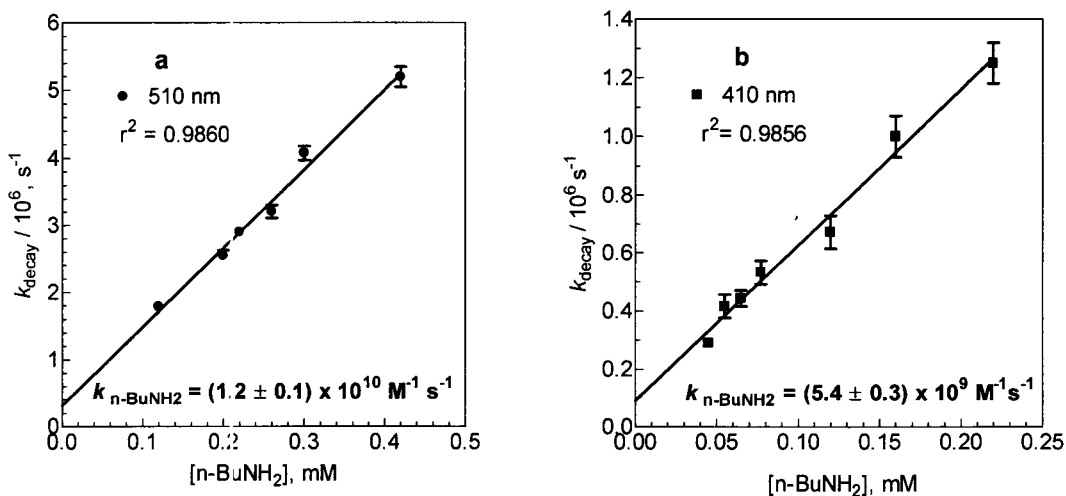
Figure 18. Plot of the rate constants for the decay of **29** and **30** generated upon nLFP of **28** in dried, deoxygenated hexane solution at 23 ^{0}C *vs.* n-BuNH$_2$ concentration recorded at 510 nm and 410 nm, respectively.

Figure 19 shows the Stern-Volmer plot resulting from analysis of the digermene signal intensities as a function of amine concentration. The plot is linear with a slope K_{SV} = 14,750 ± 320 M^{-1}.
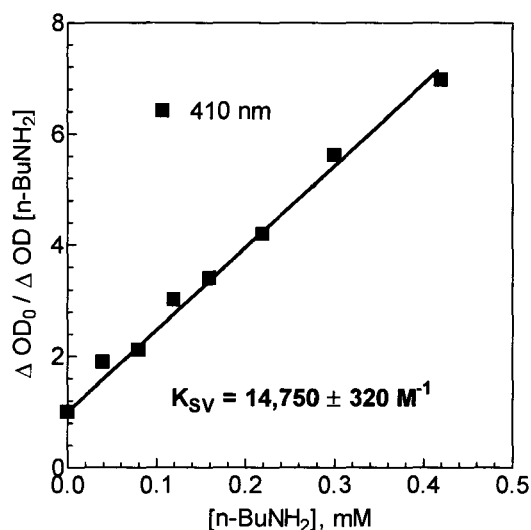
Figure 19. Stern-Volmer quenching of **30** by n-BuNH$_2$ in dry, deoxygenated hexane solution at 23 ^{0}C.

The absolute rate constant determined for the reaction of **29** with n-BuNH$_2$ in hexane is roughly three times larger than that for reaction with AcOH. Similar relative reactivities were observed with diphenylgermylene.[67, 68] Overall, **29** and **30** are both slightly more reactive than diphenylgermylene and tetraphenyldigermene, respectively, with these reagents.[67, 68]

In spite of the fact that amines are known to react with transient germylenes,[114, 120, 124, 132] absolute rate constants for the reaction of **29** and **30** with n-BuNH$_2$ have not been reported yet. Thus, the only reliable existing data for comparison are the values reported by our group for [Ph$_2$Ge:] and its dimer.[67, 68]

The results indicate that in both cases reaction with primary amines proceeds at close to the diffusion controlled rate in hexane at 23 ^{0}C (k_{diff} ~ 2.2 x 10^{10} M^{-1}s^{-1}).[67, 68]

Investigation of the transient UV-VIS absorption spectra recorded at 0.3 mM

n-BuNH$_2$ concentration shows the formation of a new transient species that

decays with mixed-order kinetics and a lifetime, $\tau \approx 8$ μs and exhibits λ_{max} = 310

nm. Representative transient absorption spectra are shown in Figure 20.
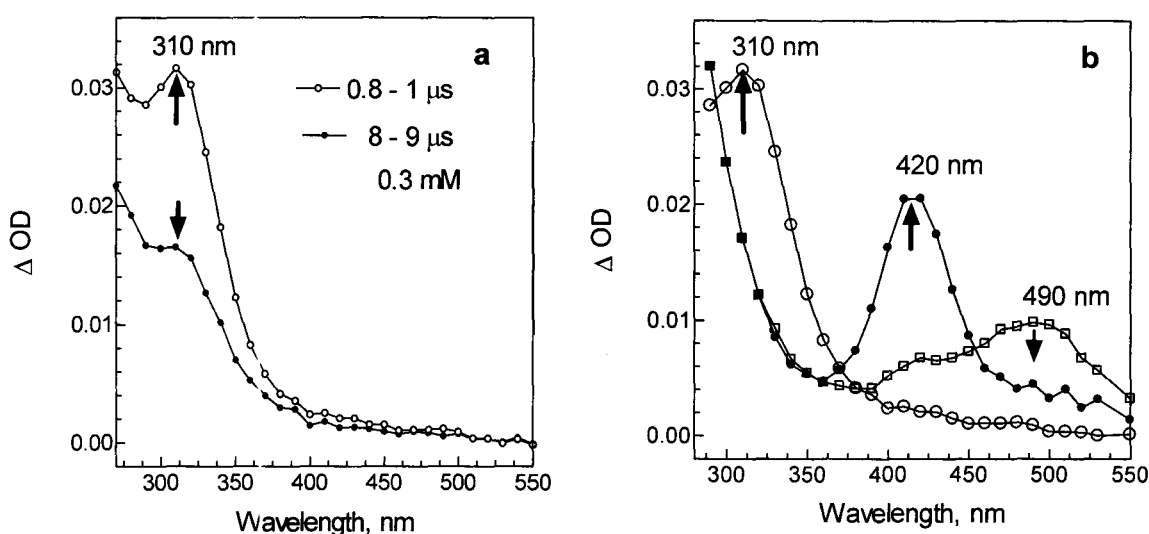
Figure 20. **a**) Transient UV-VIS absorption spectra recorded after addition of (0.3 mM) n-BuNH$_2$. **b**) Transient absorption spectra recorded in the presence and absence of n-BuNH$_2$. The spectra were recorded 0.8-1 μs and 8-9 μs (λ_{max} = 310 nm), 3.4-3.6 μs (λ_{max} = 420 nm) and 96-218 ns (λ_{max} = 490 nm) after 248 nm excitation.

This species can be identified as the initially formed product of the

reaction, and is tentatively assigned to the Lewis acid-base complex between the

germylene and the amine (**37**; Figure 21).
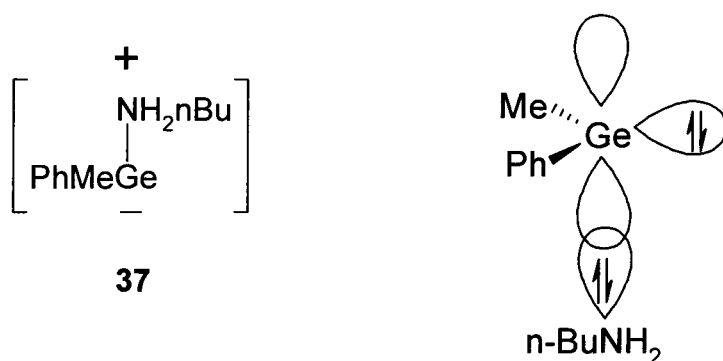
Figure 21. Lewis acid-Lewis base complex between [PhMeGe:] and n-BuNH$_2$.

The new intermediate with λ_{max} = 310 nm is assigned to the phenylmethylgermylene-butylamine Lewis acid-base complex based on data previously reported by Ando *et al*.[114, 120] in low temperature glasses, our own group for diphenylgermylene-butylamine complex in hexane solution (λ_{max} = 310 nm)[67, 68] and by comparison with the spectra of analogous silylene complexes with Lewis bases (Table 7).[41, 42, 128, 139, 140]
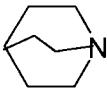
Reagent	Medium	$\lambda_{max}[RR'Ge:]$ (nm)				Ref.
		Me_2Si	Ph_2Ge	PhMeGe	Mes_2Ge	
Et_3N	C_6H_{12}, C_6H_{14}	≤ 270	- 330	-	-	41 68
n-$BuNH_2$	C_6H_{14}	-	310	310	-	68 this work
n-Bu_3N	3 MP, 77 K	287	-	-	-	42
<chemical structure: quinuclidine/azabicyclic amine>	3 MP/IP, 77 K	-	334	-	349	114

Table 7. Comparison between absorption maxima of Lewis acid-Lewis base complexes formed between [Me_2Si:] and amines and [Ph_2Ge:], [PhMeGe:], [Mes_2Ge:] with the same amines which provides good support for our assignment of phenylmethylgermylene-butylamine Lewis acid-base complex.

Figure 20 shows that the band due to the [PhMeGe:]←n-$BuNH_2$ complex is shifted to shorter wavelengths compared to that of the free germylene.

To consider the structure of simple germylene amines complexes, particularly [PhMeGe:]←n-$BuNH_2$, the crystal structures of dihalogermylene complexes are informative.[172-176] Analysis of the crystal structures of diiodo- and dichlorogermylene complexes[173-176] indicate that the monomeric dihalogermylene unit is coordinated with a lone pair of electrons from the donor. The structure of

diorganogermylene complexes seems to be similar: the donor coordinates *via* its lone pair of electrons to the vacant p orbital of the germylene (see Figure 21).[114]

Previously, it was suggested that the position of the absorption maximum of germylene complexes provides an indication of the strength of the interaction between germylene and the donor. The interaction between [PhMeGe:] and n-BuNH$_2$ seems to be relatively strong compared with that of the Lewis acid-base complex formed with MeOH (see also section 2.2).

However, at room temperature none of these complexes survive. This instability of the simple germylene complexes with amines seems to be consistent with the observations of Collins *et al.*,[124] which claimed that the diarylgermylenes did not form stable complexes at room temperature and with our observations, which indicate that the complex between [PhMeGe:] and *n*-BuNH$_2$ decays with a lifetime of *ca.* 8 μs (Figure 22).
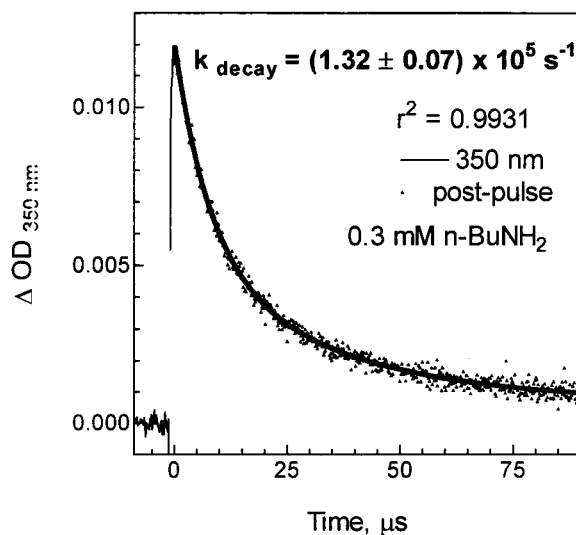
Figure 22. Transient decay profile of the [PhMeGe]←n-BuNH$_2$ complex (λ = 310 nm) recorded by laser flash photolysis of a solution of **28** in dried, deoxygenated hexane at 23 ^{0}C in presence of 0.3 mM n-BuNH$_2$. The data were fit to a second order exponential decay, which is represented in the figure by a solid line.

It is noteworthy that our ability to detect the complex as a detectable intermediate indicates that unimolecular [1, 2]-H migration within the complex to yield the formal N-H insertion product **39** is relatively slow (see Scheme 32). Figure 22 shows that the complex decay follows second-order kinetics in the presence of submillimolar concentration of amine, and its lifetime is $\tau \approx 8$ μs.

Interestingly, the reaction shows the characteristic of an *irreversible* reaction probably because the equilibrium constant for formation of the complex

is relatively large and because reaction of n-BuNH$_2$ with **30** is relatively fast (this will make the digermene growth/decays look like the reaction with **29** is reversible) (see Scheme 32).[67]

[PhMeGe:] $\xrightarrow{\text{n-BuNH}_2}$ $\left[\overset{\delta-\ \ \delta+}{\text{PhMeGe-NH}_2\text{Bu}} \right]$

29   **37**

x 2 $\downarrow$ $\downarrow$ slow

$\left[\text{PhMeGe=PhMe} \right]$
30

n-BuNH$_2$ $\downarrow$ fast

PhMeGe-GeMePh
$\ \ \ |\ \ \ \ \ |$
$\ \ \ H\ \ \ $NHBu
38

$\overset{\text{H}}{\underset{|}{\text{PhMeGe-NHBu}}}$

39
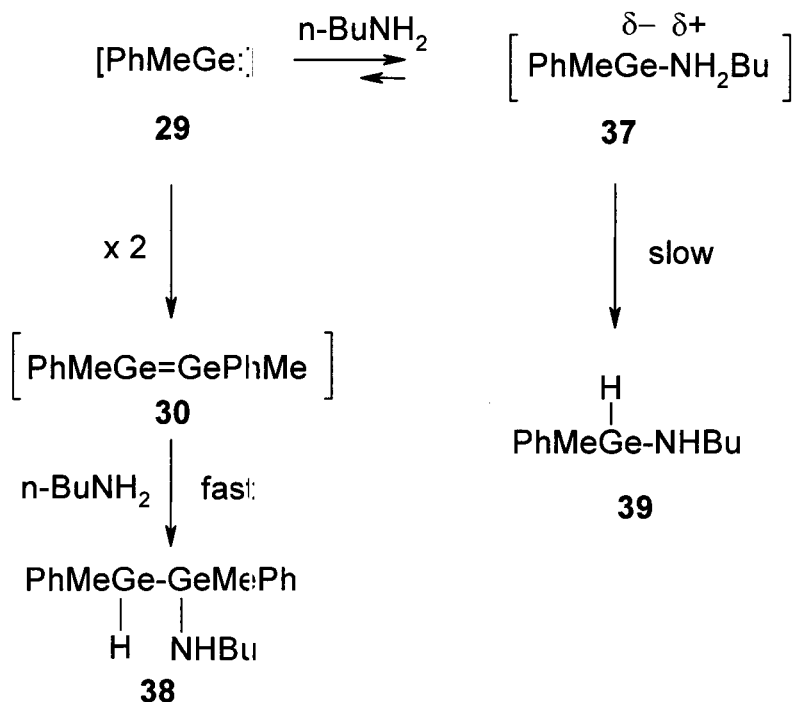
Scheme 32. Proposed behavior of **29** and **30** in the presence of n-BuNH$_2$.

The course of the reaction of **30** with *n*-BuNH$_2$ has not been determined, but is tentatively identified as [1+2]-addition across the Ge=Ge bond.[67, 68] The greater reactivity of **30** towards *n*-BuNH$_2$ compared to the carboxylic acid

suggests a mechanism involving initial nucleophilic attack at germanium, analogous to the addition of nucleophiles to disilenes (Scheme 33).[52, 177]
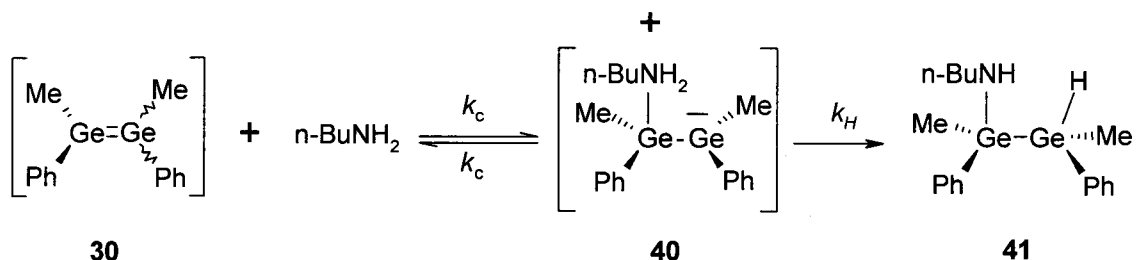
Scheme 33. Proposed mechanism of the reaction of **30** with n-BuNH$_2$.

2.6.3. Carbon tetrachloride as a scavenger

Addition of carbon tetrachloride (CCl$_4$) to the solution of **28** has the effect of accelerating the decay rate of the signal due to **29** and reducing the maximum intensity of the signal due to **30**, in proportion to the concentration of CCl$_4$ (Figure 23).
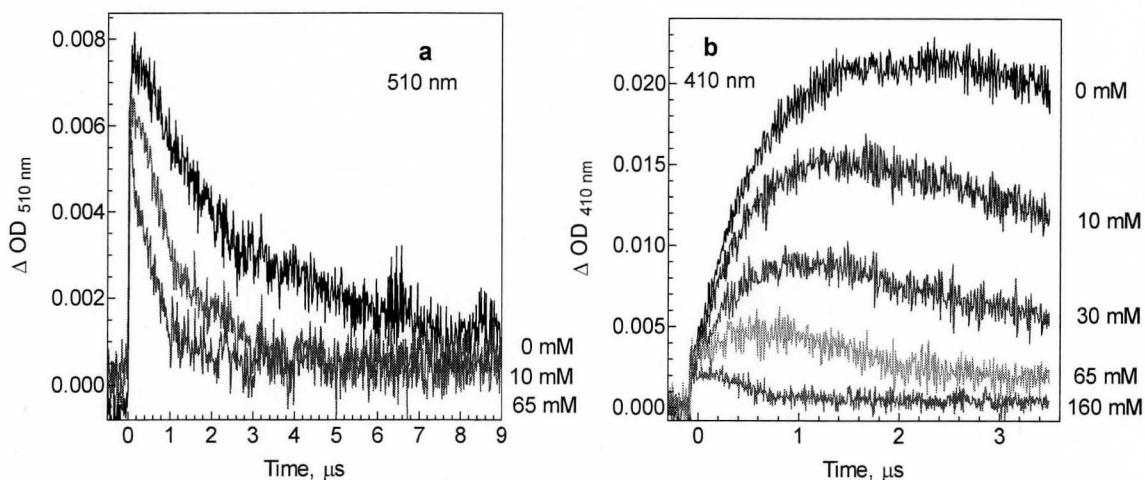
Figure 23. The effect of addition of the CCl_4 on decay/growth signal profiles of **29** recorded at 510 nm and of **30** recorded respectively, at 410 nm in dry, deoxygenated hexane solutions at 23 ^{0}C.

This is consistent with formation of a product between **29** and CCl_4, in competition with dimerization to **30**. Plots of rate constant (k_{decay}) vs. CCl_4 concentration for **29** exhibited positive curvature over the ranges of carbon tetrachloride concentration studied, indicating that the quenching kinetics in this particular case may be more complex that a simple analysis would imply. The decay rate constant for reaction of **29** with CCl_4 is $k_Q = (2.4 \pm 0.4) \times 10^7 \, M^{-1}s^{-1}$.

The decay rate constants (k_{decay}) vs. concentration of CCl_4 in the case of **30** were linear (Figure 24**b**) afforded a quenching rate constant of $k_Q = (6.2 \pm 0.1) \times 10^6 \, M^{-1}s^{-1}$.
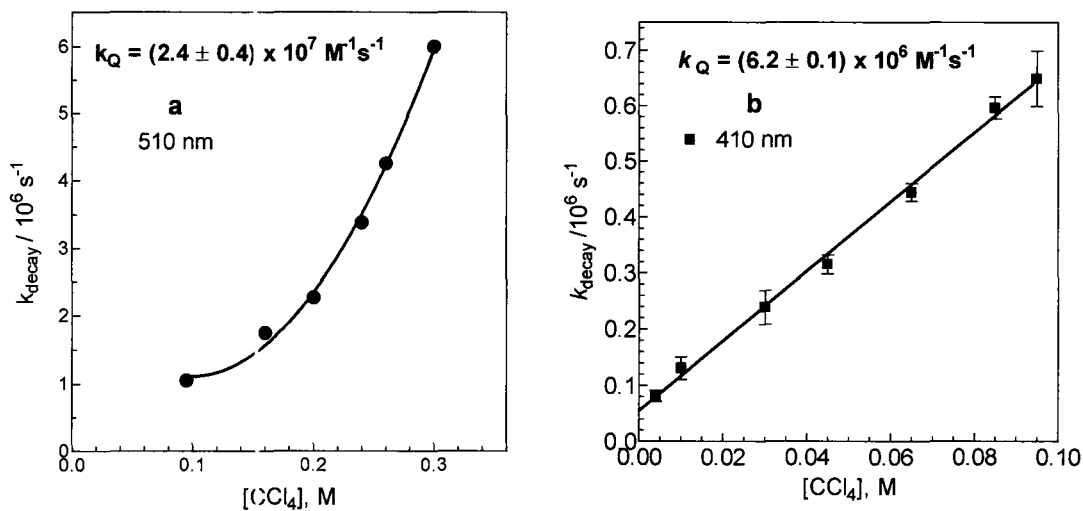
Figure 24. Plots of k_{decay} vs. CCl_4 concentration for quenching of **29** and **30** in the presence of CCl_4 in dried, deoxygenated hexane solution at 23 ^{0}C.

As mentioned in the Introduction, insertion of simple germylenes into carbon-halogen bonds has been widely reported in the literature.[45, 46, 48, 49, 52, 53]

Unfortunately, previously reported liquid-phase rate constants are highly variable, so are of little use for comparison to the present results (Table 8).

$k_{CCl_4}/10^7$ M^{-1}s^{-1}								
RR'Ge			Precursors					
	1c	**28**	**4b**	**4c**	**(PhMeGe)$_n$**	**2a**	**2b**	Ref.
Me$_2$Ge	-	-	-	-	-	73	49	53, 52
PhMeGe	-	2.4 ± 0.4^c	6.5	-	16	-	-	this work, 49, 48
Ph$_2$Ge	1.1 ± 0.1	-	-	15	-	-	-	67, 68, 46, 48

Table 8. Comparison of liquid-phase rate constants obtained in our laboratory and reported in the literature for simple germylenes in reaction with CCl$_4$ in hydrocarbon solutions (C$_6$H$_{14}$, C$_6$H$_{12}$) at room temperature.

a.   There are no errors listed for references 46, 48, 49, 52, 53.

b.   For references 67, 68 and for this work, [PhMeGe:] references are listed as $\pm 2\sigma$.

c.   From analysis of the data of figure 24a according to equation 5a.

The rate constant for the reaction of **29** with CCl$_4$, $k_Q = (2.4 \pm 0.4)$ x 10^7 M^{-1}s^{-1} is in the same range as the values reported by others using different precursors and with the value reported by our group for [Ph$_2$Ge:] (see Table 8).

Mochida et al.[52, 53, 178] have reported that the reaction of tetramethylgermylene with CCl$_4$ is slower than that of dimethylgermylene and is ~ 10^7 M^{-1}s^{-1}. In the present work, we report a value for the reaction of **30** with CCl$_4$ of (6.2 ± 0.1) x 10^6 M^{-1} s^{-1}.

However, the latter value is in good agreement with the absolute rate constant for reaction of tetraphenyldigermene with CCl_4 as reported by our group $((2.0 \pm 0.2) \times 10^6 \ M^{-1}s^{-1})$.[68]

Figure 25 shows a plot of the relative maximum intensities of the digermene signals at 410 nm in the absence and presence of trapping reagent vs. [CCl_4] fitting of which to equation 6 yields a value for the Stern-Volmer (K_{SV}) constant, $K_{SV} = (43.2 \pm 0.8) \ M^{-1}$
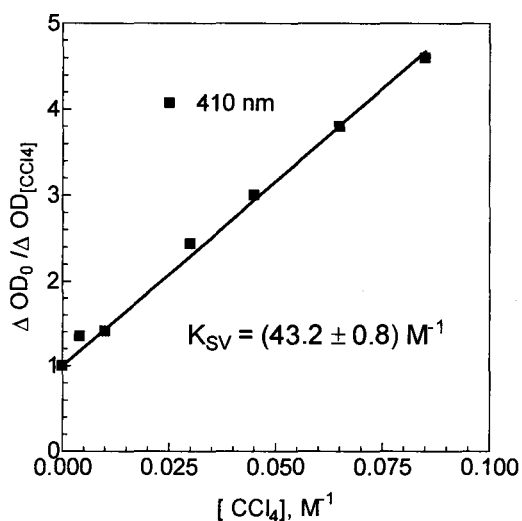
Figure 25. Stern-Volmer quenching of **30** by CCl_4 in dry, deoxygenated hexane solution at 23 ^{0}C.

Transient UV absorption spectra recorded in the presence of 0.34 M CCl_4 (Figure 26**a**, **b**) show no new absorption bands that might be attributed to products or intermediates in the reaction of **29** with the halocarbon.
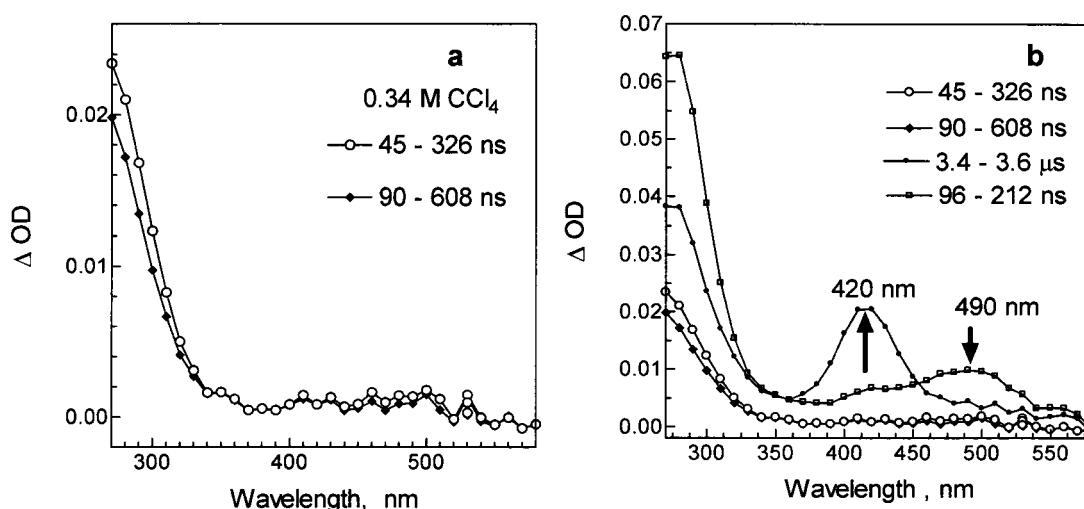
Figure 26 **a**. Transient absorption spectra recorded at the end of the addition of CCl_4 (0.34 M) in dry, deoxygenated hexane solution at 23 ^{0}C. **b**. Transient absorption spectra recorded in the presence and absence of trapping reagent, CCl_4 (0.34 M).

The reaction of $[Me_2Ge:]$ with halocarbons, in particular with CCl_4 has been much more extensively investigated compared to the other carbene analogues.[14, 137, 138, 179, 180] Thermal and photochemical decomposition of the 7-norbornadiene derivative **3a** in the presence of CCl_4 results in the formation of the C_2Cl_6 and insertion products Me_2GeCl_2 and $ClMe_2GeCCl_3$.[14, 137, 138, 179, 180] The formation of these products suggests a radical mechanism for the reaction, as shown in Scheme 34.

The first step of the interaction is abstraction of a halogen atom.[137] The radical pair $\bullet$ GeMe$_2$Cl and $\bullet$ CCl$_3$ recombines to give the insertion product ClMe$_2$GeCCl$_3$. Diffusion apart of the radicals followed by the abstraction of a second halogen atom leads to the formation of Me$_2$GeCl$_2$ (Scheme 34).[137, 180]

$$3a \xrightarrow{\text{h}\upsilon} [Me_2Ge{:}]$$

$$[Me_2Ge{:}] \xrightarrow{+\ CCl_4} [Me_2(Cl)Ge\bullet \quad \bullet CCl_3] \xrightarrow{\text{recombination}} ClMe_2GeCCl_3$$

$$[Me_2(Cl)Ge\bullet \quad \bullet CCl_3] \xrightarrow[+\ CCl_4]{\text{escape}} Me_2GeCl_2 \ + \ \bullet CCl_3$$

$$\bullet CCl_3 \ + \ \bullet CCl_3 \rightarrow C_2Cl_6$$
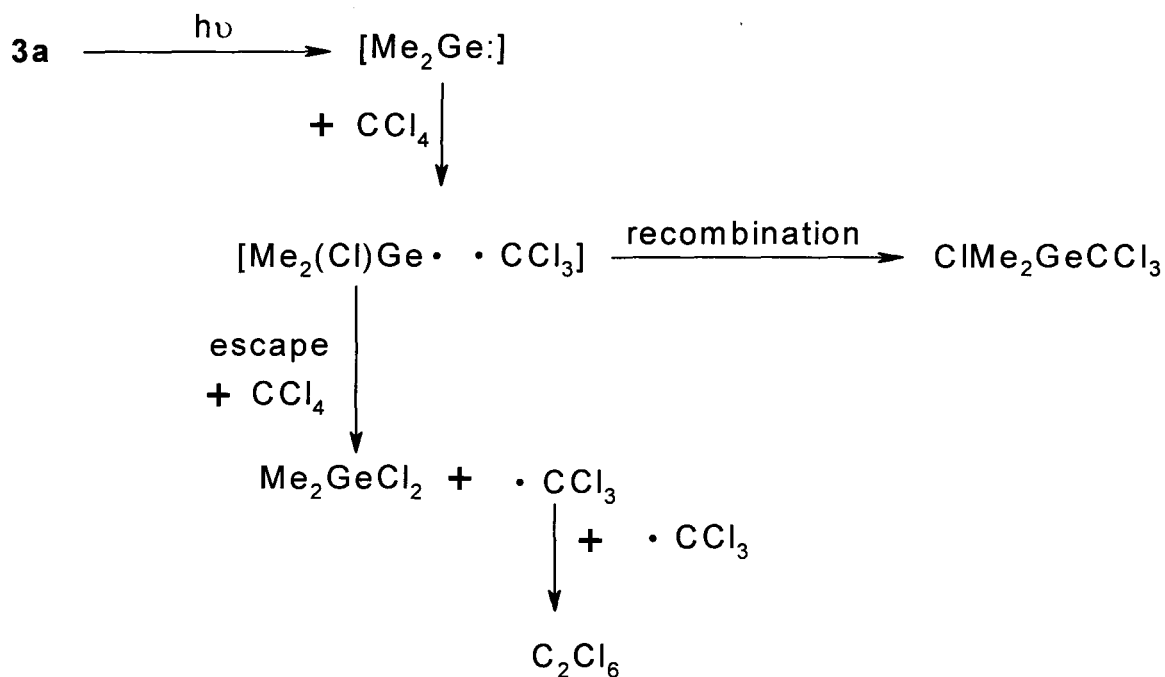
Scheme 34. Proposed mechanism for formation of the major products in the reaction of [Me$_2$Ge:] with CCl$_4$.

2.6.4. Irreversible Scavenging by n-Bu₃SnH

The transient behavior observed upon laser photolysis of **29** in the presence of n-Bu$_3$SnH is similar to that discussed earlier for AcOH, n-BuNH$_2$. Increasing the reagent concentration results in reductions in the maximum intensity of the signal due to **30**, acceleration of the apparent rate of digermene growth and acceleration of the germylene decay. This is consistent with irreversible quenching of **29** by Bu$_3$SnH, in competition with dimerization to the corresponding digermene, **30**. The decay profile of the germylene signal followed clean pseudo-first order kinetics once sufficient scavenger was added to reduce the maximum signal intensity due to the digermene to less than *ca.* 20 % of its value in the absence of added reagent (Figure 27).
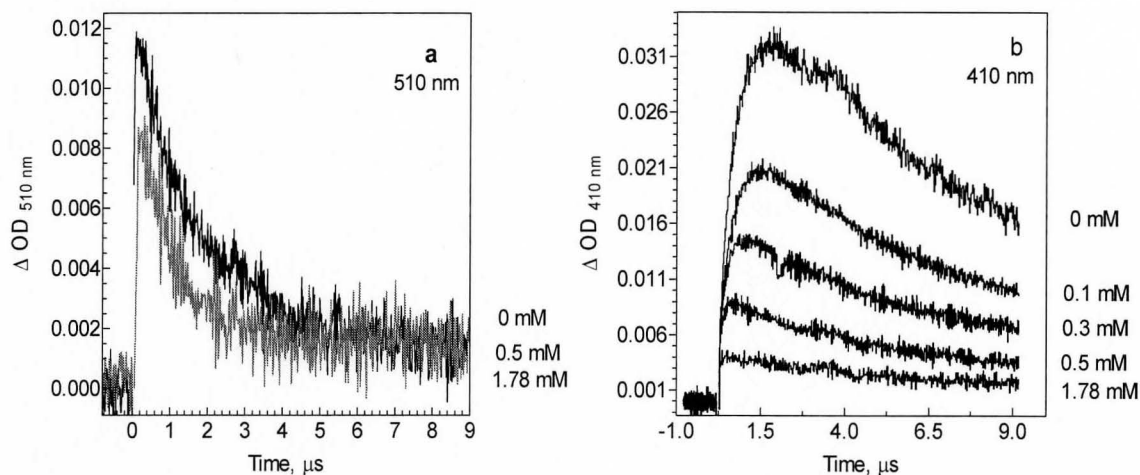
Figure 27. Transient decay/growth profiles due to **29** and **30** recorded at different concentrations of n-Bu$_3$SnH in dry, deoxygenated hexane solution at 23 ^{0}C.

A plot of the pseudo-first order decay rate constants (k_{decay}) for **29** vs. the concentration of added reagent was linear, consistent with the relationship of equation 5 (Figure 28).
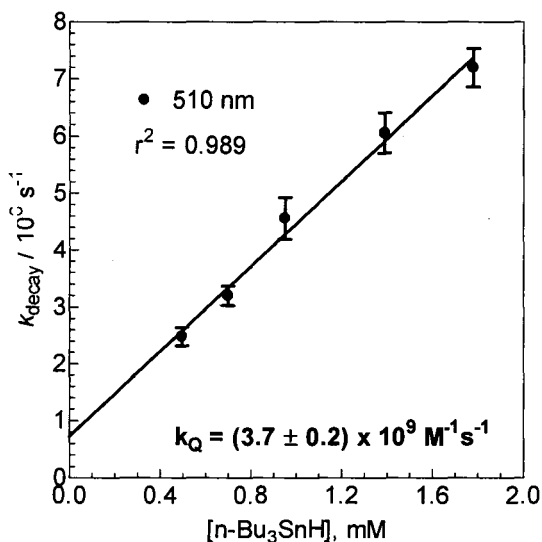
Figure 28. Plot of k_{decay} vs. [nBu$_3$SnH] for quenching of **29** upon 248 nm laser flash photolysis of **28** in dry, deoxygenated hexane solution at 23 ^{0}C at concentrations at which the formation of **30** is more than 70% quenched.

The slope of the line is the second order rate constant for reaction of **29** with the added reagent: k_{Bu3SnH} = (3.7 ± 0.2) x 10^9 M^{-1} s^{-1}. It should be noted that in the presence of 0.5 mM of the scavenger, the maximum intensity of the digermene signal was reduced to *ca.* 27% of its value in pure hexane solution; thus, the germylene signal decays cleanly to the pre-pulse level (within our detection limits) in traces recorded for solutions containing higher concentration than 0.5 mM of the added scavenger. In this case, over the 0.5 mM to 1.78 mM concentration, the decay of the germylene was dominated by reaction with the n-Bu$_3$SnH.

As with the cases of scavenging with AcOH or n-BuNH$_2$ or CCl$_4$ plots of the relative maximum intensities of the digermene signals (410 nm) in the absence and presence of added reagent were linear. This linearity is consistent with the Stern-Volmer relationship of equation 6 and affords a value of the Stern-Volmer constant K$_{SV}$ = (5,047 ± 86) M^{-1} (Figure 29).
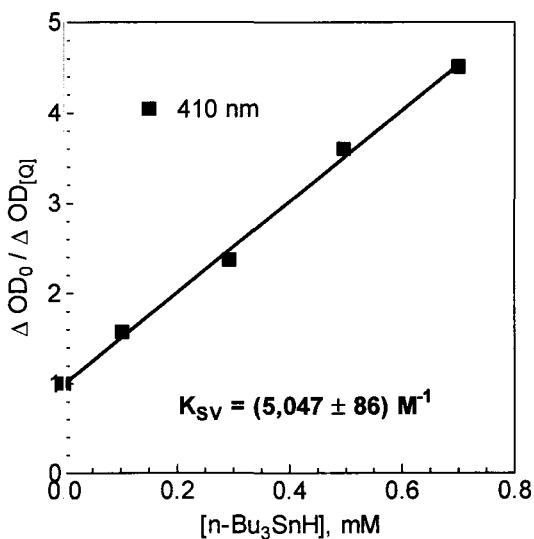
Figure 29. Stern-Volmer plot of [(Δ OD$_{410}$)$_{max, 0}$ / (Δ OD$_{410}$)$_{max, Q}$] vs. [n-Bu$_3$SnH] in dry, deoxygenated hexane solution at 23 ^{0}C.

The present data can be compared with the values obtained previously for [Ph$_2$Ge:] and [Me$_2$Si:] as shown in Table 9.[41, 68]

		$k_{Bu3SnH}/10^9$ M^{-1}s^{-1}			
		Source			
Germylenes	Medium	**Me$_{12}$Si$_6$**	**1c**	**28**	Ref.
Me$_2$Si	C$_6$H$_{12}$	10.1 ± 0.1	-	-	41
Ph$_2$Ge	C$_6$H$_{14}$	-	3.5 ± 0.1	-	68
PhMeGe	C$_6$H$_{14}$	-	-	3.7 ± 0.2	this work

Table 9. Rate constants for the reaction of [Me$_2$Si:] and [Ph$_2$Ge:], [PhMeGe:] with n-Bu$_3$SnH in hydrocarbon solvents at room temperature. Errors for this work and reference 68 were listed as ± 2σ.

The nearly identical rate constants (see table 9) for reaction of the two germylenes with tin hydride suggests only small influence on reactivity when the Ph group is substituted by Me.

Transient absorption spectra recorded at higher concentrations of quencher (1.78 mM Bu$_3$SnH) shows a broad band (380-540 nm) due to the presence of the germylene and the digermene as well. In this particular case the maximum intensity of the digermene signal is reduced to ca. 10% of its value in pure hexane solution that indicates and ensures that the decay of the germylene is dominated by the reaction with the added trapping reagent (Figure 30).
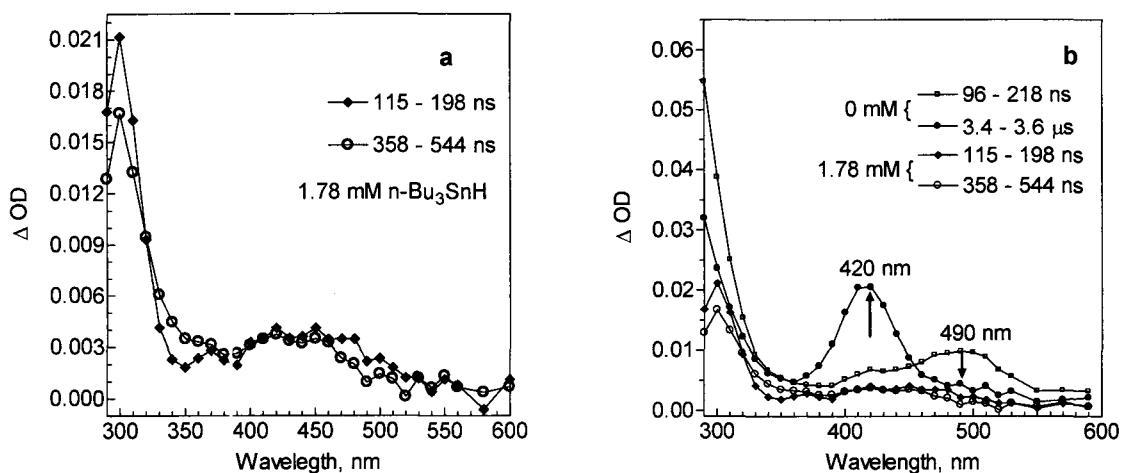
Figure 30. **a.** Transient absorption spectra recorded at 1.78 mM [n-Bu₃SnH] in dry, deoxygenated hexane solution at 23 °C. **b.** Transient absorption spectra recorded in the presence and absence of trapping reagent (n-Bu₃SnH).

A mechanism analogous to that shown in Scheme 35 has been suggested for the reaction of germylenes with Ge-H and Si-H bonds, on the basis of theoretical calculations and kinetic results. Thus, for the present work we propose the following mechanism for the reaction of **29** with n-Bu₃SnH (Scheme 35).
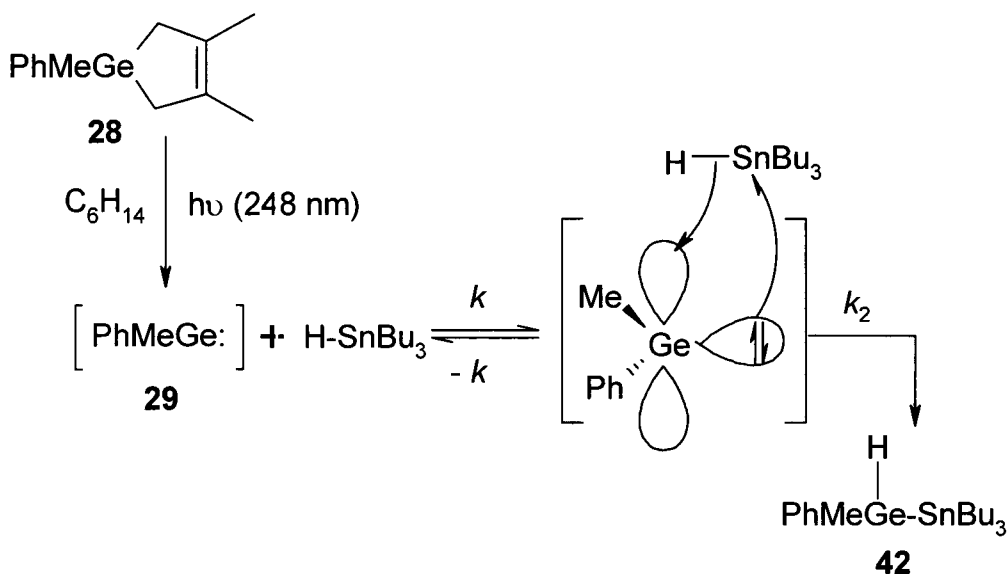
Scheme 35. Proposed mechanism for phenylmethylgermylene insertion reaction into Sn-H bond.

This pathway can be proposed based on the previously reported data[181] and on nearly identical rate constants for the reaction of **29** and diphenylgermylene with Bu_3SnH (see table 9) and the correlation observed in our group for the reaction of [Ph_2Ge:] and [Mes_2Ge:] with other hydrides (Et_3SiH, Et_3GeH).[68]

2.6.5. Reaction with t-Butylacetylene

Laser flash photolysis experiments with **28** in the presence of tert-butylacetylene (t-BuCCH) gave similar results as were observed with AcOH, n-BuNH$_2$ and Bu$_3$SnH, consistent with irreversible trapping of **30** by t-BuCCH (Figure 31).
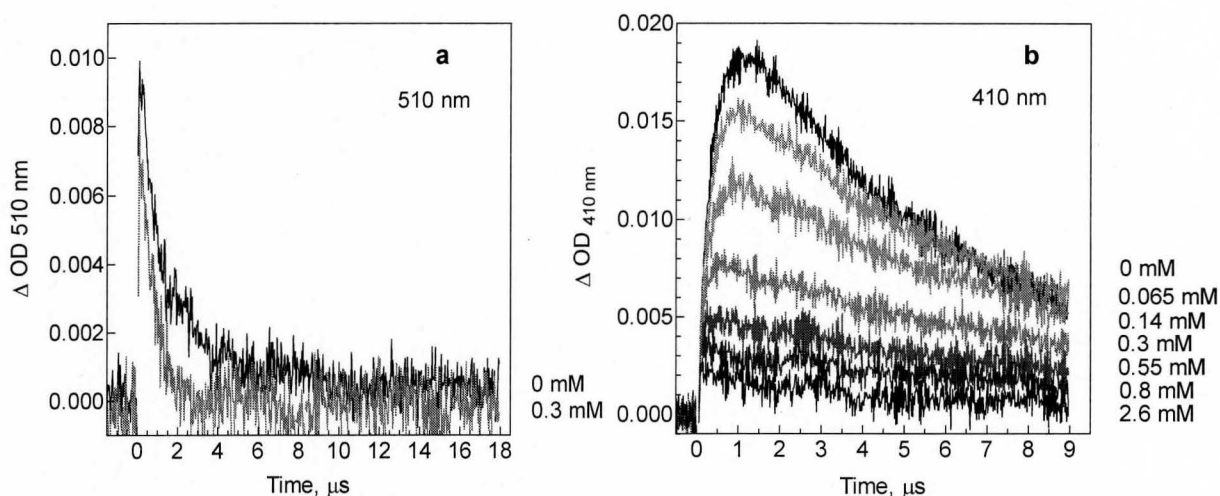
Figure 31. Decay/Growth profiles of **29** and **30** recorded at 410 nm and 510 nm in the presence of increasing amounts of t-BuCCH in dry, deoxygenated hexane solution at 23 ^{0}C.

Plots of the relative maximum intensities of the digermene signals at 410 nm in the absence and presence of added scavenger [(Δ OD$_{410}$) $_{max, 0}$ / (Δ OD$_{410}$) $_{max, Q}$] *vs.* concentration of the quencher were linear; this linear expression is the

form of the normal 'Stern-Volmer' quenching plot (equation 6). The K_{SV} obtained

in this case from the slope of the line was $(5,650 \pm 120)$ M^{-1} (Figure 32).
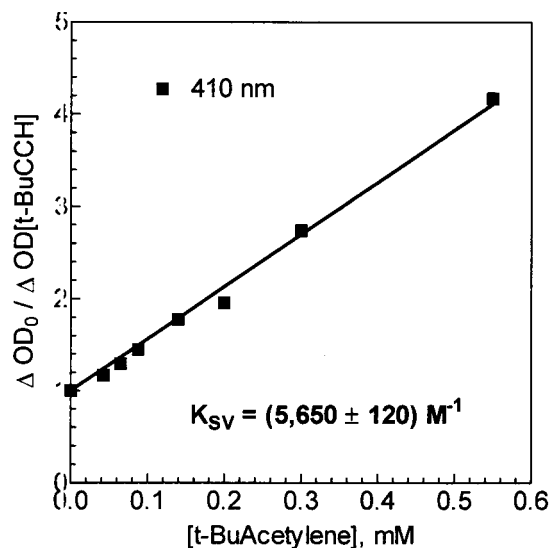
Figure 32. Stern-Volmer quenching of **30** by t-BuCCH in dry, deoxygenated hexane solution at 23 ^{0}C; at 0.55 mM t-BuCCH the intensity of the digermene signal was reduced to less than 26% of its initial value.

Similarly, a plot of the decay rate constants for the germylene *vs.* [t-BuCCH] were also linear (see Figure 33), analysis of which yielded a rate constant $k_Q = (6.0 \pm 0.4) \times 10^9$ M^{-1}s^{-1}.
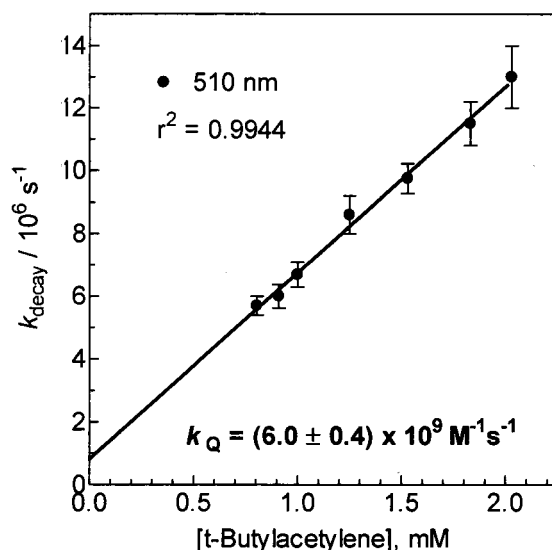
Figure 33. Plot of decay rate constants, k_{decay} vs. [t-BuCCH] in dried, deoxygenated hexane solution at 23 ^{0}C at concentrations at which the formation of **30** is more than 80% quenched.

Our observation of irreversible reaction with t-BuCCH is in good accord with the results obtained for [Ph$_2$Ge:] with the same quencher[68] and the value reported for the rate constant is in good agreement with the previously determined value for [Ph$_2$Ge:].[68] As might be expected from the behavior with the other irreversible quenchers studied, [PhMeGe:] reacts slightly faster than [Ph$_2$Ge:] but slower than [Me$_2$Ge:].

The absolute rate constant obtained in this work may also be compared with the reaction of [Me$_2$Ge:] with acetylene in the gas-phase, which proceeds with a rate constant of $(1.3 \pm 0.3) \times 10^{-11}$ cm^3 molecule^{-1} s^{-1} ($\sim (7.8 \pm 0.3) \times 10^9$ M^{-1}

s^{-1}).[60] It can also be compared to the rate constant for reaction of dimethylsilylene, [Me_2Si:] with trimethylsilylacetylene in cyclohexane solution, which was reported to be $(8.0 \pm 0.1) \times 10^9$ $M^{-1}s^{-1}$.[41]

The transient absorption spectrum recorded at higher concentration of the quencher (1.2 mM t-BuCCH) shows the disappearance of bands due to **29** and **30** and formation of a new transient absorption band at shorter wavelengths, centered at λ = 270 nm. We tentatively assign this band to the primary product of the reaction with t-BuCCH, the three-membered ring formed by [1+2] cycloaddition (see Scheme 36). The new intermediate with λ_{max} = 270 nm is assigned to the initial product of the reaction with t-BuCCH based on data previously reported by Billeb et al.[146-148] and our own group.[68] It is noteworthy to mention that the primary product formed in the reaction of diphenylgermylene with t-BuCCH in hexane solution exhibits an absorption maximum centered at λ_{max} = 275 nm.[68]
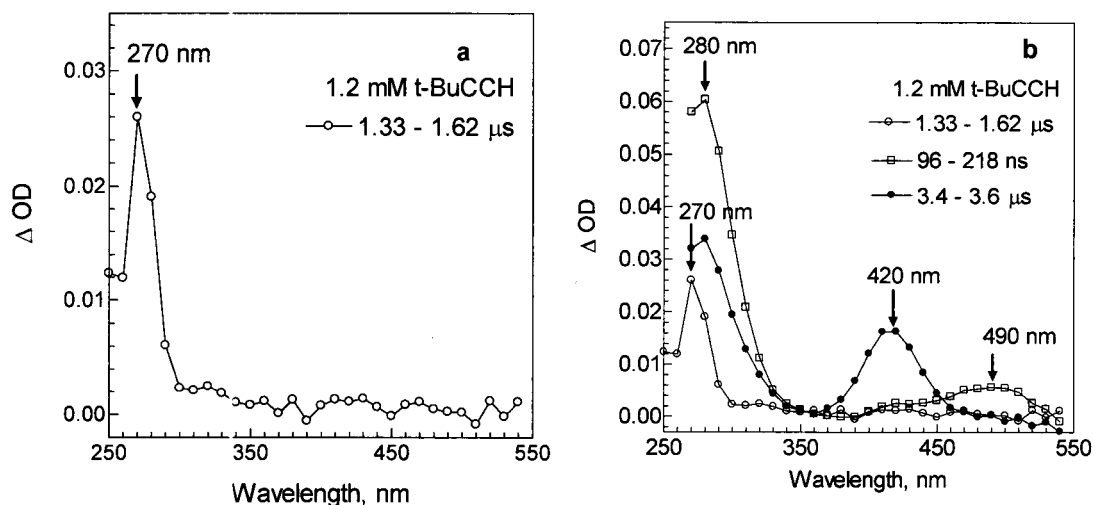
Figure 34. a.Transient absorption spectrum recorded in the presence of 1.2 mM t-BuCCH in dry, deoxygenated hexane solution at 23 ^{0}C; **b**. Transient absorption spectra recorded in the presence and absence of the added reagent, to show the differences.

The reaction of [Me$_2$Ge:] with alkynes has been studied mainly by Billeb et al.[146-148] and reviewed by Neumann.[27] Depending on the alkyne substituents and the reaction conditions, a variety of germanium heterocycles containing one, two, or even three Me$_2$Ge units, acyclic germanium compounds, or polymeric materials are formed.[27, 146, 147]

However, the primary product of the reaction with alkynes is thought to be a three-membered germanocycle (germirene) resulting from [1+2]-

cycloaddition.[68, 146, 147] The only one that has been identified is **43**[182], although a few examples of stable, sterically hindered germirene derivatives are known.
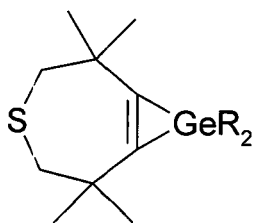
$$S \overset{}{\underset{}{\diagup}} \hspace{-0.5em} \overset{}{\underset{}{\bigtriangledown}} GeR_2 \qquad R = Me, Et$$

43

The kinetic stability of **43** is thought to be due to steric protection by the four Me groups, preventing dimerization or other possible consecutive reactions such as shown in Scheme 36.[27, 182]

R = H, alkyl, aryl; R' = n-BuCCH, t-BuCCH.
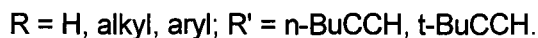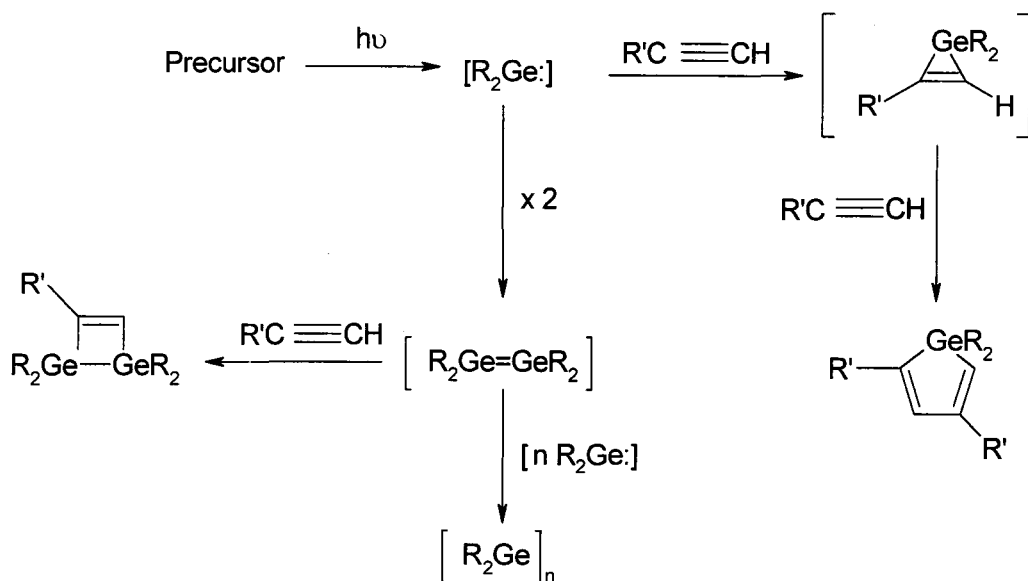
Scheme 36. Mechanistic consideration regarding reaction of simple germylene with a terminal alkyne (t-BuCCH).

2.6.6. Isoprene as Trapping Agent

The results for isoprene as scavenger appear similar to those observed for t-BuCCH, and are suggestive of irreversible reaction. Representative decay and growth/decay profiles for **29** and **30** in the presence of the diene are shown in Figure 35.
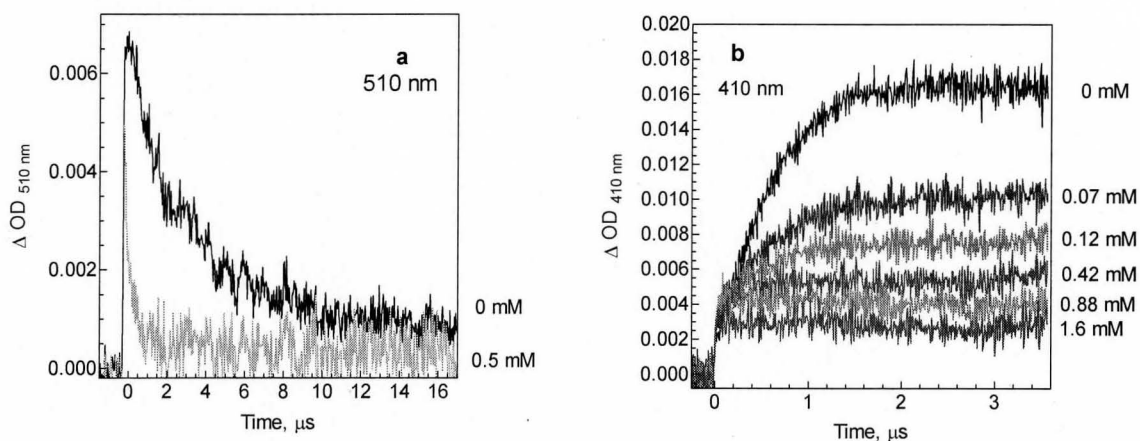
Figure 35. The effect of addition of isoprene over the germylene decay signal profile recorded at 510 nm (**a**) and over the digermene growth profile recorded at 410 nm (**b**) in dry deoxygenated hexane solution at 23 ^{0}C.

Plots of k_{decay} and $\Delta OD_{410,0} / \Delta OD_{410,Q}$ *vs.* isoprene concentration are shown in Figure 36 and 37.

The slope of the linear plots of the pseudo-first-order decay (k_{decay}) versus isoprene concentration over the range in which the formation of **30** was almost suppressed (at 0.42 mM isoprene ~ 70 % of the dimer was quenched), yields the second-order rate constant $k_Q = (8.0 \pm 0.4) \times 10^9$ M^{-1}s^{-1} (Figure 36 and equation 5, 5a).
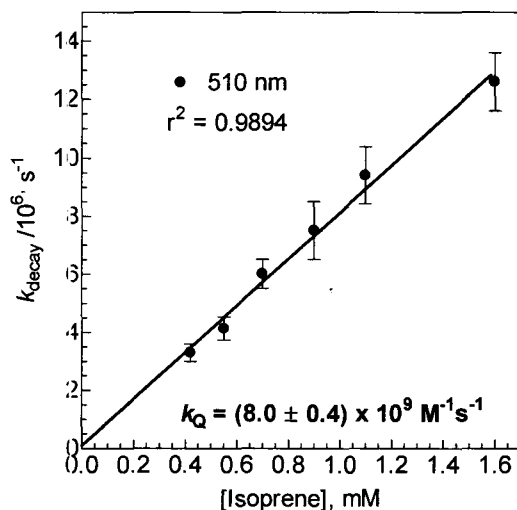
Figure 36. Plot of the decay rate constant k_{decay} vs. [Isoprene] for quenching of 29 in dry, deoxygenated hexane at 23 °C.

Reaction of **30** with isoprene was found to be too slow to be measured with our system and so only an upper limit for the quenching rate constant could be estimated from the k_{decay} value of the signal in the presence 1.6 mM isoprene: $k_Q \leq (4.1 \pm 0.2) \times 10^6 \ M^{-1}s^{-1}$.

A plot of the relative maximum intensities of the digermene signals at 410 nm in the absence and presence of isoprene [$(\Delta\ OD_{410})_{max, 0}$ / $(\Delta\ OD_{410})_{max, Q}$] vs. concentration of the quencher was linear, with a slope $K_{SV} = 3,830 \pm 87 \ M^{-1}$ (Figure 37).
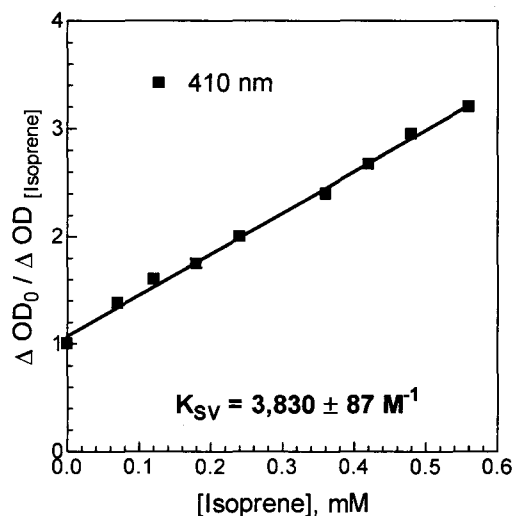
Figure 37. Stern-Volmer plot of $[(\Delta\ OD_{410})_{max,\ 0} / (\Delta\ OD_{410})_{max,\ Q}]$ *vs.* [Isoprene] in dry, deoxygenated hexane solution at 23 ^{0}C.

Interestingly, the reported rate constant for quenching of [Me$_2$Si:] formed upon 266 nm laser flash photolysis of cyclohexane solution of dodecamethylcyclohexasilane by **DMB** was $(9.4 \pm 0.15) \times 10^9\ M^{-1}s^{-1}$.[41]

Reliable gas-phase kinetic data have been also reported for [Me$_2$Ge:] in reaction with 1,3-butadiene[60] of $1.1 \times 10^{-11}\ cm^3\ molecule^{-1}\ s^{-1}$ (*ca.* $6.6 \times 10^9\ M^{-1}s^{-1}$) which compares favorably with the values obtained here for **29**.

As might now be expected, the absolute rate constant determined for reaction of **29** with isoprene is very similar to the corresponding value for diphenylgermylene[68] ($k_Q = (5.5 \pm 0.1) \times 10^9\ M^{-1}s^{-1}$).

Tetraphenyldigermane is similarly unreactive toward the diene as **30**.

Transient UV absorption spectra were recorded in the presence of 1.6 mM isoprene and are shown in Figure 38. One observes only a long-lived ($\tau \approx 1.78$ μs) absorption centered at 280 nm, which appears in the same position as the short wavelength bands in the spectra of **29** and **30** (Figure 38 **b**).
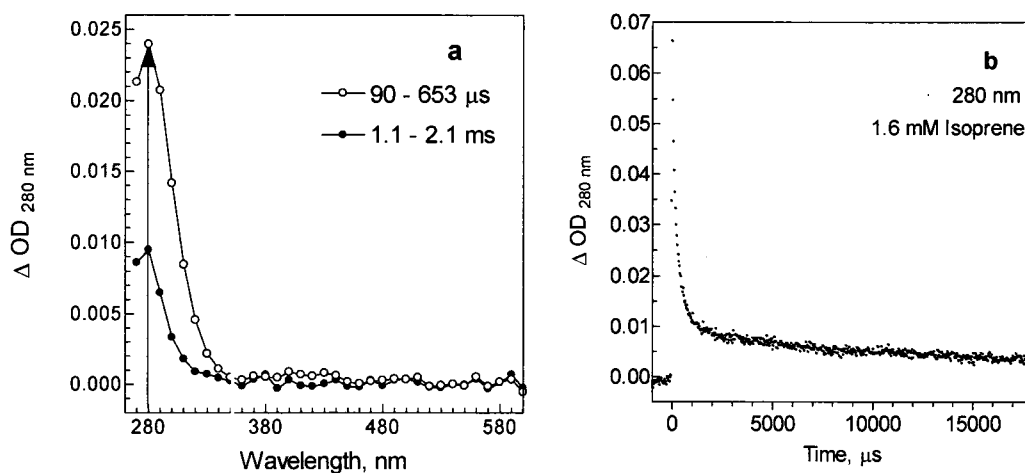
Figure 38. **a**. Transient absoption spectra recorded in the presence of 1.6 mM isoprene; **b**. Decay trace of the species with λ = 280 nm recorded at 1.6 mM isoprene.

PhMeGe
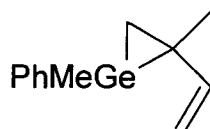
44

The assignment is based on recent work on the reaction of [Ph$_2$Ge:] with

the diene[68], which showed that the initial product of the reaction is a transient

with λ = 285 nm and a lifetime, $\tau \approx$ 0.5 ms in hexane at 23 ^{0}C. The reaction with

[Ph$_2$Ge:] is reversible, with $K_{eq} \approx$ 6000 M^{-1}; our results for **29** indicate that if it too

reacts with isoprene reversibly, the equilibrium constant must be significantly

larger than 10,000 M^{-1}.

However, at 1.6 mM isoprene concentration, which is the highest

employed in our experiment the formation of the intermediate is competitive with

dimerization and oligomerization which generate products which absorb in the

same spectral region as vinylgermirane (280 nm). Therefore, a higher

concentration of isoprene (*e. g.* for [Ph$_2$Ge:] in reaction with the same scavenger

a concentration > 15 mM was used in order to identify the initial product of the

reaction[68]) will be necessary to suppress the dimerization and to obtain reliable

data for the final product (**31**) and the corresponding intermediate (**44**).
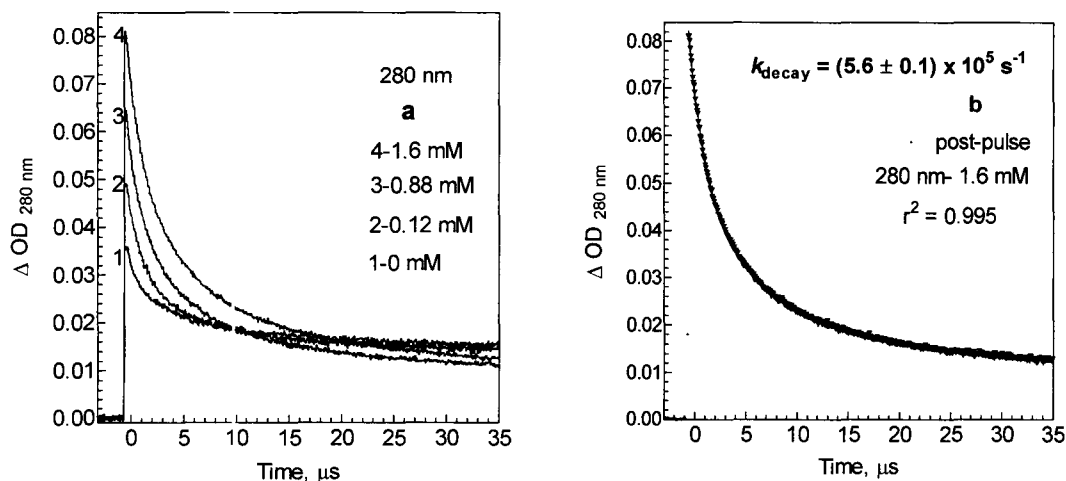
Figure 39. **a**. The effect of addition of isoprene on the 280 nm species in dry, deoxygenated hexane solution at 23 ^{0}C; **b**. Decay trace recorded at 280 nm in the presence of 1.6 mM isoprene. The solid line represents the best fit of the data to a second order exponential decay.

Figure **39b** shows a series of decay traces for the new species recorded in the presence of 1.6 mM isoprene on a shorter timescale in order to better illustrate the enhanced absorption in this wavelength range.

The enhanced transient absorption at 280 nm (Figure **39a**) is consistent with the formation of an intermediate in the reaction of isoprene with **29**, which presumably leads ultimately to the final product of the reaction germacyclopentene (**31**). We tentatively assign the structure of this species to vinylgermirane (**44**). Since the only product detected in steady state experiments with isoprene as scavenger is **31**, we suggest that the process responsible for the decay of **44** is ring expansion to **31**.

Becerra *et al.*[57, 60] suggested a similar route to the final product in the case of [H_2Ge:] and [Me_2Ge:] in their studies of the reaction with conjugated dienes in the gas phase. This proposed pathway is also consistent with the analogous reaction of [Me_2Si:] with conjugated dienes.[36, 152, 155, 158] More work is required in order to make a conclusive assignment of the structure of this species.

2.7. Reversible Scavenging by MeOH

Addition of MeOH to hexane solutions of **28** caused somewhat different transient behavior. Our observations can be summarized as follows:

(a)   - increasing amounts of MeOH appeared to cause a drop in the signal intensity at 510 nm, but had only a small effect on the lifetime (Figure 40 **a**).

(b)   - the growth rate of the signal at 410 nm due to **30** appeared to decrease upon addition of 0.1-30 mM MeOH. The signal persisted at concentrations in excess of that required to render the signal at 510 nm undetectable (30-50 mM; see Figure 40 **b**).

(c)   - new absorptions centered at 320 nm were formed with increasing yields with addition of increasing amounts of MeOH. (They were observed to grow in on a similar time scale as that of the germylene decay).

We interpret the apparent drop in signal intensity at 510 nm to a rapid, unresolvable decay of the germylene, which is due to reversible reaction of the

germylene with the alcohol, and the resolvable portion of the decay to dimerization of residual free germylene after equilibration is complete.

The time evolution of the digermene signal shows an initially rapid growth due to dimerization followed by an elongated decay. Increasing the MeOH concentration also has the effect of reducing the maximum intensities of the signals due to **30**, but with only a slight shift of the maximum in time (after the laser pulse). The slightly accelerated decay of the signal, which can be discerned in the traces recorded in the presence of 30 mM and 50 mM MeOH, indicates that **30** also reacts with the trapping reagent, but much more slowly than **29** does. Representative data are shown in Figure 40 **b**.
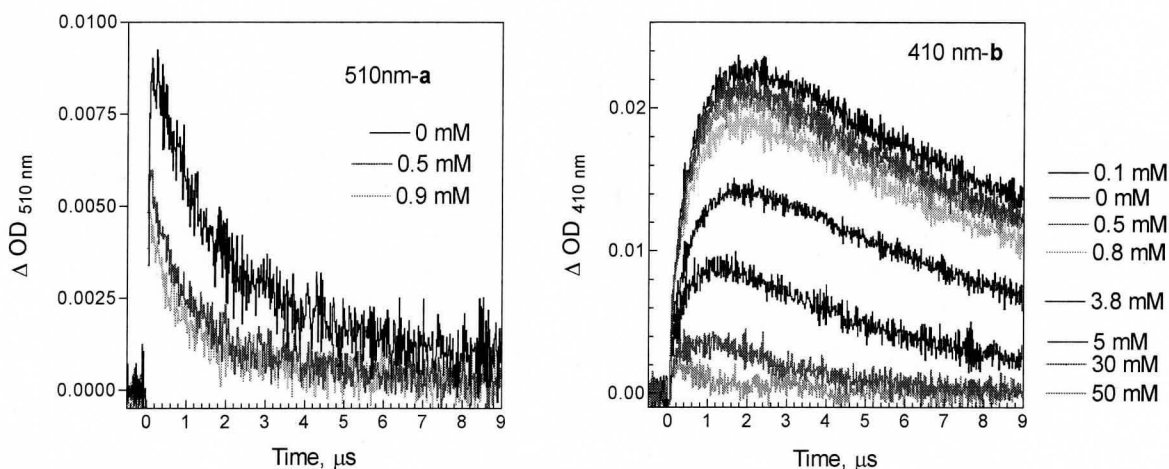
Figure 40 **a**. The effects of added MeOH on the transient absoptions due to **a**. [PhMeGe:] recorded at 510 nm and **b**. its corresponding dimer recorded at 410 nm in dry, deoxygenated hexane at 23 ^{0}C.

The linear dependence of the relative maximum intensities of the digermene signals at 410 nm in the absence and in the presence of added scavenger, $[(\Delta \, OD_{410})_{max,0} \, / \, (\Delta \, OD_{410})_{max, \, MeOH}]$ on MeOH concentration affords the Stern-Volmer constant for this process, $K_{SV} = (410 \pm 15) \, M^{-1}$ (see Figure 41).
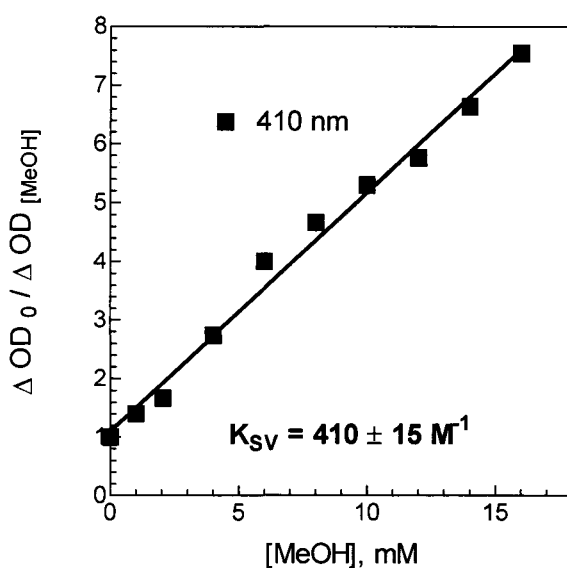
Figure 41. Stern-Volmer quenching of **30** by MeOH in dry, deoxygenated solution of hexane at 23 ^{0}C.

By analogy with previous observations for [Ph$_2$Ge:] with MeOH, the results are consistent with reversible formation of the Lewis acid base complex of **29** with methanol, which occurs as a very fast pseudo-first-order approach to equilibrium that competes with dimerization of **29** to form **30**. This approach to

equilibrium is too fast to be resolved with our system, and consequently the extraction of a rate constant for the reaction is not possible.

On the other hand, a plot of k_{decay} vs. [MeOH] for reactive quenching of **30** by MeOH exhibits good linearity, as illustrated in Figure 42; least-squares analysis of the data according to equation 5 yields a value for the rate constant of $k_Q = (2.4 \pm 0.2) \times 10^7 \ M^{-1}s^{-1}$.
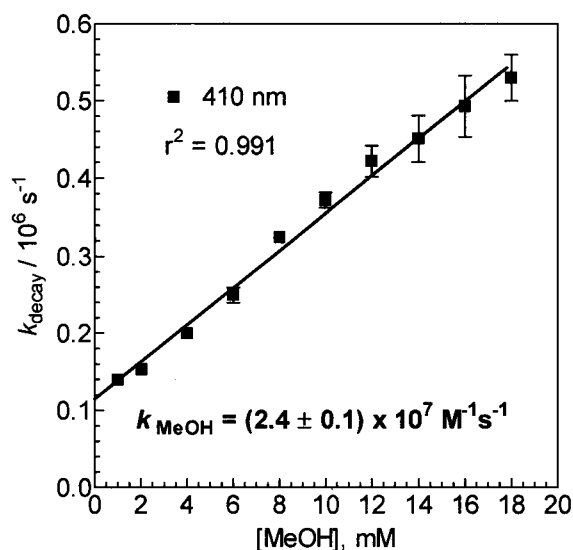
Figure 42. Plot of k_{decay} vs. [MeOH] for quenching of **30** upon 248 nm laser flash photolysis of **28** in dry, deoxygenated hexane solution at 23 ^{0}C.

The absolute rate constant recorded in this work is in reasonably good agreement with the value reported for the reaction of tetramethyldigermene with ethanol in cyclohexane solution, $k_Q = 4.9 \times 10^7 \ M^{-1}s^{-1}$ reported by Mochida *et*

al.[178] They suggested that nucleophilic attack of the alcohol oxygen at the unsaturated germanium center is the rate-determining step of the addition reaction based on the absence of a deuterium isotope effect.

Figure 43 **a** illustrates that on gradual addition of millimolar amounts of MeOH to the solution of **28,** the intensities of the signals due to **29** and **30** are progressively reduced with concomitant formation of a band centered at 320 nm, which is assigned to the Lewis acid-base complex of [PhMeGe:] with MeOH (**46**). Thus, at 5 mM MeOH ~ 50 % of **30** has been quenched and the complex is barely evident, at 30 mM MeOH ~ 85 % of the germylene has been scavenged and the complex is clearly evident, while at 50 mM MeOH the absorption spectrum of the complex is well defined and the absorptions due to the germylene and digermene are essentially completely suppressed.
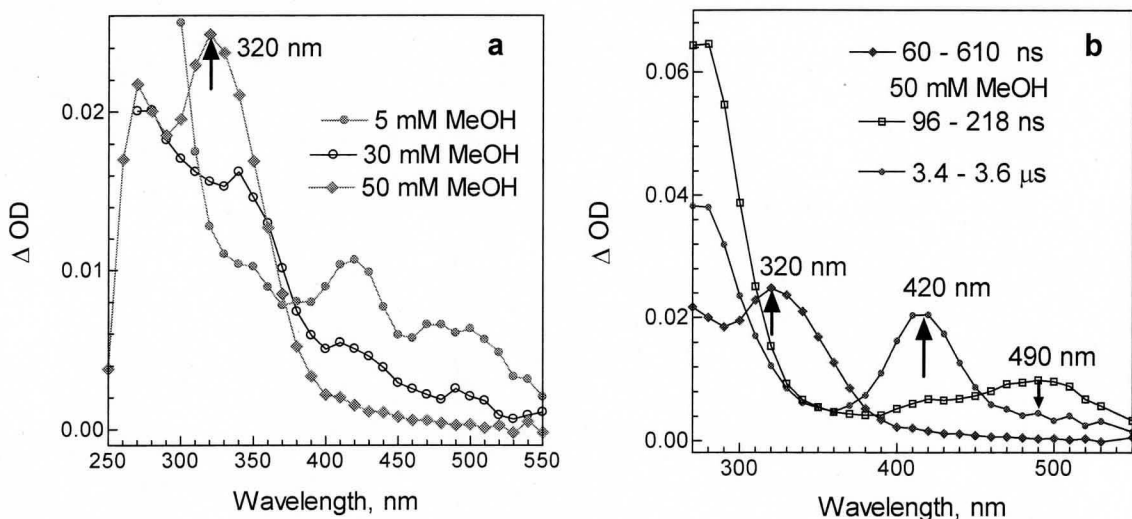
Figure 43 **a**) Transient absorption spectra recorded at different concentrations of MeOH, showing the gradual formation of the Lewis acid-base complex in dry hexane solution at 23 ^{0}C; **b**) Transient absorption spectra recorded in the absence and in the presence of the trapping reagent (50mM) under otherwise similar conditions.

Ando *et. al.*[114] reported electronic absorption maxima for several germylene-alcohol complexes in the range (320-367 nm) in hydrocarbon matrixes at 77 K (see Table 2). These results are in line with what we recorded for the phenylmethylgermylene-MeOH complex.

Therefore, our assignement of the new intermediate with λ_{max} at 320 nm to the PhMeGe-MeOH complex is based on comparison to data previously reported by Ando *et al.*[114] in low temperature glasses, results from our group for the

product reaction of [Ph$_2$Ge:] with MeOH in hexane solution (λ_{max} = 350 nm)[67] and

by comparison to the analogous silylene complexes with Lewis bases.[42, 139]

Figure 43 also demonstrates that the band due to the Lewis acid-base

complex with MeOH, as in the case of the complex with n-BuNH$_2$, is shifted to

shorter wavelengths compared to those of the corresponding free germylene and

its dimer. Furthermore, when the Me group is substituted by Ph on going from

[PhMeGe:], to [Ph$_2$Ge:] a red shift is observed in the absorption maximum

([PhMeGe:] λ_{max} = 320 nm; [Ph$_2$Ge:] λ_{max} = 350 nm). It should be pointed out that

as was previously mentioned,[114] the position of the absorption maxima of

germylene complexes provides an indication of the strength of the interaction

between the germylenes and the donor. The stronger the interaction of the lone

pair electrons of the Lewis base with the empty p-MO of the germylene the more

stable is the complex, the larger is the HOMO-LUMO separation in the complex,

and the larger the hypsochromic shift that is observed. In our particular case it

seems that the interaction between **29** and n-BuNH$_2$ is stronger (λ_{max} = 310 nm)

than the complex formed between the same germylene and MeOH (λ_{max} = 320

nm). This is in good agreement with what was suggested by Ando *et al.*, given

the much stronger basicity of the amine relative to the alcohol.[114, 140]

Our observations point to a relatively slow insertion into the OH bond of

the complex to form the final product. A typical decay trace of the 320 nm at

species at 50 mM MeOH is shown in Figure 44; the species decays with second

order kinetics and a lifetime $\tau \approx 1$ μs.
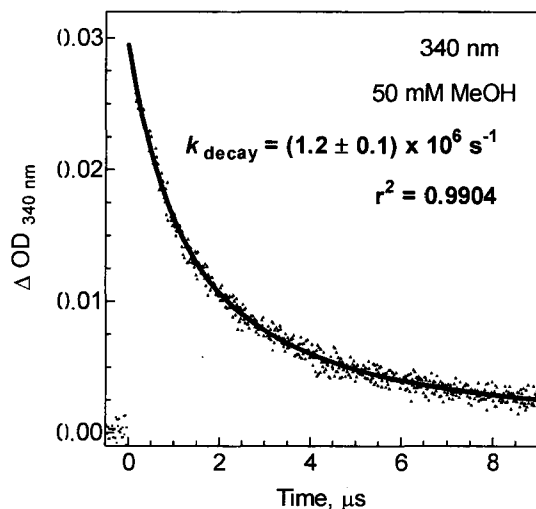
Figure 44. Decay trace of the species observed at 320 nm in dried, deoxygenated hexane containing 0.05 M MeOH (23 ^{0}C); the solid line represents the best fit of the data to a second order exponential decay.

A mechanistic model that is compatible with our data can be proposed based on observations for the reaction of [Me$_2$Si:] with alcohols in solution[41] and in the gas-phase.[183] Thus, we suggest that the reaction proceeds by initial electron pair donation into the empty p-orbital of **29**, with the reversible formation of the zwitterionic acid base complex. Proceeding to the final (alkoxygermane) product requires donation of the lone pair on germanium to the H as it migrates from O to Ge. (see Scheme 37). Alternatively, formation of **33** from the complex may proceed via a catalyzed proton transfer mechanism.
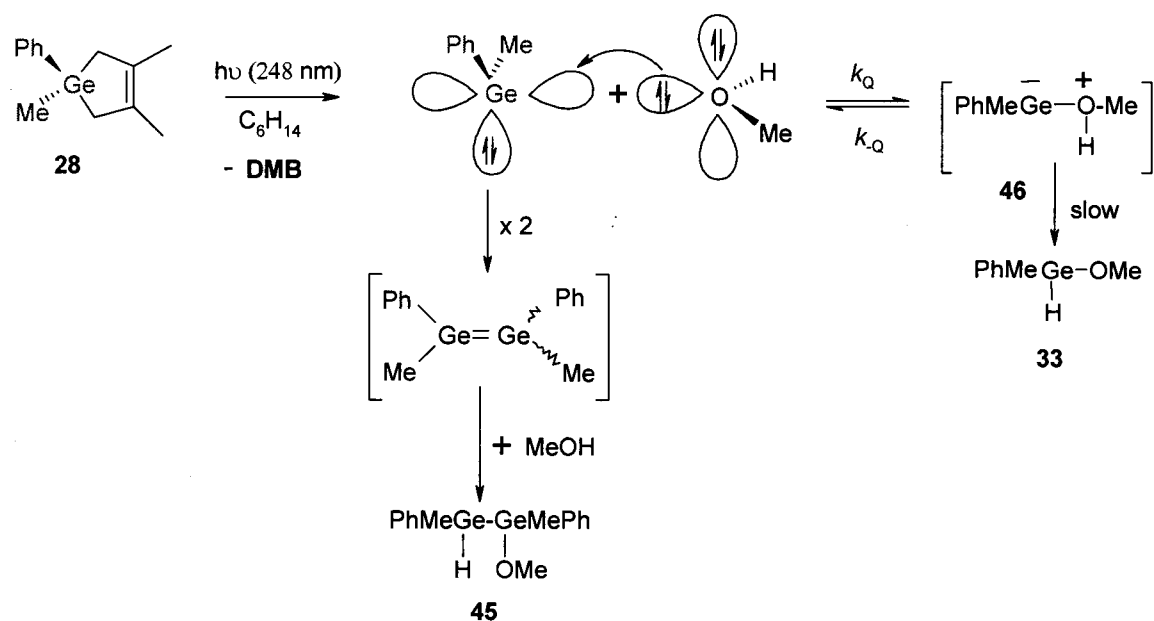
Scheme 37. Mechanistic considerations for the reaction of **29** with MeOH in dry, deoxygenated hexane solution at 23 ^{0}C.

Further studies are underway in our laboratory in the attempt to clarify this mechanism.[68]

2.8. Summary

The results of our exploratory laser flash photolysis study of the reactivity of **29** and **30** with a variety of irreversible and reversible germylene scavengers are listed in full detail in Table 10.

Reagent (Q)	PhMeGe[a]		PhMeGe=GeMePh[d]
	$k_Q / 10^9 M^{-1}s^{-1}$ [b]	K_{SV} / M^{-1} [c]	$k_Q / 10^9 M^{-1}s^{-1}$
n-BuNH$_2$	11.7 ± 0.7	14,750 ± 320	5.4 ± 0.3
Isoprene	8.0 ± 0.4	3,830 ± 87	(≤ 0.0041 ± 0.0002)[e]
t-BuAcetylene	6.0 ± 0.4	5,650 ± 120	-
AcOH	5.6± 0.2	5,300 ± 100	0.14 ± 0.01
n-Bu$_3$SnH	3.7 ± 0.2	5,047 ± 86	-
CCl$_4$	0.02 ± 0.01	43.2 ± 0.8	0.006 ± 0.001
MeOH	-	410 ± 15	0.024 ± 0.002

Table 10. Absolute rate (k_Q) and Stern-Volmer (K_{SV}) constants for reactions of phenylmethylgermylene (**29**) and diphenyldimethyldigermene (**30**) with the studied scavengers in dry, deoxygenated hexane solution at 23 °C.

a. Measured by laser flash photolysis of ca. 0.009 M solution of **28**. Errors are listed as ± 2σ from least squares analysis of data according to equation 5.
b. Measured according to equation 6, from a plot of [(Δ OD$_{410}$)$_{max, 0}$ / (Δ OD$_{410}$)$_{max,Q}$] vs. concentration of the quencher [Q], which are also linear.
c. Measured from linear dependency between rate constants k$_{decay}$ of **29** and scavengers concentrations, [Q] over the range where the intensity of the digermene signal is reduced to less than ca. 20 % of its initial value, according to equation 5.
d. Determined from plots of k$_{decay}$ of **30** vs. [Q]. Errors are listed as ± 2σ in the same manner as **29**.
e. Reported as upper limit and determined from decay kinetics of the digermene signal at the highest concentration of the scavenger.

For comparison Table 11 lists absolute rate constants for reaction of **29**, [Ph$_2$Ge:], and [Mes$_2$Ge:] with various scavengers.

| Reagent | k_Q / 10^9 $M^{-1}s^{-1}$ | | | |
	[PhMeGe:][a]	[Ph$_2$Ge:][b]	[Mes$_2$Ge:][c]	Ref.
n-BuNH$_2$	11.7 ± 0.7	10.1 ± 0.6	7.0 ± 0.3	this work, 67, 68
Isoprene	8.0 ± 0.4	5.5 ± 1.2	-	this work, 68
t-BuAcetylene	6.0 ± 0.4	5.2 ± 0.5	-	this work, 68
AcOH	5.6 ± 0.2	3.9 ± 0.7	1.6 ± 0.3	this work, 67, 68
n-Bu$_3$SnH	3.7 ± 0.2	3.5 ± 0.1	-	this work, 68
CCl$_4$	0.02 ± 0.01	0.01 ± 0.01	-	this work, 68

Table 11. Comparison of absolute rate constants for the reaction of simple germylenes with various scavengers in dry, deoxygenated hexane solutions at 23 ^{0}C.

a. Measured by laser flash photolysis of ca. 0.009 M solution of **28**. Errors are listed as ± 2σ from least squares analysis of data according to equations 5.

b. Measured by laser flash photolysis of ca. 0.003 M solution of **1c**. Errors are listed as ± 2σ from least squares analysis of data according to equations 5, 5a (from references 67, 68).

c. Measured by laser flash photolysis of ca. 0.004 M solution of **15**. Errors are listed in the same way (reference 68).

The results for all the trapping reagents studied in this work except MeOH

are consistent with irreversible reaction between [PhMeGe:] and the

corresponding scavenger. Generally, in irreversible cases the decay of the

germylene (**29**), at low reagent concentrations follows mixed pseudo-first and

second order kinetics due to competition with dimerization to **30**. As [Q]

increases and dimerization is largely suppressed (*i.e.* > 80 % quenching) the

signal decay profile of **29** follows first-order kinetics. Over this range of

concentrations the absolute rate constants for the germylene reaction are

determined. The behavior observed in the decay signals of **29** is accompanied by

a reduction in the maximum intensities of the signals due to **30**, an increase in its

apparent growth rate, and a shift of the concentration maximum to shorter time

scales (see Scheme 38).

28

248 nm $\quad$ hυ

Product $\xleftarrow{\quad +\cdot Q \quad}_{k_Q}$ [PhMeGe:] $\xrightarrow{\quad + \text{[PhMeGe:]} \quad}_{k_{dim}}$ Dimer

$\qquad\qquad\qquad\qquad$ **29** $\qquad\qquad\qquad\qquad$ **30**
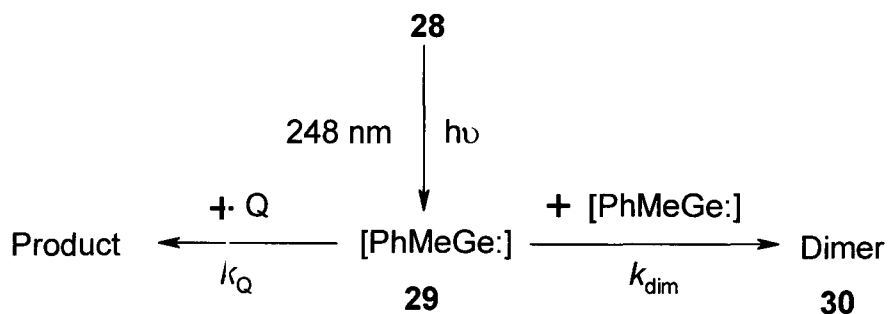
$d[\text{PhMeGe:}]/dt = \{2k_{dim}[\text{PhMeGe:}] + k_Q[Q]\}[\text{PhMeGe:}]$

- at low [Q] when $k_Q[Q] < k_{dim}[\text{PhMeGe:}]$ $\Longrightarrow$ mixed pseudo-first and second order kinetics

- as [Q] increses when $k_Q[Q] >> k_{dim}[\text{PhMeGe:}]$ $\Longrightarrow$ pseudo-first order kinetics

Scheme 38. The hallmarks of irreversible reaction of [PhMeGe:] with studied scavengers.

In the case of reaction of **29** with MeOH, the results are consistent with reversible behavior. In this situation the germylene decay profiles should show a fast component due to competition between dimerization and pseudo-first order approach to equilibrium with the formation of the Lewis acid-base complex, and a slower one that involves the dimerization of the residual free **29** after equilibration is complete. The time evolution of the digermene signals shows an initially rapid growth, a reduction in the maximum intensities on gradual addition of MeOH, and a shift of the maximum to longer times after the laser pulse (see Scheme 39).

28

248 nm │ hʋ

+ MeOH
k_Q

Intermediate ⇌ [PhMeGe:] $\xrightarrow{+ [PhMeGe:]}$ Dimer

k_{-Q} **29** k_{dim} **30**

slow │ k_2

[PhMeHGeOMe]
44
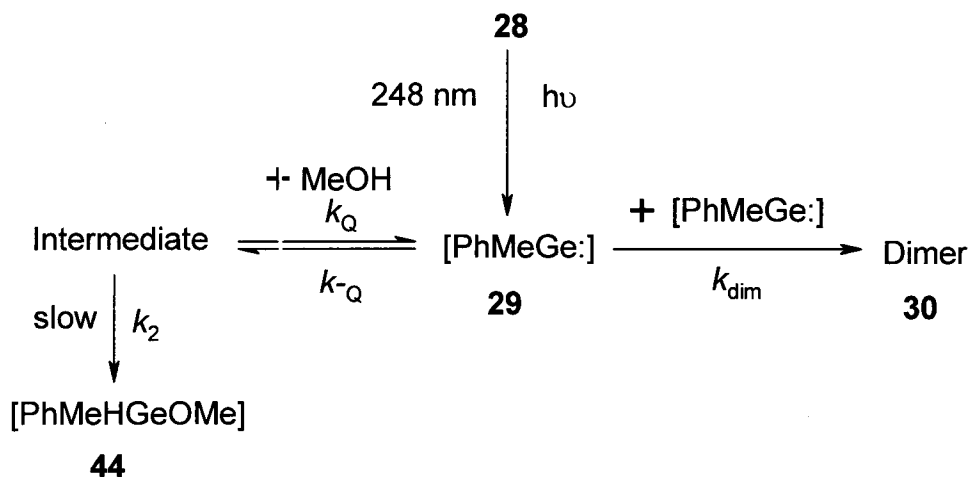
$$d[\textbf{44}]/dt = \text{Rate} = k_Q k_2 [\text{PhMeGe:}][\text{MeOH}]/(k_{-Q} + k_2)$$

- when $k_{-Q} \gg k_2 \implies$ Rate = $(k_2 k_Q / k_{-Q})[\text{PhMeGe:}][\text{MeOH}]$ or

$$\text{Rate} = k_2 K_{eq} [\text{PhMeGe:}][\text{MeOH}]$$

- when $k_{-Q} \approx k_Q$ there is a rapid established pre-equilibrium between

reactants and the intermediate (equilibrium constant Keq).

Scheme 39. The hallmarks of reversible reaction of [PhMeGe:] with MeOH.

Chapter 3

CONCLUSIONS AND FUTURE WORK

3.1 Conclusions

Phenylmethylgermylene (**29**) and 1,2-dimethyl-1,2-diphenyldigermene (**30**) have been detected and characterized directly in hydrocarbon solution by nanosecond laser flash photolysis. The germylene of interest is formed by photodecomposition of 1,3,4- trimethyl-1-phenylgermacyclopent-3-ene (**28**).

This photochemical precursor was demonstrated to be a clean and efficient source of **29** by steady-state trapping experiments. Using conventional UV lamps (254 nm) as the excitation source, trapping experiments with isoprene and methanol show that [PhMeGe:] extrusion is the major reaction pathway, leading to the expected products of reaction of the germylene with the corresponding scavengers in essentially quantitative yields.

Laser flash photolysis of a continuously flowing, deoxygenated hexane solution of **28** leads to the prompt formation of a weak transient which exhibits a long-wavelength UV-VIS absorption at λ_{max} = 490 nm and which was assigned to [PhMeGe:] (**29**). The species dimerizes in hexane solution at ambient temperature to form a second transient (**30**) which is a significantly stronger absorber, exhibiting λ_{max} = 420 nm and decaying with mixed first- and second-

order kinetics and a lifetime, $\tau \sim 8 \, \mu s$. The UV-VIS spectra and kinetic behavior of **29** and its dimer, **30,** are similar to those for other simple germylenes such as dimethyl-, diphenyl-, and dimesitylgermylene, and also with the reported spectra of the corresponding silicon analogues.

The present thesis demonstrates that the successful detection of **29** in hydrocarbon solution depends on several key factors, of which the choice of the photochemical precursor employed for generation of the species is the major one. Generation of short-lived germylenes from cyclopolygermanes (**2**), 7-germanorbornadiene derivatives (**3**), polygermanes or disilagermanes (**4**) or germetanes (**5**) seems to be accompanied by the formation of germanium-centered radicals or conjugated germenes, which absorb much more strongly in the same UV-VIS region where the germylenes of interest do. This makes an unequivocal assignment of the transients observed very difficult. This complication is not a factor with **28**, as the trapping experiments show that it yields only **29** upon photolysis in solution. This greatly simplifies the task of assigning the transients observed upon laser flash photolysis of the compound.

The kinetic studies of selected reactions of **29** allow us to compare its reactivity to those of other simple heavy carbene analogues quantitatively. The reactions studied include N-H, O-H and Sn-H insertion reactions, the [1+2] addition to alkynes and isoprene, and halogen atom abstraction from carbon tetrachloride.

With most of the scavengers analyzed (all but MeOH) the data are consistent with irreversible scavenging. Generally, addition of increasing amounts of corresponding scavenger to the deoxygenated hexane solution of **28** results in an enhancement in the decay rate of the signal attributed to **29** and a shortening of its lifetime. The maximum intensities of the signal due to **30** show a reduction after each addition and a shift of its concentration maximum to shorter times, which occurs because dimerization dominates the early part of the germylene decay where the concentration of the transient is highest. Once sufficient trapping reagent is added and the competitive formation of the digermene is almost suppressed (70- 80% quenched) the decay kinetics of **30** changes from mixed first- and second-order to pseudo-first-order.

Gradual addition of methanol also has the effect of reducing the maximum intensities of the signals due to **30** but the maximum shifts to longer times scales after the laser pulse, indicating that dimerization persists even when the germylene can no longer be detected. This, along with other aspects of the kinetic behavior, is consistent with reversible reaction of the germylene with the scavenger, to form a product whose subsequent reaction is relatively slow. This product has been identified as the Lewis acid-base complex of the germylene with methanol.

It has also been shown that the reactivity towards the studied reagents decreases on going from dimethyl to diphenyl *via* phenylmethylgermylene. However the decrease is not very pronounced. Thus, this thesis serves as a link

between dimethyl-and diphenylgermylene and provides the first indication of the effects of substitution on the spectral properties and reactivity of simple germylenes in solution.

Moreover, the experiments performed in this work have conclusively demonstrated that the pattern of reactivity of germylenes is similar to that of silylenes. These species react with the same types of scavengers at comparable rates, and the mechanisms of these reactions appear to be much the same. This conclusion may seem to be in contradiction with the impression created by the previous studies in solution, which suggested a stronger decrease in reactivity and a difference in kinetic behavior on going from silylenes to germylenes.

3. 2. Future Work

The photolysis of **28** provides a versatile methodology for the clean and remarkably efficient generation of [PhMeGe:] (**29**) and its dimerization products, E- and Z-1,2-dimethyl-1,2-diphenyldigermene (**30**), under conditions where they can be detected directly and the kinetics of some of their reactions determined. This has provided very important quantitative information about the reactivity, spectroscopic properties, and influence of phenyl-substitution on the reactivities of these species. Nevertheless, the list of reactions that have been studied is still fairly limited. Further work needs to be done to fully explore germylene and

digermene reactivity towards other types of molecules, such as oxygen, secondary and tertiary amines, alkenes, other group 14 hydrides R_3MH (M = Si, Ge), secondary and tertiary-alcohols and ethers. As well, our understanding of the mechanisms by which germylenes react with is still incomplete. These reactions are not simple and often include several stages. Therefore, a lot remains to be done to elucidate the pre-reaction complexes proposed as the first formed intermediates in some of these reactions.

Further efforts should focuse on revealing the kinetic and mechanistic differences between irreversible and reversible scavengers. We mentioned that **28** represent an ideal photochemical precursor to phenylmethylgermylene for time-resolved spectroscopic experiments. Para-substituents on the phenyl group of **29** should have little effect on the photochemistry of the precursor, but significant and mechanistically informative effects on the reactivities of the resulting germylene. For example, adding electron-withdrawing substituents to the para position of the phenyl groups may enhance the reactivity of the resulting germylene while electron-donating groups will have the opposite effect. It is noteworthy to study the reactivity of **28** in these conditions.

Chapter 4

EXPERIMENTAL

4.1. General

^{1}H and ^{13}C NMR spectra were recorded on Bruker AV 200 or AV 600 NMR spectrometers in deuterated chloroform or cyclohexane-d_{12} solutions and are reported in parts per million downfield from tetramethylsilane using residual solvent-proton resonances as the internal standard. Ultraviolet absorption spectra were recorded on a Cary 50 Scan (Varian) UV-VIS spectrophotometer interfaced to a Pentium microcomputer. Gas chromatographic (GC) analyses were carried out using a Hewlett-Packard 5890 Series II gas chromatograph equipped with a HP3396A integrator, a flame ionization detector and a DB-5 column (30 m, 0.25 μm; Supelco, Inc.). All gas chromatograms were recorded under the following conditions:

-injection temperature 220 ^{0}C, detector temperature 250 ^{0}C,

-initial temperature 50 ^{0}C for 1 min,

-10^0/min ramp to the final temperature 250 ^{0}C,

-final temperature 250 ^{0}C for 5 min.

Gas chromatographic/mass spectrometric (GC/MS) separations employed a Hewlett-Packard 5890 Series II gas chromatograph equipped with a HP-5971A mass selective detector and a SPB-5 capillary column (25 m, 0.25 μm; Supelco,

Inc.). High-resolution electron impact mass spectra and exact masses were determined on a Micromass TofSpec 2E mass spectrometer. Exact masses were determined for the molecular ion (M^+), employing a mass of 12.000000 for carbon-12. Radial chromatographic separations were carried out using a Chromatotron® (Harrison Research, Inc.), with silica gel 60 plates (4 mm thick) and using pentane as the eluant. Column chromatography employed a 30 mm x 800 mm column using Silica Gel (120 g, acid washed, 230-400 mesh ASTM, particle size 0.040-0.063 mm) (Silicycle) and pentane as the eluant. Steady state photolyses employed a Rayonet® photochemical reactor (Southern New England Ultraviolet Co.) equipped with a merry-go-round apparatus and 6 RPR-2537 lamps (254 nm).

4.2. Commercial Reagents and Solvents

Germanium tetrachloride (99.9%) and 1,1,3,3-tetramethyldisiloxane were were used as received from Gelest Inc., 1,4-Dioxane (99.9%), 2,3-dimethyl-1,3-butadiene, isoprene, phenylmagnesium bromide (3.0 M solution in diethyl ether), methylmagnesium bromide (3.0 M solution in diethyl ether) and magnesium were used as received from Sigma-Aldrich. Methanol (99.9%) was of the highest purity available from Sigma-Aldrich Co and was used as received. Hexane (Caledon Reagent or Omnisolv HPLC grade) was dried by refluxing for several days under

nitrogen with sodium/potassium amalgam followed by distillation. Diethyl ether (Caledon Reagent) and tetrahydrofuran (Caledon Reagent) were dried by passage through activated alumina under nitrogen using a Solv-Tec solvent purification system (Solv-Tec, Inc.). Pentane (Omnisolv HPLC grade) was used as received from Caledon. n-Buthylamine (Sigma-Aldrich) was refluxed for 12 hours over potassium hydroxide followed by distillation. Isoprene (Sigma-Aldrich) was purified by distillation. Glacial acetic acid was used as received from Caledon. Deuterated materials were used as received from Cambridge Isotopes Laboratories.

4.3. Nanosecond Laser Flash Photolysis

Nanosecond laser flash photolysis experiments employed the pulses from a Lambda Physik Compex 120 excimer laser, filled with F_2/Kr/Ne (248 nm; ~25 ns; 100 ± 5 mJ) gas mixtures and a Luzchem Research nLFP-111 laser flash photolysis system. An external 150-watt high pressure Xe lamp as monitoring source, powered by a Kratos LPS-251HR power supply, was incorporated in the latter system to provide a dynamic range in time of 10^6 (1 μs to 1 s full scale). A Pyrex filter inserted between the sample cell and monochromator protects the PMT from scattered light from the laser when the monitoring wavelength is ≥ 300 nm; the excitation beam is delivered at a 90^0 angle relative to the monitoring

beam through a 5 mm diameter circular slit, which defines the path length over which the transients are produced.[67, 105, 184]

Solutions were prepared at concentrations such that the absorbance at the excitation wavelength (248 nm) was ~ 0.7-0.8, and were flowed continuously through a 7x7 mm Suprasil flow cell connected to a calibrated 100 mL Pyrex reservoir, fitted with a glass frit to allow bubbling of nitrogen gas through the solution for ~ 1 hour prior to and then throughout the duration of each experiment. Solution temperatures were controlled to within 0.1 ^{0}C with a VWR 1166 constant-temperature circulating bath plumbed to a brass sample holder. The temperature of the solutions was measured with a Teflon-coated copper/constantan thermocouple inserted directly into the flow cell. The glassware, sample cells and the transfer lines used for these experiments were stored in 65 ^{0}C vacuum oven between experiments. Prior to assembling the sample-handing system at the beginning of each experiment and every time the oven was opened to the atmosphere a stream of dry nitrogen was vented into it to minimize the contact with atmospheric moisture. Quenchers were added directly to the reservoir by microliter syringe as aliquots of standard solutions.

Raw data from the Luzchem nLFP software were imported and processed *via* Excel using the Prism 3.0 software package (GraphPad Software, Inc.).

Rate constants were calculated by linear least-squares analysis of decay rate *vs.* concentration. These data spanned as large a range in transient decay rate as possible but generally to a maximum of *ca.* 20%. Non-linear least squares

analysis of the absorbance-time profiles and the appropriate user-defined fitting equations allowed the calculation of transient decay and growth rate constants. Errors are quoted as twice the standard deviation obtained from the least-squares analysis in each case. Transient absorption spectra at a particular time after the laser flash were constructed from the kinetic traces at many wavelengths.

4.4. Preparation and Characterization of Compounds

4.4.1. Preparation of 1,1-dichloro-3,4-dimethyl-1-germacyclopent-3-ene (27)

The complex of germanium dichloride with 1,4-dioxane was prepared by a modified procedure of *Kolesnikov et al.*[185] and *Viktorov et al.*[186]

Into a flame-dried, 500 mL one neck round-bottom flask equipped with a reflux condenser and a nitrogen inlet were placed 1,4-dioxane (18.0 g, 0.204 mol, 17.4 mL), 1,1,3,3-tetramethyldisiloxane (17.3 g, 0.129 mol, 22.8 mL) and germanium tetrachloride (25.0 g, 0.117 mol, 13.3 mL). The reaction mixture was heated at 50 ^{0}C until the first bubbles of HCl were formed, and then the temperature was raised to 80-85 ^{0}C. At this temperature after 1 h long white crystals were formed on the bottom of the flask. After another 12 h at 85 ^{0}C the resulting suspension of colorless crystals was cooled and the excess solution was decanted off. The crystals were washed with pentane (5 x 20 mL), and then pumped on under

vacuum for 30 min to yield the $GeCl_2$-dioxane complex as colorless needles (22.0 g, 0.095 mol, 82 %, mp =100-150 ^0C).[67]

Compound **27** was prepared by a modification[67] of the procedures of *Nefedov et al.*[187] and *Kolesnikov et al.*[188, 189] $GeCl_2$-dioxane (5.0 g, 0.0216 mol) and dry THF (50 ml) were combined in a flame-dried two-necked round bottom 100 mL flask fitted with a reflux condenser, addition funnel, nitrogen inlet and magnetic stir bar. The reaction mixture was heated to reflux (70-75 ^0C) with stirring under nitrogen, and after *ca.* 10 min at this temperature a solution of 2,3-dimethyl-1,3-butadiene (2.3 g, 0.028 mol, 3.2 mL) in dry THF (10 mL) was added dropwise over 1 h. The solution was stirred for another 2 h and the apparatus was quickly reconfigured for distillation. When most of the solvent had distilled off, the apparatus was connected to a vacuum pump and the resulted colorless liquid (4.30 g, 0.019 moles, 88%; bp = 60-63 ^0C, 0.5 mmHg) was collected. The boiling point and ^1H NMR spectrum of the compound were in good agreement with previously reported data for the desired product, **27**.[187]

^1H NMR ($CDCl_3$, 200 MHz): δ = 1.78 (s, 6 H, CMe), 2.20 (s, 4H, CH_2); ^{13}C NMR ($CDCl_3$, 200 MHz): δ = 18.65 (CMe), 32.76 (CH_2Ge), 129.03 (-C=).

4.4.2. Preparation of 1,3,4-Trimethyl-1-phenyl-1-germacyclopent-3-ene (28)

1,3,4-Trimethyl-1-phenyl-1-germacyclopent-3-ene (**28**) was synthesized by a procedure similar to that of *Mazerolles et al.*[190] In a flame-dried apparatus consisting of a 250 mL two-necked round-bottom flask, reflux condenser, nitrogen inlet, addition funnel, and magnetic stirrer was prepared a solution of 1,1-dichloro-3,4-dimethyl-1-germacyclopent-3-ene (3.7 g, 0.0163 mol) in anhydrous diethyl ether (80 ml). The solution was cooled to 0 ^{0}C using an ice-bath and then from the addition funnel was added dropwise over 1 h, with stirring, a solution of phenylmagnesium bromide (5.7 mL of a 3.0 M solution in diethyl ether, 0.01713 mol) in dry diethyl ether (20 mL). The cooling bath was removed after 2 h and the reaction mixture, which contained a large amount of white precipitate, was stirred at room temperature for another 20 h under nitrogen. A solution of methylmagnesium bromide (6.3 mL of a 3.0 M solution in diethyl ether, 0.01885 mol) in anhydrous diethyl ether (20 mL) was then added dropwise via addition funnel over 1 h with continuous stirring. After the addition the reaction mixture was stirred under reflux for another 3 h. After cooling, the resulting yellow solution was hydrolyzed with saturated aqueous ammonium chloride (40 mL) over 20 min, transferred to a separatory funnel, and the aqueous and organic fractions were separated. The aqueous fraction was extracted with diethyl ether (3 x 60 mL), and then the combined ether fractions were washed with distilled water (2 x 30 mL), 5 % aqueous sodium bicarbonate (2 x 30 mL), dried with anhydrous magnesium sulfate (30 min), and filtered. The

solvent was removed on a rotary evaporator to yield a yellow-green liquid (4.4 g).

Distillation under vacuum (bp = 103-105 ^{0}C at 0.3 mmHg) afforded **28** (3.78 g;

0.0152 mol, 86 %), as a colourless liquid. Further purification of **28** by column

chromatography using pentane as eluent was performed until the purity of the

compound was at least 99% according to GC analysis. The ^{1}H NMR spectrum of

the compound agreed well with that previously reported.[45]

^{1}H NMR (CDCl$_3$, 200 MHz): δ = 0.56 (s, 3H, GeMe), 1.74 (s, 10 H, CH$_2$, CMe),

7.31-7.51 (m, 5H, Ar-H); ^{13}C NMR (CDCl$_3$): δ = - 4.45 (GeMe), 19.41 (CH$_2$),

26.44 (CMe), 127.99 (ortho or meta CH), 128.45 (para CH), 130.90 (-C=), 133.25

(ortho or meta CH); MS: m/z = 248 (65), 246 (40), 233 (38), 231 (36), 229 (20),

166 (70), 151 (base, 100), 149 (85), 147 (80); Exact mass: calc. for C$_{13}$H$_{18}$Ge,

248,0620; found 248.0617 (Figure 45, 46) .
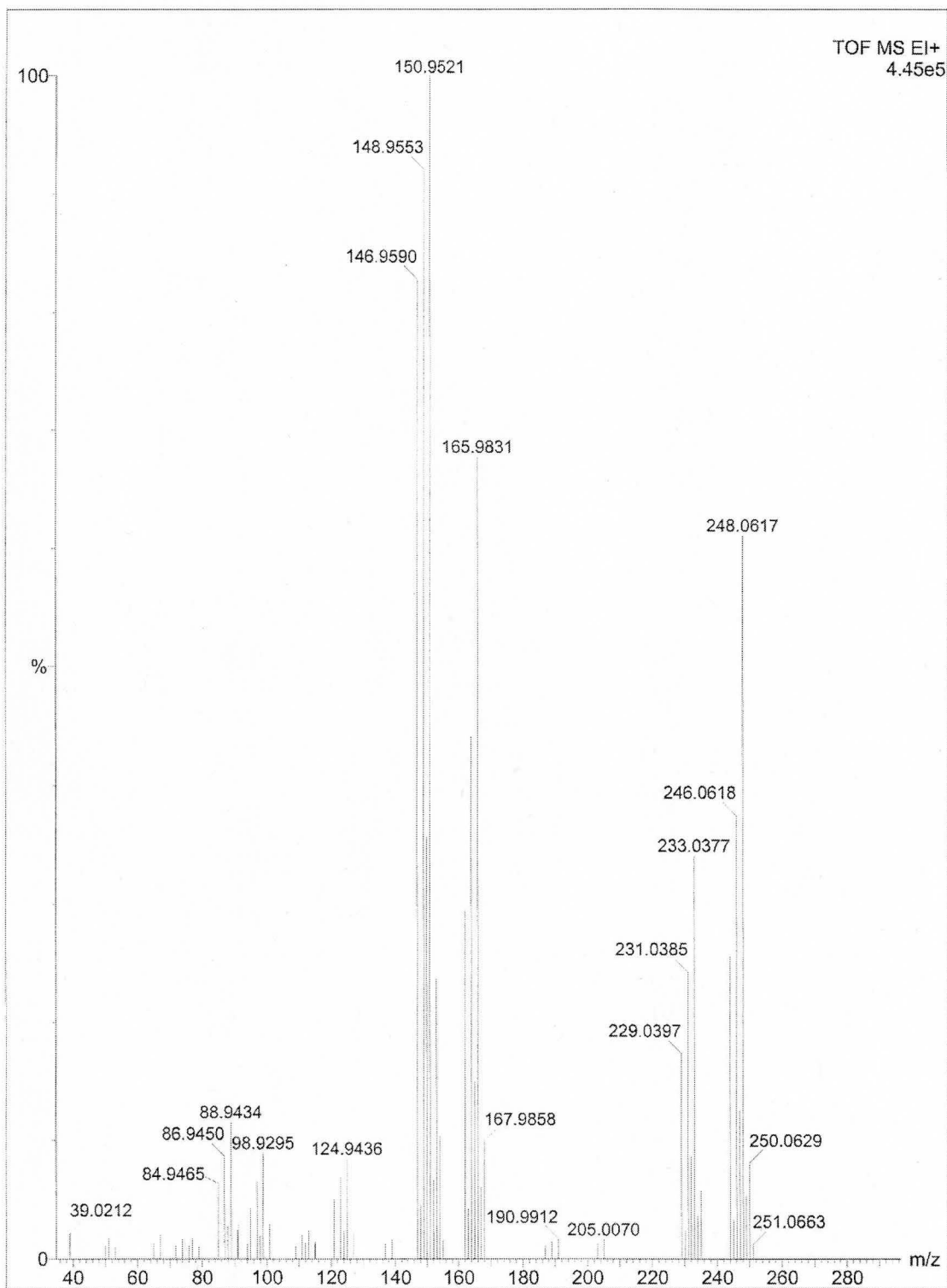
Figure 45. Mass Spectrum of **28**.

Single Mass Analysis
Tolerance = 10.0 mDa   /   DBE: min = -1.5, max = 50.0
Isotope cluster parameters: Separation = 1.0   Abundance = 1.0%

Monoisotopic Mass, Odd and Even Electron Ions
9 formula(e) evaluated with 2 results within limits (up to 50 closest results for each mass)

| Minimum: | | | | -1.5 | | |
| Maximum: | | 10.0 | 5.0 | 50.0 | | |

Mass	Calc. Mass	mDa	PPM	DBE	Score	Formula
248.0617	248.0620	-0.4	-1.4	5.0	2	C13 H18 Ge
	248.0626	-0.9	-3.7	17.0	1	C20 H8

Figure 46. Elemental composition report of **28**.

4.4.3. Preparation of 1,3-dimethyl-1-phenyl-1-germacyclopent-3-ene (31)

1,3-Dimethyl-1-phenyl-1-germacyclopent-3-ene **(31)** was prepared in a similar way as **28**. A solution of GeCl₂-dioxane (4.0 g, 0.0173 mol) in anhydrous THF (50 mL) was placed in a flame-dried apparatus consisting of a 100 mL two-necked round-bottom flask, reflux condenser, nitrogen inlet, addition funnel, and magnetic stirrer. The solution was heated to reflux with stirring under nitrogen, and then a solution of isoprene (1.53 g, 2.2 mL, 0.0225 mol) in dry THF (10 mL) was added dropwise over 1.5 h. After addition, the solution was stirred for

another 10 h under nitrogen at room temperature. The apparatus was reconfigured for distillation, and most of the solvent was distilled off. The distillation was continued under vacuum to afford 1,1-dichloro-3-methyl-1-germacyclopent-3-ene as a colorless liquid (2.0 g, 0.009 mol, 56%, bp = 28-30 ^{0}C, 0.2 mmHg) which was identified based on ^{1}H NMR and ^{13}C NMR spectra.

^{1}H NMR (CDCl$_3$, 200 MHz): δ = 1.85 (s, 3H, CMe), 2.07 (s, 2H, CH$_2$CMe), 2.22 (s, 2H, CH$_2$CH), 5.75 (s, 1H, CH=); ^{13}C NMR (CDCl$_3$, 200 MHz): δ = 22.82 (Me), 27.57(C-CH=), 29.41 (C-CMe), 122.06 (-CH=), 137.84 (-C=).

The product from above (2.0 g, 0.009 mol) in anhydrous diethyl ether (40 mL) was introduced into a flame-dried apparatus consisting of two-necked round-bottom flask (100 mL), reflux condenser, nitrogen inlet, addition funnel, and magnetic stirrer. After cooling to 0 ^{0}C using an ice-bath, a solution of phenyl magnesium bromide (3.3 mL of a 3.0 M solution in diethyl ether, 0.0098 mol) in dry diethyl ether (20 mL) was added dropwise over 1.5 h with stirring. The cooling bath was removed after 2 h and the reaction mixture, which contained a large amount of white precipitate, was stirred at room temperature for another 15 h under nitrogen. A solution of methyl magnesium bromide (4.1 mL of a 3.0 M solution in diethyl ether, 0.0122 mol) in anhydrous diethyl ether (20 mL) was then added dropwise via addition funnel over 1.5 h with continuous stirring. At the end of the addition the reaction mixture was stirred under reflux for another 4 h. After cooling, the resulting yellow solution was hydrolyzed with saturated aqueous

ammonium chloride (40 mL) over 20 min, transferred to a separatory funnel, where the aqueous and organic fractions were separated. The aqueous fraction was extracted with diethyl ether (3 x 60 mL), and then the combined ether fractions were washed with distilled water (2 x 30 mL), 5 % aqueous sodium bicarbonate (2 x 30 mL), dried with anhydrous magnesium sulfate (30 min), and filtered. The solvent was removed on a rotary evaporator to yield a yellow oil (2.3 g). Purification was accomplished using silica gel column chromatography with pentane as the eluting solvent, affording the product **31** (2.2 g, 0.0094 mol, 56 %) in > 99 % purity according to GC analysis. It was identified as **31** on the basis of the following spectroscopic data: ^{1}H NMR (CDCl$_3$, 200 MHz): δ = 0.58 (s, 3H, GeMe), 1.23-1.80 (m, 7 H, CH$_2$, CMe), 5.64 (s, 1H, -CH=), 7.24-7.50 (m, 5H, Ar-H); ^{13}C NMR (CDCl$_3$,): δ= - 4.15 (GeMe), 14.16 (CMe), 22.74 (CH$_2$), 31.69 (C-CMe), 125.44 (CH-CH$_2$), 128.09 (para CH), 128.58 (ortho or meta CH), 130.90 (-C=), 133.21 (ortho or meta CH), 140,33 (ipso C); MS: m/z = 234 (35), 220 (67), 219 (36), 217 (15), 166 (40), 151 (base, 100), 149 (85), 147 (50), 122 (20); Exact mass: calc. for C$_{12}$H$_{16}$Ge, 234.0464; found 234.0446 (Figure 47, 48, 49)
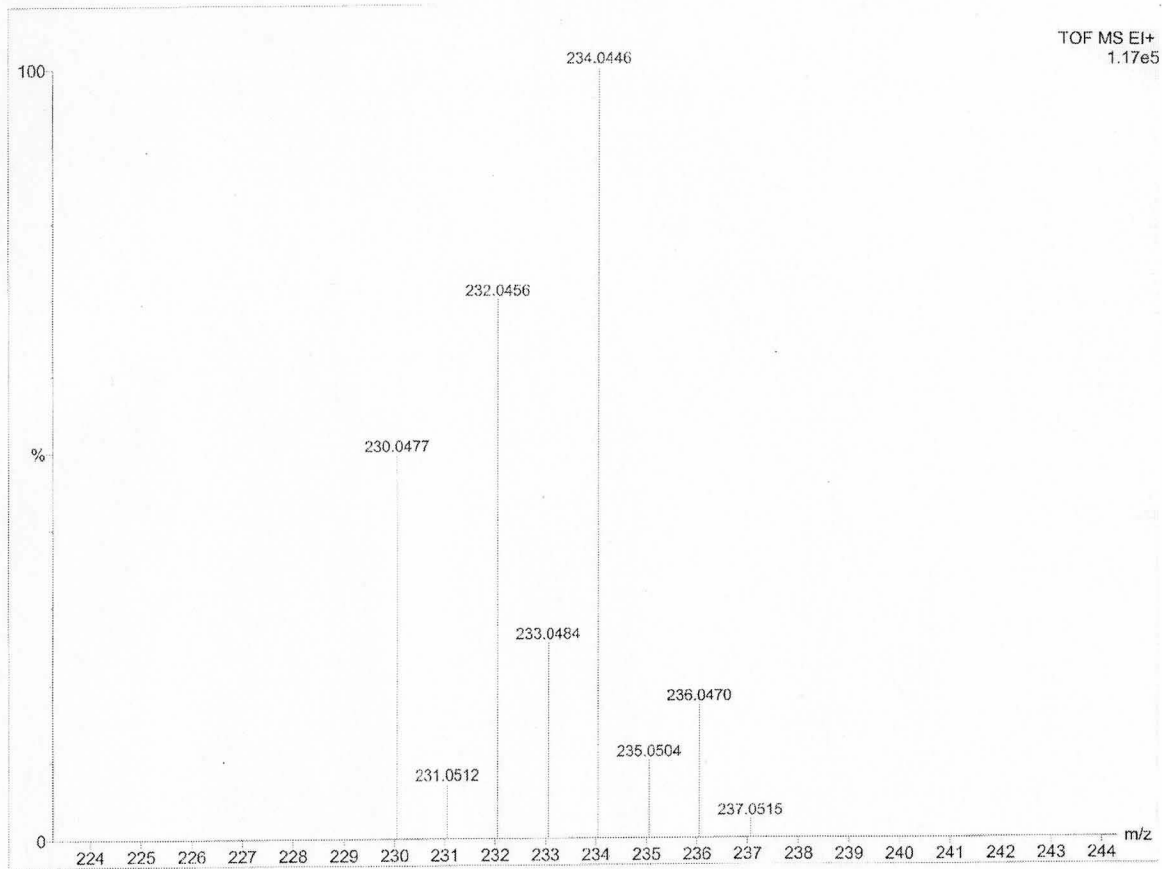
Figure 47. Mass Spectrum of **31**.

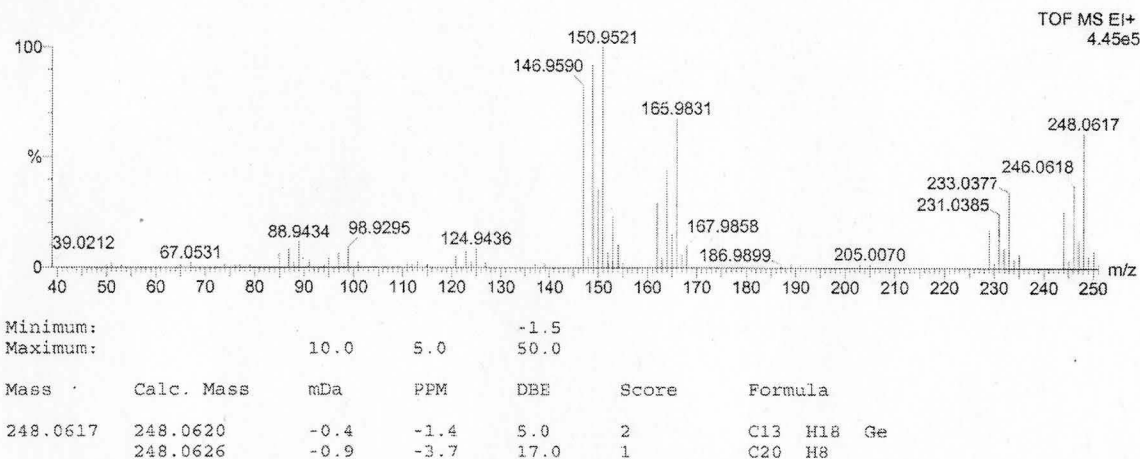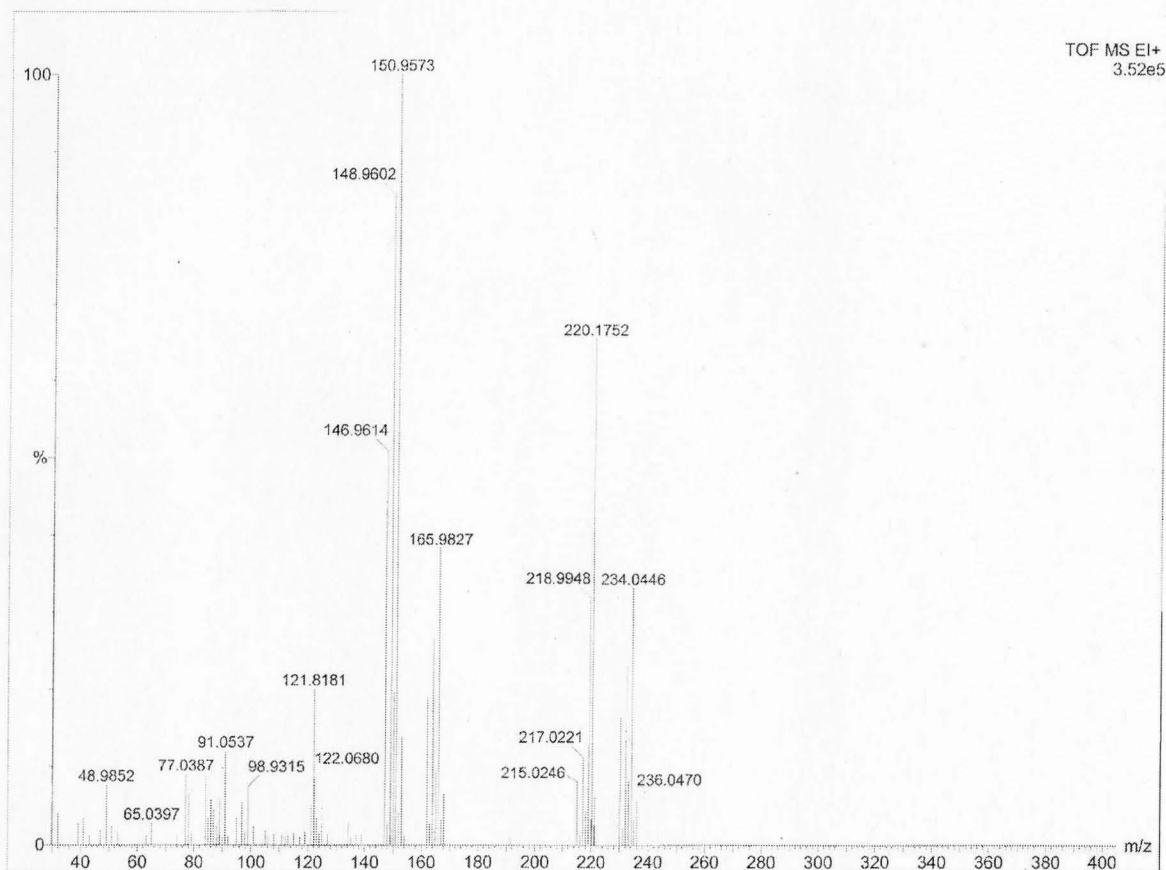Figure 48. Mass spectrum of **31**.

Single Mass Analysis
Tolerance = 10.0 mDa / DBE: min = -1.5, max = 50.0
Isotope cluster parameters: Separation = 1.0 Abundance = 1.0%

Monoisotopic Mass, Odd and Even Electron Ions
6 formula(e) evaluated with 2 results within limits (up to 50 closest results for each mass)

I7133: CH MW=243
WJL7133 100 (1.666) Cm (100:110-204:214x2.000)   TOF MS EI+
                                                                                            1.17e5
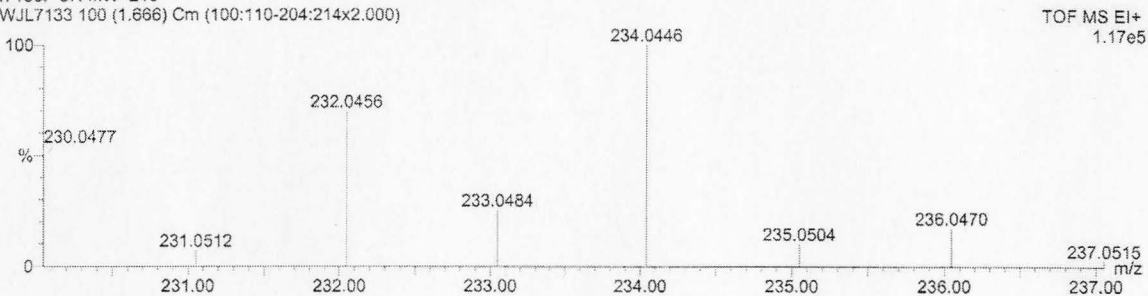
Minimum:				-1.5		
Maximum:		10.0	15.0	50.0		
Mass	Calc. Mass	mDa	PPM	DBE	Score	Formula
234.0446	234.0464	-1.8	-7.7	5.0	2	C12 H16 Ge
	234.0470	-2.4	-10.1	17.0	1	C19 H6

Figure 49. Elemental Composition Report of **31**.

4.5 Steady-State Photolysis

4.5.1. Steady State Photolysis of 1,3,4-Trimethyl-1-phenyl-1-germacyclopent-3-ene (28) in presence of Methanol

Photolysis of **28** was carried out in septa-sealed quartz NMR tubes (5 mm) using solutions of 0.05 M substrate containing 0.5 M methanol and 0.5 M MeOD in argon-saturated cyclohexane-d_{12}, and was monitored by ^{1}H NMR. The conversion was taken to *ca.* 40 % (*ca.* 25 min total irradiation time) with periodic monitoring by ^{1}H NMR over the course of the photolysis. The formation of

phenylmethylgermylene adduct with methanol was accompanied in every experiment by an equal yield of 2,3-dimethyl-1,3-butadiene (**DMB**). Accurate detection of the methoxygermane (**33**) by GC was difficult due to decomposition on the column. Our assignment was based on previously reported data[67, 130] and on the following spectroscopic data:

^{1}H NMR (C$_6$D$_{12}$, 600 MHz): δ = 0.6 (d, 3H, GeMe), 3.45 (s, 3H, GeOCH$_3$), 5.7 (q, 1H, Ge-H), 7.2-7.5 (m, 5H, Ar-H); MS (EI) m/z = 183 (17), 167 (base, 100), 151 (55), 123 (22), 89 (98), 85 (50), 51 (37).
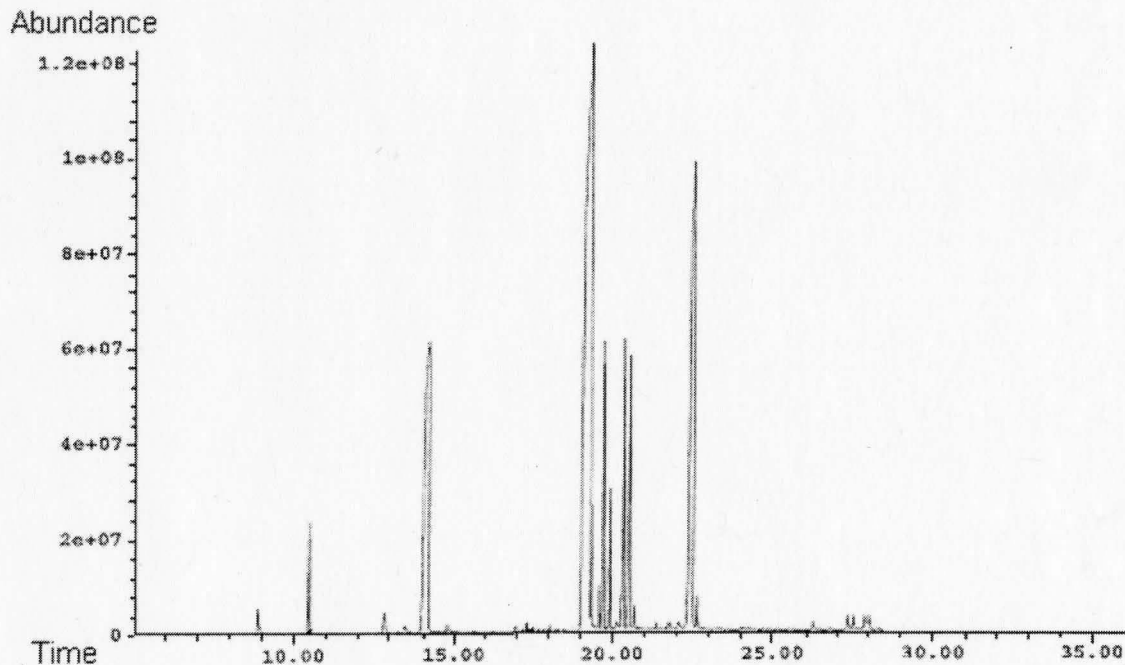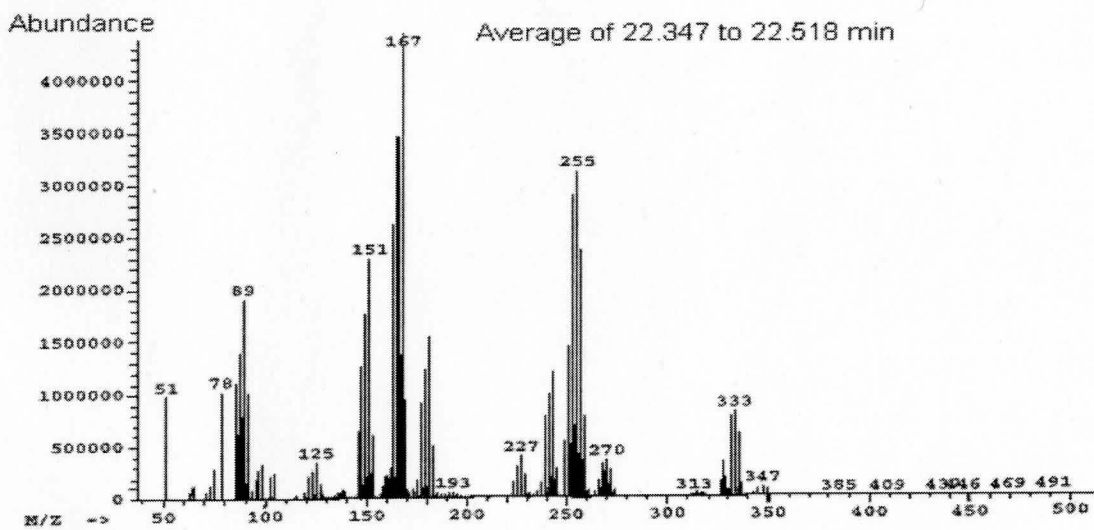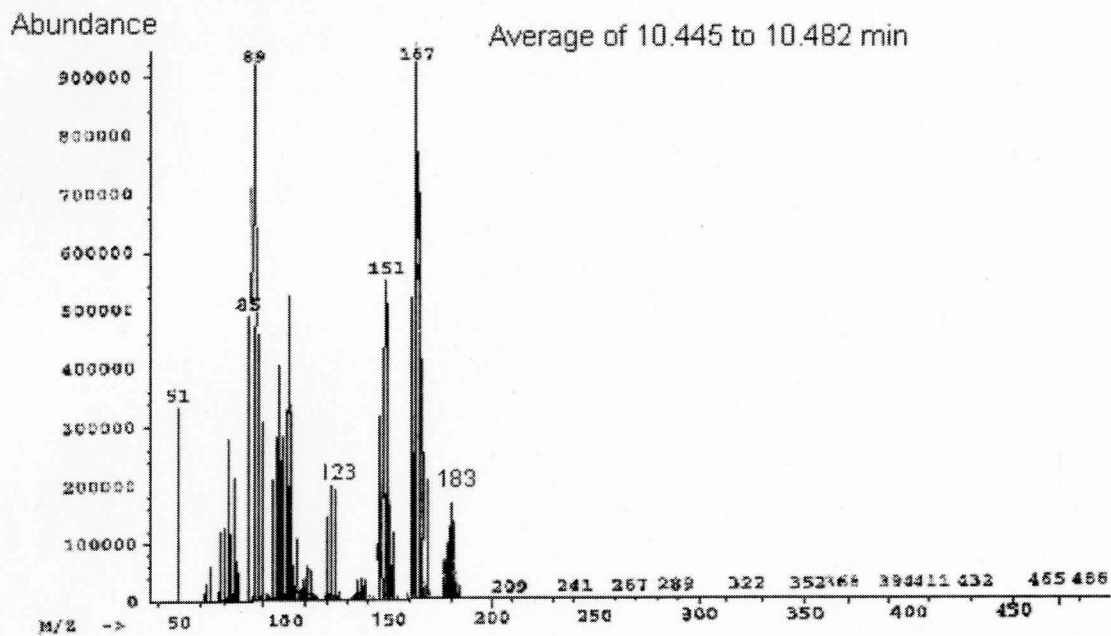
Figure 50. Mass spectrum of 33.

4.5.2. Steady State Photolysis of 1,3,4-Trimethyl-1-phenyl-1-germacyclopent-3-ene (28) in the presence of Isoprene

The photolysis of **28** was performed in septa-sealed quartz tubes (3 x 6 mm) using a 0.05 M solution of substrate in hexane containing 0.1 M isoprene and n-dodecane as internal standard. The conversion was taken to ~ 80% (*ca.* 50 min total irradiation time), as determined by GC analysis over the course of the photolysis. The identity of the crude photolyzed product **31** was verified by co-injection of **31** with the authentic sample on two different GC columns (see experimental section 4.4.3 and Figure 9).

REFERENCES

(1)   Winker, C. A. *Chem. Ber.* **1886,** *19,* 210.

(2)   Winker, C. A. *Chem. Ber.* **1887,** *20,* 677.

(3)   O'Connor, J. A. *Chem. Eng.* **1952,** *59,* 158.

(4)   Dennis, L. M.; Papish, J. *J. Am. Chem. Soc.* **1921,** *43,* 2131.

(5)   Allred, A. L.; Rochow, E. G. *J. Am. Chem. Soc.* **1957,** *79,* 5361.

(6)   Mazerolles, P.; Morancho, R.; Reynes, A. *Silicon, Germanium, Tin and Lead Compounds* **1986,** *9,* (2-3), 155.

(7)   Lukevics, E.; Germane, S.; Ignatovich, L. *Appl. Organomet. Chem.* **1992,** *6,* (7), 543.

(8)   Thayer, J. S. *Appl. Organomet. Chem.* **1987,** *1,* (3), 227.

(9)   Lukevics, E.; Ignatovich, L. *Appl. Organomet. Chem.* **1992,** *6,* (2), 113.

(10)   Asai, K. In *Miracle Cure, Organic Germanium.* 3rd. ed.; Japan Publication Inc/Kodansa International via Harper and Row: New York, Japan, 1980; pp 8-20.

(11)   Griller, D.; Nazran, A. S.; Scaiano, J. C. *Acc. Chem. Res.* **1984,** *17,* 283.

(12)   Creary, X. *J. Am. Chem. Soc.* **1980,** *102,* (5), 1611.

(13)   Bodor, N.; Dewar, J. S.; Wasson, J. S. *J. Am. Chem. Soc.* **1972,** *94,* (26), 9095.

(14)   Nefedov, M. O.; Egorov, M. P.; Ioffe, A. I.; Menchikov, L. G.; Zuev, P. S.; Minkin, V. I.; Simkin, B. Y.; Glukhovtsev, M. N. *Pure and Appl. Chem.* **1992,** *64,* (2), 265.

(15)   Bourissou, D.; Guerret, O.; Gabbai, P. F.; Bertrand, G. *Chem. Rev.* **2000,** *100*, 39.

(16)   Kirmse, W. Part II. Structure and Reactivity of Carbenes and Carbenoids. In *Carbene Chemistry*, 2nd ed.; Academic Press: New York, 1971; pp 209-612.

(17)   Noyori, R.; Yamakawa, M.; Ando, W. *Bull. Chem. Soc. Jpn.* **1978,** *51*, (3), 811.

(18)   Chatgilialoglu, C.; Ingold, K. U.; Lusztyk, J.; Nazran, A. S.; Scaiano, J. C. *Organometallics* **1983,** *2*, 1332.

(19)   Chatgilialoglu, C. *Chem. Rev.* **1995,** *95*, 1229.

(20)   Scaiano, J. C. *Acc. Chem. Res.* **1982,** *15*, 252.

(21)   Mochida, K. Kikkawa, H.; Nakadaira, Y. *J. Organomet. Chem.* **1991,** *412*, 9.

(22)   Reed, C. A. *Acc. Chem. Res.* **1998,** *31*, (6), 325.

(23)   Olah, G. A. *J. Am. Chem. Soc.* **1972,** *94*, (*3*), 808.

(24)   Budac, D.; Wan, P. In *Advances in Carbanion Chemistry*. Snieckus, V., JAI Press Inc. ed.; London, 1996; Vol. 2, pp 147-189.

(25)   Buncel, E.; Dust, J. M. In *Carbanion Chemistry, Structures and Mechanism*. ed.; Oxford Univ. Press, American Chemical Society: Washington, DC, 2003; pp 3-343.

(26)   Escudie, J.; Barrau, J.; Satge, J. *Chem. Rev.* **1990,** *90*, 283.

(27)   Neumann, W. P. *Chem. Rev.* **1991,** *91*, 311.

(28)   Raabe, G.; Michl, J. *Chem. Rev.* **1985,** *85*, 419.

(29)   Baines, K. M.; Cooke, J. A. *Organometallics* **1991,** *10*, 3419.

(30)   Brook, A. G.; Brook, M. A. *Adv. Organomet. Chem.* **1996,** *34*, 71.

(31)   Gaspar, P. P. Silylenes. In *Reactive Intermediate*, ed.; Moss, R. A.;Jones, M., Wiley, J.: New York, 1985; Vol. III, pp 333-366.

(32)   Gaspar, P. P. Silylenes. In *Reactive Intermediates*, ed.; Moss, R.A.; Jones, M.: New York, 1978; Vol. III, pp 362-380.

(33)   Conlin, R. T.; Netto - Ferreira, J. C.; Zhang, S.; Scaiano, J. C. *Organometallics* **1990,** *9*, 1332.

(34)   Atwell, W. H.; Weyenberg, D. R. *Angew. Chem. Int. Ed. Engl.* **1969,** *8*, (7), 469.

(35)   Braddock-Wilking, J.; Chiang, M. Y.; Gaspar, P. P. *Organometallics* **1993,** *12*, 197.

(36)   Gaspar, P. P.; Holten, D.; Konieczny, S. *Acc. Chem. Res.* **1987,** *20*, 329.

(37)   Gaspar, P. P.; Boo, B. H.; Chari, S.; Ghosh, A. K.; Holten, D.; Kirmaier, C.; Konieczny, S. *Chem. Phys. Lett.* **1984**, (*105*), 153.

(38)   Shizuka, H.; Tanaka, H.; Tonokura, K.; Murata, K.; Hiratsuka, H.; Ohshita, J.; Ishikawa, M. *Chem. Phys. Lett.* **1988,** *143*, (3), 225.

(39)   Hawari, J. A.; Lesage, M.; Griller, D. *Organometallics* **1987,** *6*, 880.

(40)   Lei, D.; Gaspar, P. P. *Organometallics* **1985,** *4*, 1471.

(41)   Levin, G.; Das, P. K.; Bilgrien, C.; Lee, C. L. *Organometallics* **1989,** *8*, 1206.

(42)   Gillette, G. R.; Noren, G. H.; West, R. *Organometallics* **1989, 8**, 487.

(43)   Gaspar, P. P.; West, R. Silyenes. In *The Chemistry of Organic Silicon Compounds.* ed.; John Wiley & Sons Ltd.: New York, 1998; Vol. 2, pp 2463-2568.   .

(44)   Nazran, A. S.; Hawari, J. A.; Griller, D. *J. Am. Chem. Soc.* **1984, 106**, 7267.

(45)   Bobbitt, K. L.; Maloney, M. V.; Gaspar, P. P. *Organometallics* **1991, 10**, 2772.

(46)   Mochida, K.; Yoneda, I.; Wakasa, M. *J. Organomet. Chem.* **1990, 399**, 53.

(47)   Konieczny, S.; Jacobs, J. S.; Braddock Wilking, K. J.; Gaspar, P. P. *J. Organomet. Chem.* **1988, 341**, C17.

(48)   Wakasa, M.; Yoneda, I.; Mochida, K. *J. Organomet. Chem.* **1989, 366**, C1.

(49)   Mochida, K.; Kimijima, K.; Chiba, H.; Wakasa, M.; Hayashi, H. *Organometallics* **1994, 13**, 404.

(50)   Ando, W.; Tsumuraya, T.; Sekiguchi, A. *Chem. Lett.* **1987**, 317.

(51)   Mochida, K.; Tokura, S.; Murata, S. *J. Chem. Soc., Chem. Commun.* **1992**, 250.

(52)   Mochida, K.; Kanno, N.; Kato, R.; Kotani, M.; Yamaguchi, S.; Wakasa, M.; Hayashi, H. *J. Organomet. Chem.* **1991, 415**, 191.

(53)   Mochida, K.; Tokura, S. *Bull. Chem. Soc. Jpn.* **1992, 65**, (6), 1642.

(54)   Toltl, N. P.; Kollegger, G. M.; Stibbs, W. G.; Baines, K.; Leigh, W. J. *Organometallics* **1996, 15**, 3732.

(55)   Alexander, U. N.; Trout, N. A.; King, K. D.; Lawrance, W. D. *Chem. Phys. Lett.* **1999,** *299*, 291.

(56)   Becerra, R.; Boganov, S. E.; Nefedov, O. M.; Egorov, M. P.; Faustov, V. I.; Walsh, R. *Phys. Chem. Chem. Phys.* **2001,** *3*, 184.

(57)   Becerra, R.; Nefedov, O. M.; Egorov, M. P.; Boganov, S. E.; Walsh, R. *Chem. Phys. Lett.* **1996,** *260*, 433.

(58)   Taraban, M. B.; Volkova, O. S.; Plyusnin, V. F.; Ivanov, Y. V.; Leshina, T. V.; Egorov, M. P.; Nefedov, O. M.; Kayamori, T.; Mochida, K. *J. Organomet. Chem.* **2000,** *601*, 324.

(59)   Becerra, R.; Nefedov, O. M.; Egorov, M. P.; Krylova, I. V.; Walsh, R. *Chem. Phys. Lett.* **2002,** *351*, 47.

(60)   Becerra, R.; Boganov, S. E.; Egorov, M. P.; Nefedov, O. M.; Lee, V. Y.; Walsh, R. *Chem. Phys. Lett.* **1996,** *250*, 111.

(61)   Becerra, R.; Walsh, R. *Phys. Chem. Chem. Phys.* **1999,** *1*, 5301.

(62)   Becerra, R.; Boganov, S. E.; Nefedov, O. M.; Egorov, M. P.; Faustov, V. I.; Walsh, R. *Mendeleev Commun.* **1997**, 87.

(63)   Becerra, R.; Boganov, S. E.; Nefedov, O. M.; Egorov, M. P.; Faustov, V. I.; Walsh, R. *Can. J. Chem.* **2000,** *78*, 1428.

(64)   Egorov, M. P.; Dvornikov, A. S.; Kuzmin, V. A.; Kolesnikov, S. P.; Nefedov, O. M. *Bull. Acad. Sci. USSR, Div. Chem. Sci.* **1987,** *36*, 1114.

(65)   Mochida, K.; Hasegawa, A. *Chem. Lett.* **1989**, 1087.

(66)   Boganov, S. E.; Egorov, M. P.; Faustov, V. I.; Nefedov, O. M.; Krylova, I. V.; Becerra, R.; Walsh, R. *Russ. Chem. Rev.* **2005,** *in press.*

(67)   Leigh, W. J.; Harrington, C. R.; Vargas-Baca, I. *J. Am. Chem. Soc.* **2004,** *126*, 16105.

(68)   Leigh, W. J.; Harrington, C. R. *J. Am. Chem. Soc.* **2005,** *submitted.*

(69)   Curtius, T.; Buchner, E. *Ber. Dtsch. Chem. Ges.* **1885,** *8*, 2377.

(70)   Staudinger, H.; Kupfer, O. *Ber. Dtsch. Chem. Ges.* **1912,** *45*, 501.

(71)   Mass, G. Silicon - Substituted Carbenes, Chap. 13. In *The Chemistry of Organic Silicon Compounds*, ed.; Wiley, J. & Sons: New York, **1998**; Vol. 2, pp 703-775.

(72)   Schuster, G. B. *Adv. Phys. Org. Chem.* **1986,** *22*, 311.

(73)   Clayden, J.; Greeves, N.; Warren, S.; Wothers, P. Synthesis and Reaction of Carbenes. In *Organic Chemistry*, ed.; Oxford University Press Inc.: New York, 2001; pp 1054-1077.

(74)   McKellar, A. R. W.; Bunker, P. R.; Sears, T. J.; Evenson, K. M.; Saykally, R. J. *J. Chem. Phys.* **1983,** *79*, 5251.

(75)   Slipchenko, L. V.; Krylov, A. I. *J. Chem. Phys.* **2002,** *117*, 4696.

(76)   Leopold, D. G.; Murray, K. K.; Miller, A. E. S.; Lineberger, W. C. *J. Chem. Phys.* **1985,** *83*, 4849.

(77)   Gleiter, R.; Hofmann, R. *J. Am. Chem. Soc.* **1968,** *90*, 1475.

(78)   Sander, W.; Bucher, G.; Wierlacher, S. *Chem. Rev.* **1993,** *93*, 1583.

(79)   Shimizu, H.; Gordon, M. S. *Organometallics* **1994,** *13*, 186.

(80)   Richards, C. A.; Yamaguchi, Y.; Schafer III, H. F.; Kim, S. J. *J. Am. Chem. Soc.* **1995,** *117*, 10104.

(81)   Myers, D. R.; Senthilnathan, V. P.; Platz, M. S.; Jones, J. *J. Am. Chem. Soc.* **1986,** *108*, 4232.

(82)   Irikura, K. K.; Goddard, W. A. I.; Beauchamp, J. L. *J. Am. Chem. Soc.* **1992,** *114*, 48.

(83)   Harrison, J. F.; Liedtke, C. R.; Liebman, J. F. *J. Am. Chem. Soc.* **1979,** *101*, 7162.

(84)   Moss, R. A.; Mallon, C. B. *J. Am. Chem. Soc.* **1975,** *97*, 344.

(85)   Gilbert, B. C.; Griller, D.; Nazran, A. S. *J. Org. Chem.* **1985,** *50*, 4738.

(86)   Gano, J. E.; Wettach, R. H.; Platz, M. S.; Senthilnathan, V. P. *J. Am. Chem. Soc.* **1982,** *104*, 2326.

(87)   Hoffmann, R.; Zeiss, G. D.; Van Dine, G. W. *J. Am. Chem. Soc.* **1968,** *90*, 1485.

(88)   Baird, N. C.; Tailor, K. F. *J. Am. Chem. Soc.* **1978,** *100*, 1333.

(89)   Jones, J. M.; Ando, W.; Hendrick, M. E.; Kulczycki, J. A.; Hawley, P. M.; Hummel, K. F.; Malament, D. S. *J. Am. Chem. Soc.* **1972,** *94*, 7469.

(90)   Berkowitz, J. L.; Green, J. P.; Cho, H.; Ruscic, R. *J. Chem. Phys.* **1987,** *86*, 1235.

(91)   Balasubramanian, K.; McLean, A. D. *J. Chem. Phys.* **1986,** *85*, 5117.

(92)   Grev, R. S.; Schaefer, H. F., III;; Baines, K. M. *J. Am. Chem. Soc.* **1990,** *112*, 9458.

(93) Dyall, J. *J. Chem. Phys.* **1992,** *96*, 1210.

(94) Luke, B. T.; Pople, J. A.; Krogh Jespersen, M. B.; Apeloig, Y.;

Chandrasekhar, J.; Schleyer, P. R. *J. Am. Chem. Soc.* **1986,** *108*, 270.

(95) Escribano, R.; Campargue, A. *J. Chem. Phys.* **1998,** *108*, 6249.

(96) Smith, T. C.; Clouthier, D. J.; Sha, W.; Adam, A. G. *J. Chem. Phys.* **2000,**

113, 9567.

(97) Harrison, J. F.; Allen, L. C. *J. Am. Chem. Soc.* **1971,** *93*, 4112.

(98) Apeloig, Y.; Pauncz, R.; Karni, M.; West, R.; Steiner, W.; Chapman, D.

Organometallics **2003,** *22*, 3250.

(99) Gaspar, P. P.; Xiao, M.; Dong, H. P.; Berger, D. J.; Haile, T.; Chen, T.; Lei,

D.; Winchester, W. R.; Jian, P. *J. Organomet. Chem.* **2002,** *646*, 68.

(100) Sekiguchi, A.; Tanaka, T.; Ichinohe, M.; Akiyama, K.; Tero - Kubota, S. *J.*

Am. Chem. Soc. **2003,** *125*, 4962.

(101) Grev, R. S.; Schaefer III, H. F.; Gaspar, P. P. *J. Am. Chem. Soc.* **1991,**

113, 5638.

(102) Holthausen, M. C.; Koch, W.; Apeloig, Y. *J. Am. Chem. Soc.* **1999,** *121*,

2623.

(103) Dunkin, I. R *Chem. Soc. Rev.* **1980,** *9*, 1.

(104) Chapman, O. L. *Pure Appl. Chem.* **1974,** *40*, 511.

(105) Leigh, W. J.; Workentin, M. S.; Andrew, D. *J. Photochem. Photobiol. A:*

Chem. **1991,** *57*, 97.

(106) Bonneau, R.; Wirtz, J.; Zuberbuhler, A. D. *Pure Appl. Chem.* **1997,** *69*, 1.

(107) Hadel, L. M. Laser Flash Photolysis (Chapter 11). In *CRC Handbook of Organic Photochemistry*, ed.; CRC Press, Boca Raton: 1989; Vol. 1, pp 279-290.

(108) Eaton, D. F. *Pure Appl. Chem.* **1990,** *62*, 1631.

(109) Brittain, E. F. H.; George, W. O.; Wells, C. H. J. Electronic Spectroscopy (Chapter 2). In *Introduction to Molecular Spectroscopy-Theory and Experiment*, ed.; Academic Press INC.: London, 1970; pp 37-114.

(110) Wells, C. H. J. In *Introduction to Molecular Photochemistry.* ed.; Chapman and Hall Ltd : London, 1972; pp 24-55.

(111) Beker, A. D.; Engel, R. In *Organic Chemistry*, ed.; West Publishing Company: New York, 1992; pp 984-987.

(112) Kishikawa, K.; Tokitoh, N.; Okazaki, R. *Chem. Lett.* **1998**, 239.

(113) Boganov, S. E.; Egorov, M. P.; Faustov, V. I.; Nefedov, O. M. Spectroscopic Studies and Quantum-Chemical Calculations of Short-Lived Germylenes, Stannylenes and Plumbylenes. In *The Chemistry of organic germanium, tin and lead compounds*, ed.; Wiley, Johns.& Sons: New York, 2002; Vol. 2, pp 749-841.

(114) Ando, W.; Itoh, H.; Tsumuraya, T. *Organometallics* **1989,** *8*, 2759.

(115) Conlin, R. T.; Namavari, M. *Organometallics* **1992,** *11*, 3307.

(116) Potter, G. D. Substituent Effects on the Photochemistry of 1,1-Diarylgermacyclobutanes and the Reactivity of Transient 1,1-Diarylgermenes. McMaster, Hamilton, 2003, pp 111-114.

(117) Toltl, N. P. The Direct Detection of Germenes in solution: The Photochemistry of 1,1-Diphenylgermetane, Arylgermasilanes, and Aryldigermanes. McMaster University, Hamilton, 1999, pp 30-103.

(118) Leigh, W. J.; Toltl, N. P.; Apodaca, P.; Castruita, M.; Pannell, K. H. *Organometallics* **2000,** *19*, 3232.

(119) Sluggett, G. W.; Leigh, W. J. *Organometallics* **1992,** *11*, 3731.

(120) Ando, W.; Itoh, H.; Tsumuraya, T.; Yoshida, H. *Organometallics* **1988,** 7, 1880.

(121) Deqing, L.; Gaspar, P. P. *Organometallics* **1985,** *4*, 1471.

(122) Masamune, S.; Collins, S.; Murakami, S.; Snow, T. J. *Tet. Lett.* **1985,** *26*, 1281.

(123) Gaspar, P. P. Silylenes. In *Reactive Intermediates*, ed.; Wiley Interscience Publication: New York, 1978; Vol. II, pp 368-368.

(124) Collins, S.; Murakami, S.; Snow, T. J.; Masamune, S. *Tet. Lett.* **1985,** *26*, 1281.

(125) Lange, L.; Meyer, B.; Du Mont, W. W. *J. Organomet. Chem.* **1987,** *329*, C17.

(126) Su, M. D.; Chu, S. Y. *J. Phys. Chem. A* **1999,** *103*, 11011.

(127) Gillette, G. R.; Noren, G. H.; West, R. *Organometallics* **1990,** *9*, 2925.

(128) Yamaji, M.; Hamanishi, K.; Takahashi, T.; Shizura, H. *J. Photochem. Photobiol. A: Chemistry* **1994,** *81*, 1.

(129) Ragahavachari, K.; Chandrasekhar, J.; Gordon, M. S.; Dykema, K. J. *J. Am. Chem. Soc.* **1984,** *106*, 5853.

(130) Massol, M.; Satge, J.; Riviere, P.; Barrau, J. *J. Organomet. Chem.* **1970,** *22*, 599.

(131) Satge, J.; Massol, M.; Riviere, P. *J. Organomet. Chem.* **1973,** *56*, 1.

(132) Klein, B.; Neumann, W. P.; Weisbeck, M. P.; Wienken, S. *J. Organomet. Chem.* **1993,** *446*, 149.

(133) Riviere, P.; Satge, J.; Riviere, M.; Dousse, G.; Couret, C. *J. Organomet. Chem.* **1974,** *72*, 339.

(134) Riviere, P.; Satge, J.; Soula, D. *J. Organomet. Chem.* **1974,** *72*, 329.

(135) Riviere, P.; Satge, J. *J. Organomet. Chem.* **1973,** *49*, 157.

(136) Lappert, M. F.; Miles, S. J.; Atwood, J. L.; Zaworotko, M. J.; Carty, A. J. *J. Organomet. Chem.* **1981,** *212*, C4.

(137) Kocher, J.; Lehnig, M.; Newmann, W. P. *Organometallics* **1988,** *7*, 1201.

(138) Kocher, J.; Lehnig, M. *Organometallics* **1984,** *3*, 937.

(139) Bharatam, P. V.; Moudgil, R.; Kaur, D. *Organometallics* **2002,** *21*, 3683.

(140) Ando, W.; Sekiguchi, A.; Hagiwara, K.; Sakakibara, A.; Yoshida, H. *Organometallics* **1988,** *7*, 558.

(141) Ishikawa, M.; Nakagawa, K. I.; Kumada, M. J. *J. Organomet. Chem.* **1979,** *178*, 105.

(142) Seyferth, D.; Annareli, D. C.; Duncan, D. P. *Organometallics* **1982,** *1*, 1288.

(143) Tortorelli, V. J.; Jones, M. J. *J. Am. Chem. Soc.* **1980,** *102*, 1425.

(144) Tortorelli, V. J.; Jones, M. J.; Wu, S. H.; Li, Z. H. *Organometallics* **1983,** *2*, 759.

(145) Ohgaki, H.; Kabe, Y.; Ando, W. *Organometallics* **1995,** *14*, 2139.

(146) Billeb, G.; Brauer, H.; Neumann, W. P.; Weisberck, M. *Organometallics* **1992,** *11*, 2069.

(147) Billeb, G.; Neumann, W. P.; Steinhoff, G. *Tet. Lett.* **1988,** *29*, (41), 5245.

(148) Billeb, G.; Brauer, H.; Maslov, S.; Neumann, W. P. *J. Organomet. Chem.* **1989,** *373*, 11.

(149) Billeb, G.; Brauer, H.; Neumann, W. P. *Synlett* **1990**, 113.

(150) Brauer, H.; Neumann, W. P. *Synlett* **1991**, 431.

(151) Lei, D.; Gaspar, P. P. *J. Chem. Soc., Chem. Commun.* **1985**, 1149.

(152) Hwang, R. J.; Conlin, R. T.; Gaspar, P. P. *J. Organomet. Chem.* **1975,** *94*, C38.

(153) Neumann, W. P.; Michels, E.; Kocher, E. *Tet. Lett.* **1987,** *28*, (33), 3783.

(154) Davidson, M. T. I.; Clarke, M. P. *J. Chem. Soc., Chem. Comm.* **1988**, 241.

(155) Zhang, S.; Conlin, R. T. *J. Am. Chem. Soc.* **1991,** *113*, 4272.

(156) Kocher, J.; Neumann, W. P. *Organometallics* **1985,** *4*, 400.

(157) Bobbitt, K. L.; Gaspar, P. P. *J. Organomet. Chem.* **1995,** *499*, 17.

(158) Atwell, W. H.; Weyenberg, D. R. *J. Am. Chem. Soc.* **1968,** *90*, 3438.

(159) Schriewer, M.; Neumann, W. P. *J. Am. Chem. Soc.* **1983,** *105*, 897.

(160) Kocher, J.; Neumann, W. P. *J. Am. Chem. Soc.* **1984,** *106*, 3861.

(161) Weyenberg, D. R.; Atwell, W. H. *Pure Appl. Chem.* **1969,** *19*, 343.

(162) Atwell, W. H.; Uhlmann, J. G. *J. Organomet. Chem.* **1973,** *52*, C21.

(163) Clarke, M. P.; Davidson, M. T. I. *J. Chem. Soc., Chem. Commun.* **1988**, 241.

(164) Lei, D.; Hwang, R. J.; Gaspar, P. P. *J. Organomet. Chem.* **1984,** *271*, 1.

(165) Lei, D.; Gaspar, P. P. *Polyhedron* **1991,** *10*, 1221.

(166) Horner, D. A.; Grev, R. S.; Schaefer III, H. F. *J. Am. Chem. Soc.* **1992,** *114*, 2093.

(167) Vancik, H.; Raabe, G.; Michalczyz, J. M.; West, R.; Michl, J. *J. Am. Chem. Soc.* **1985,** *107*, (13), 4097.

(168) Michalczyk, M. J.; Fink, M. J.; De Young, D. J.; Carlson, C. W.; Wesh, K. M.; West, R.; Michl, J. *Silicon, Germanium, Tin and Lead Compd.* **1986**, (*9*), 75.

(169) West, R.; Fink, M. J.; Michl, J. *Science* **1981,** *214*, 1343.

(170) Barltrop, J. A.; Coyle, J. D. Kinetics of Quenching. In *Excited States in Organic Chemistry*, ed.; A Wiley- Interscience publication: 1975; pp 148-154.

(171) Fujii, Y.; Yamada, H.; Mizuta, M. *J. Am. Chem. Soc.* **1988,** *92*, 6768.

(172) Denk, M. K.; Khan, M.; Lough, A. J.; Shuchi, K. *Acta Cryst.* **1998,** *C54*, 1830.

(173) du Mont, W. W.; Neudert, B.; Schumann, H. *Angew. Chem. Int. Ed. Engl.* **1976,** *15*, 308.

(174)   King, R. B. *Inorg. Chem.* **1963,** *2*, 199.

(175)   Inoguchi, Y.; Okui, S.; Mochida, K.; Itai, A. *Bull. Chem. Soc. Jpn.* **1985,** *58*, 974.

(176)   Jutzi, P.; Hofmann, J.; Brauner, D. J.; Kruger, C. *Angew. Chem. Int. Ed. Engl.* **1973,** *12*, 1002.

(177)   Morkin, T.; Owens, T. R.; Leigh, W. J. Kinetic studies of the reactions of Si=C and Si=Si bonds. In *The chemistry of organic silicon compounds,* ed.; Rappoport, Z.; Apeloig, Y.: New York, 2001; Vol. *3*, pp 976-978.

(178)   Mochida, K.; Kayamori, T.; Wakasa, M.; Hayashi, H.; Egorov, M. P. *Organometallics* **2000,** *19*, 3379.

(179)   Adachi, M.; Mochida, K.; Wakasa, M.; Hayashi, H. *Main Group Met. Chem.* **1999**, *22*, 227.

(180)   Taraban, M. B.; Volkova, O. S.; Kruppa, A. I.; Leshina, T. V. Radical reaction mechanisms of and at organic germanium, tin and lead. In *The chemistry of organic germanium, tin and lead compounds,* ed.; Wiley, J & Sons Ltd.: Chichester, 2002; Vol. *2*, pp 579-581.

(181)   Baggott, J. E.; Blitz, M. A.; Frey, H. M.; Walsh, R. *J. Am. Chem. Soc.* **1990,** *112*, 8337.

(182)   Krebs, A.; Berndt, J. *Tet. Lett.* **1983,** *24*, 4083.

(183)   Baggott, J. E.; Blitz, M. A.; Frey, H. M.; Lightfoot, P. D.; Walsh, R. *International Journal of Chemical Kinetics* **1992,** *24*, 127.

(184)   Leigh, W. J.; Bradaric, C. J. *Can. J. Chem.* **1997,** *75*, 1393.

(185) Kolesnikov, S. P.; Rogozhin, I. S.; Nefedov, O. M. *Izv. Acad. Nauk SSSR, Ser. Khim.* **1974,** *10*, 2379.

(186) Viktorov, N. A.; Gar, T. K.; Mironov, V. F. *Zh. Obshch. Khim.* **1985,** *55*, 1208.

(187) Nefedov, M. O.; Kolesnikov, S. P.; Ioffe, A. I. *Izv. Acad. Nauk SSSR, Ser. Khim.* **1976,** *3*, 619.

(188) Kolesnikov, S. P.; Ioffe, A. I.; Nefedov, O. M. *Izv. Acad. Nauk SSSR, Ser. Khim.* **1975,** *4*, 978.

(189) Kolesnikov, S. P.; Rogozhin, I. S.; Safarov, M. G.; Nefedov, O. M. *Izv. Acad. Nauk SSSR, Ser. Khim.* **1981,** *6*, 1423.

(190) Mazerolles, P.; Manuel, G. *Bull. Soc. Chim. Fr.* **1965,** *56*, 327.